SEGREGATION OF POWDER MIXTURES IN SILOS WITH PARTICULAR REFERENCE TO DRY MINERAL-BASED CONSTRUCTION MATERIALS

Niklas Engblom

Academic dissertation

Thermal and Flow Engineering Laboratory

Department of Chemical Engineering

Division for Natural Sciences and Technology

Åbo Akademi University

2012

Supervisors

Professor Henrik Saxén
Thermal and Flow Engineering Laboratory
Department of Chemical Engineering
Åbo Akademi University
Åbo, Finland

and

Professor Gisle G. Enstad
Department for Powder Science and Technology
Telemark College
Porsgrunn, Norway

and

Industrial Director Henrik Nylander
Saint-Gobain Weber Oy Ab
Parainen, Finland

Opponent and reviewer

Prof. Dr. Dietmar Schulze
Institute for Recycling
Hochschule Braunschweig/Wolfenbüttel
Wolfsburg, Germany

Reviewer

Dr. Janne Henrik Pärssinen
BAXTER
Braine l'Alleud, Belgium

ISBN 978-952-12-2723-3
Finlands Universitetstryckeri Ab Uniprint

Preface

The work included in this thesis has involved close co-operation between the Laboratory of Thermal and Flow Engineering at Åbo Akademi University (ÅAU) in Turku, Finland, Tel-Tek, Dept. POSTEC in Porsgrunn, Norway, and Saint-Gobain Weber (SGW). SGW is gratefully acknowledged for financial support. Rector Jorma Mattinen at ÅAU is thanked for funding the last months of this thesis work.

I wish to thank my official supervisors Prof. Henrik Saxén at ÅAU, Prof. Gisle G. Enstad at POSTEC and Mr. Henrik Nylander at SGW for invaluable guidance, support and encouragement. Prof. Ron Zevenhoven at ÅAU provided significant input during the course of this work and, in effect, acted as the fourth unofficial supervisor, which I am deeply indebted for. The people at the Laboratory of Thermal and Flow Engineering, especially Vivéca and Alf, are thanked for their help. Pekka at the department's workshop deserves a tribute for his efforts to fulfill my wishes in the building of experimental equipment even though technical documentation was always insufficient. All personnel at SGW involved in this work is gratefully acknowledged for their assistance with special regards to Arto and Kai in Parainen, Harry, Jari and Auli in Kiikala, and Marko and Paavo in Ojakkala.

I have had the privilege to visit a number of different research groups during my time as a doctoral student. First and foremost, I would like to thank everyone at POSTEC for their hospitality during my visits to Porsgrunn; you made me feel at home despite being away from my family. Special thanks are in place to Mr. Franz Otto von Hafenbrädl for his help with practical matters. Prof. Ai-Bing Yu at SIMPAS at the University of New South Wales in Sydney, Australia is thanked for the opportunity to meet with his research staff and discuss different aspects related to mathematical modeling of particulate systems. I am indebted to the personnel at BlueScope Steel's Iron- and Steelmaking Research Group at the steelworks in Port Kembla, Australia for an unforgettable couple of months. Those deserving special mention are Dr. Paul Zulli for making the visit possible, and Dr. Bryan Wright and Dr. David Pinson for supervising the work carried out at the steelworks.

I wish to thank my parents, Erik and Päivikki, for their everlasting support, and for providing me with valuable capabilities and nearly endless possibilities in life. By way of your own example, you have shown me that righteousness and diligence are virtues that carry you through

even the toughest of situations in all aspects of life. My brothers Markus with family and Thomas are thanked for always being there.

I am grateful to my parents-in-law, Jussi and Eira, for all their assistance with matters at home. Benny and Carina Björkblom are thanked for their hospitality during the final stages of this thesis work.

None of this work would have seen daylight without the endless love, support and encouragement of my wife Petra. You have patiently listened at times of despair and taken care of things at home during my long hours at work and extended tours abroad. Words cannot express the gratitude I owe to our daughter Fiona (and to “Mikael”) for leading me into the extraordinary wonders of parenthood; your existence truly brings meaning to life. And finally to Emppu, my faithful friend and best of hunting buddies.

Abstract

This thesis work comprises a study of the segregation of powder mixtures in silos with particular reference to dry mineral-based construction materials. In industrial production of dry mineral-based construction materials, short term storage of final products in silos constitutes the most critical stage with respect to segregation. Segregation manifests itself as an increase of the fine particle concentration to unacceptable levels when the silo is completely emptied, which leads to tedious and costly re-processing of the final goods. During normal production conditions, the final products are often subjected to considerable free fall distances at silo filling and this was suspected to be one reason for the observed segregation.

Experimental work was performed in silos of different size with commercial (dry mineral-based) construction materials as well as other powder mixtures that resemble these in composition and behavior. The segregation patterns of commercial products in large (20 m^3 and 70 m^3) silos were reproduced with two- and three-component powder mixtures in a silo of much smaller (0.5 m^3) size. Furthermore, the segregation mechanisms causing the fine particle concentration to increase at complete emptying of silos were identified as embedding, fluidization and air current effects. These occur as a result of silo filling with free fall and lead to accumulation of fine particles away from the filling point. For centrally filled silos fines will therefore collect at the silo walls. The magnitude of this segregation was shown to depend on several factors: mass fraction of fine particles, particle size ratio or width of size distribution, and particle solid densities for the bulk solid as well as the free fall distance, silo diameter and silo inlet size. On the basis of the experimental results, a regression model was developed for quantifying the magnitude of segregation at silo filling.

It was also shown that segregation at complete emptying of silos is mainly determined by the segregation induced during filling, whereas the discharge flow pattern (mass flow or funnel flow) has minor - or negligible - effect. The size distribution at the end of complete emptying is mainly determined by the material distribution obtained at the levels of fill that discharge last. No further segregation, for example as a result of sifting, was found to occur during discharge even in the case of funnel flow.

The experimental findings were utilized to explain segregation data collected for a production plant, which showed considerable differences in the magnitude of segregation between sever-

al commercial products and strong variations in segregation for each product. Possible remedies for suppressing the detrimental effects of segregation are also discussed as well the possibilities for mathematical modeling of the flow of particulate solid assemblies.

The results of this thesis work contribute to the understanding of embedding, fluidization and air current segregation and highlight the parameters affecting these phenomena. The conclusions of this work should be of immediate interest to producers of dry mineral-based construction materials and to other industries involved in the handling of similar bulk solids.

Sammanfattning

I denna avhandling har segregering av olika pulverblandningar och speciellt torra mineralbaserade byggmaterial i siloer studerats. Korttidslagring av slutprodukter i siloer utgör den mest kritiska enhetsoperationen med tanke på segregering vid industriell produktion av dylika byggmaterial. Segregering leder till en oacceptabel ökning av massandelen finmaterial i slutändan av fullständig tömning ur siloer, vilket förorsakar arbetsam och dyr bearbetning av slutprodukterna. Under normala produktionsförhållanden utsätts materialen för anmärkningsvärda sträckor av fritt fall vid påfyllning av produktsiloer och i början av denna avhandling ansågs detta vara en möjlig orsak till den segregering som observeras.

Experimentellt arbete utfördes i siloer av olika storlek med kommersiella (mineralbaserade) byggmaterial samt med pulverblandningar som efterliknar dessa i avseende på sammansättning och beteende. Man fann att segregeringsmönstren för de stora (20 m^3 och 70 m^3) siloerna kunde reproduceras i mycket mindre skala (0.5 m^3) med blandningar bestående av två och tre olika råmaterial. Dessutom klargjordes att inbäddning (”embedding”), fluidisering och luftströmssegregering är de väsentligaste segregeringsmekanismerna vid industriell produktion av byggmaterial. Dessa segregeringstyper sker vid påfyllning av produktsiloer med fritt fall och leder till ackumulering av finmaterial längre bort från påfyllningspunkten, exempelvis vid siloväggarna då påfyllningen sker centralt. Magnituden av segregeringen påvisades bero av flera faktorer såsom massandelen finmaterial, partikelstorleksfördelning och partikeldensitet samt det fria fallets längd, silodiametern och storleken av siloinloppet. En regressionsmodell för kvantifiering av segregering vid silopåfyllning utvecklades på basis av de experimentella resultaten.

Därtill påvisades att den segregering som erhålls i slutet av fullständig silotömning huvudsakligen bestäms av den under påfyllning inducerade segregeringen medan tömningsmönstret (massa- eller trattströmning) har en mycket liten eller nästan obetydlig inverkan. Partikelstorleksfördelningen för de sista delarna av utflödet bestäms huvudsakligen av materialfördelningen vid de höjdnivåer från vilka material flödar ut sist. Detta innebär att knappast någon ytterligare segregering, exempelvis på grund av siktning, sker under tömningsfasen oavsett tömningsmönstret.

Erfarenheterna från det experimentella arbetet utnyttjades för att förklara segregeringsdata för en produktionsanläggning. Dessa data innehöll kraftiga variationer för enskilda produkter och stora skillnader mellan olika produkter.

Slutligen har möjliga åtgärder för minskning av pulversegregering i siloer samt tillämpning av numeriska metoder för simulering av partikelflöden med hjälp av datorer behandlats.

Resultaten av denna avhandling ökar den kvalitativa förståelsen för segregering som induceras av inbäddning (”embedding”), fluidisering och luftströmning, och klargör de parametrar som är betydelsefulla för dessa mekanismer. Detta arbetes konklusioner uppskattas vara av värde för producenter av torra mineralbaserade byggmaterial samt inom andra industrier där liknande pulverformiga material behandlas.

List of publications

The following peer reviewed journal publications were produced in the context of this thesis work and are enclosed as appendices to this dissertation:

I. N. Engblom, H. Saxén, R. Zevenhoven, H. Nylander and G.G. Enstad, Segregation of Construction Materials in Silos. Part 1: Experimental Findings on Different Scales, Particulate Science and Technology, 2012, 30, pp. 145-160 (DOI: 10.1080/02726351.2011.553880).

II. N. Engblom, H. Saxén, R. Zevenhoven, H. Nylander and G.G. Enstad, Segregation of Construction Materials in Silos. Part 2: Identification of Relevant Segregation Mechanisms, Particulate Science and Technology, 2012, 30, pp. 161-178 (DOI: 10.1080/02726351.2011.552097).

III. N. Engblom, H. Saxén, R. Zevenhoven, H. Nylander, G.G. Enstad and M. Murtomaa, Effects of Material Properties on Segregation of Binary and Ternary Powder Mixtures in a Small Scale Cylindrical Silo, Industrial & Engineering Chemistry Research, 2011, 50(19), pp. 11097-11108 (DOI: dx.doi.org/10.1021/ie200490a).

IV. N. Engblom, H. Saxén, R. Zevenhoven, H. Nylander and G.G. Enstad, Effects of process parameters and hopper angle on segregation of cohesive ternary powder mixtures in a small scale cylindrical silo, Advanced Powder Technology, 2011, in press (DOI: 10.1016/j.apt.2011.06.003).

V. N. Engblom, H. Saxén, R. Zevenhoven, H. Nylander and G.G. Enstad, Segregation of powder mixtures at filling and complete discharge of silos, Powder Technology, 2012, 215-216, pp. 104-116 (DOI: 10.1016/j.powtec.2011.09.033).

VI. N. Engblom, H. Saxén, R. Zevenhoven, H. Nylander and G.G. Enstad, Analysis of segregation data for a dry mineral-based construction materials plant, 2012, submitted manuscript.

The present author has performed most of the work presented in this thesis and was the main writer of the publications listed above. For work reported in Papers I and II, plant personnel assisted in performing the intermediate and large silo experiments. Dr. Matti Murtomaa determined electrostatic properties for some of the materials used in experiments reported in Paper III. Plant personnel also assisted in the collection of segregation data presented in Paper VI. DEM simulations of bunker filling (section 10) were performed by Dr. Yu Guo under the supervision of Dr. Chuan-Yu Wu at the University of Birmingham. The present author participated in planning of the simulations and analyzing of the results.

Table of contents

1. Introduction

Particles are abundantly present in our everyday lives and can be found in a variety of different forms and surroundings, such as dispersed in the atmosphere as dust, stored in jars, cups and bags in our kitchens, laid out on the ground outdoors, and submerged in rivers and oceans. Assemblies of particles are called particulate or bulk solids and there are many commercial examples of these: foodstuffs, detergents, pharmaceuticals, pigments, fertilizers, minerals, coal, animal food products, etc. The constituents of bulk solids therefore vary from large lumps of minerals or rock with sizes measured in meters to tiny ultrafine particles of nanometer scale. It is estimated that about 50 % of all matter used by man is derived from or is at some stage of its existence present in particulate form [1]. In the U.K. alone, approximately 170 Mt of bulk solids are processed by the industry on an annual basis according to estimates in the mid 1990s.

Bulk solids are a peculiar form of substance that, on the one hand, cannot be described as solid, liquid or gaseous matter, but, on the other hand, can resemble each of these in their behavior depending on the circumstances they are exposed to. The difficulties encountered in industrial handling of particulate solids were vividly illustrated by Merrow [2-4], who highlighted the problems associated with industrial processing of such materials. This was exemplified through comparison of start-up times for processing plants using gases and liquids, refined bulk solids or raw bulk solids as feedstock. Plants belonging to the latter two categories, and in particular to the last one, experienced considerably greater difficulties during commissioning. In addition, the productivity of these plants expressed in terms of percentage of design value after one year of operation was considerably lower compared to plants with gaseous or liquid feedstock. Difficulties experienced in the processing of bulk solids arise from poor and insufficient knowledge of the fundamental laws governing the behavior of these materials. Theories describing the behavior of solids, liquids and gases are much further developed and this bears the inherent advantage of increased predictability [5].

Even though problems associated with the handling of particulates are vast in number, and vary considerably in nature and magnitude depending on the materials and the processing conditions, Bates [1] postulated that "*Segregation is the most influential common factor which adversely affects the uniformity of bulk materials, raising problems of product suitability and also giving rise to many types of handling and processing difficulties within the manufactur-*

ing plant". Producing products suitable for a given purpose can be seen as one of the ultimate goals of any processing plant and segregation can be seen as a major obstacle in pursuit of this goal. This is because of the widespread adverse effects of this problem on the handling and quality of bulk solids. In addition, segregation usually has a negative impact on the economics and sustainability of industrial production.

1.1. Dry mineral-based construction materials

Dry mineral-based construction materials (termed construction materials in the following) constitute a subclass of particulate solids. Construction materials are multi-component and highly heterogeneous mixtures of different minerals and other raw materials. These materials are typically used for different constructional purposes such as building or renovating of small private houses as well as larger buildings. Examples of construction materials are grouts for tiled inner walls, renders for the facades of buildings, plasters for inner walls, floor screeds, as well as masonry and technical mortars. The exact specifications for commercial products are subject to confidentiality, but these usually include sand and limestone (sometimes also glass and Styrofoam beads) as aggregates and fillers, different types of cement, hydrated lime (calcium hydroxide) and gypsum (calcium sulphate dihydrate) as binders, as well as a vast amount of distinct additives including different glues (in particulate form), cellulose derivates, color pigments and synthetic fibers.

Each class of raw materials (aggregates/fillers, binders and additives) has a specific purpose and affects the transient and permanent properties of commercial construction materials. Aggregates and fillers are used for enhancing certain technical properties of the products, e.g., for reducing bulk density and increasing the strength of final constructions. Aggregates/fillers also lower the consumption of the more expensive binders and additives. Binders determine the kinetics of chemical reactions occurring after the addition of water and have a significant effect on the expansion/contraction during curing as well as the small enduring contraction (usual outcome) of the final application. Additives have several different functions; these influence the effect of binders by accelerating or decelerating the chemical reactions, and increase the permanent adhesive strength and resilience of the construction. Inclusion of aggregates/fillers, binders and additives in pre-determined proportions is crucial for correct functionality of construction materials. A typical outcome of using out of spec products is reduced

workability during application and the formation of cracks during the drying phase, while more serious problems include reduced strength of the final construction.

One commercial construction product can contain over ten different raw materials and the final products therefore include particles of varying shape, solid density and, especially, size. Typically, aggregates and fillers comprise the coarsest raw materials with particle sizes ranging from roughly 100 µm up to several millimeters, whereas binders and additives consist of particles from less than 1 µm up to a few hundred micrometers. The proportion of aggregates/fillers, binders and additives included in commercial products varies considerably with tentative general compositions given as 60-80 %-wt, 15-35 %-wt and < 5 %-wt, respectively, for the different groups of raw materials. The particle size distributions for construction materials, therefore, often cover several orders of magnitude and many products include significant amounts of fine particles (typically 20-80 %-wt below 125 µm). The flow properties of commercial products (in dry form) range from free flowing to cohesive, i.e., bulk materials characterized by the presence of significant inter-particle forces, depending on the composition.

Figure 1 presents images obtained with Scanning Electron Micrograph of individual particles for a subset of raw materials used in commercial construction products and shows that the shapes are similar. Individual particles of construction materials are mainly cubic or flaky with the exception of fibers that are very elongated (and lightweight). Fibers are a special type of additive usually present in very small proportions (less than 0.4 %-wt), but these influence the flow properties of the products by forming complex interconnected networks. Particle solid densities for the main raw materials cover a wide range ($\rho_s \approx$ 1200-3200 kg/m^3), but on average or apparent particle solid densities for different size fractions of commercial products are much more alike ($\rho_s \approx$ 2600-3200 kg/m^3). The affinity for individual particles to become electro-statically charged was determined for a small subset of raw materials by sliding electrically neutralized samples into a Faraday pail through a grounded stainless steel pipe and recording the charge using an electrometer. The majority of particles tested showed similar behavior by obtaining a small negative charge with the exception of hydrated lime, which charged positively, most likely because of its hygroscopic nature.

The above description of particle properties for commercial construction materials presents merely a short overview with the aim of familiarizing the reader with the materials under investigation in this work. Determining all particle properties, e.g., shape, solid density, affinity

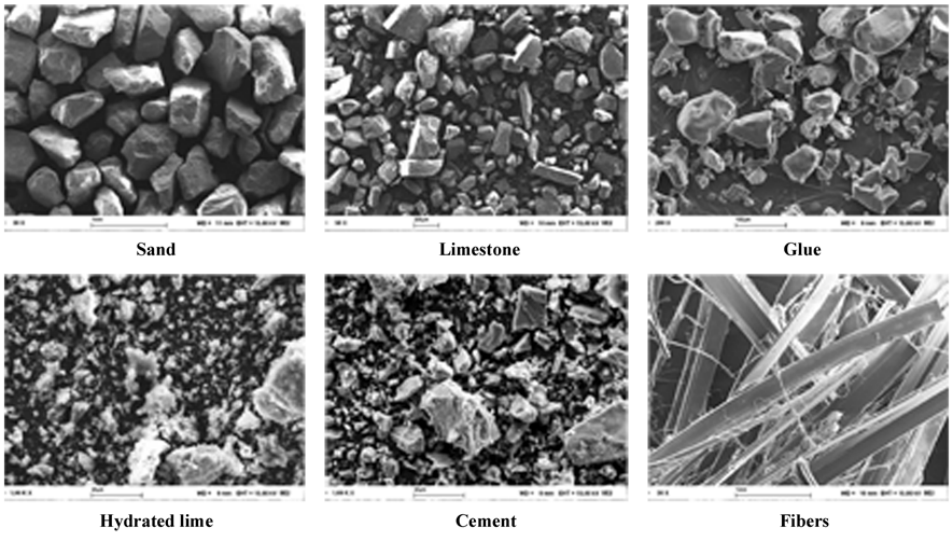

Figure 1. SEM images of individual particles for a subset of raw materials used in commercial dry mineral-based construction products.

for electrostatic charging, surface texture, micromechanical properties, and molecular surface forces, that could be relevant for segregation would be an exhaustive task because of the vast number of different raw materials used in commercial construction products. Moreover, exact compositions or "recipes" for commercial products are subject to confidentiality and these are, in fact, unknown to the author of this thesis.

1.2. Industrial production of construction materials

Industrial production of (dry mineral-based) construction materials essentially incorporates the mixing of multiple raw materials in specified proportions and maintaining the mixture quality until delivery at the customer. The supply for a local market is managed through monthly overall resource planning based on sales forecasts and weekly production schedules for individual plants. Products are usually split up into those that should be always available and delivered even during the next day and products with delivery times up to two or three weeks. Despite efforts towards a complete make-to-order production system by the sponsor of this thesis work, sales forecasting is still required because of long delivery times for some raw

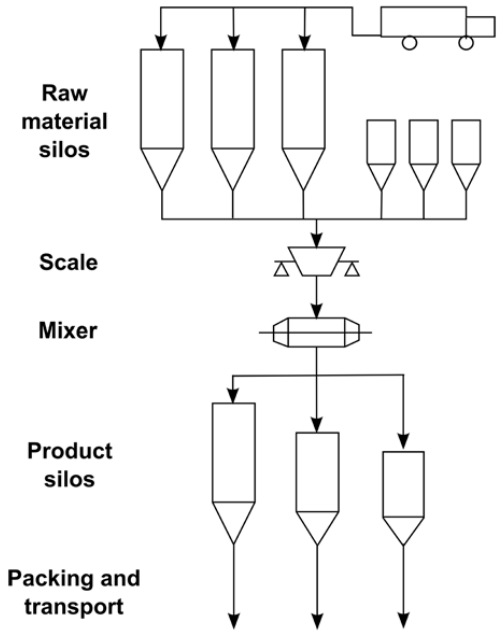

Figure 2. Simplified flow sheet for production of dry mineral-based construction materials.

materials. Even though production at plant level is planned on a weekly basis, it nearly always requires daily supervision and adjustment partly because of unexpected equipment break-downs.

Figure 2 shows a simplified flow sheet for a typical construction materials plant without sand drying and classification. Raw materials are usually delivered to plants by truck or in big bags (one ton). Materials delivered by truck are transferred pneumatically and big bags are emptied by hand into raw material silos ranging from a few to nearly one hundred cubic meters in size. Raw materials are then transferred mainly with screw feeders and belt conveyers to scales for weighing to ensure that correct proportions of raw materials are included in the products. Usually more than one scale per plant exists and volumetric dosage of raw materials may also be used. After weighing, the raw materials are fed into the mixer in a number of different ways, i.e., with belt conveyors, portable bins or by hand for example in the case of fibers. Batch wise mixers with a centric shaft and additional blenders on the mixer walls are used. Typically, there is one mixer per mixing line and in the majority of cases this unit operation comprises the core process for the plant. The capacity of the mixer is usually two or three tons with mixing times in the order of minutes (normally 1-3 min). On the basis of the above, it is

evident that the throughput of the mixer significantly affects the production rate for the entire plant.

After completion of the mixing process, the contents of the mixer are usually emptied into a separate bin situated vertically below in order to free the mixer as quickly as possible for mixing of the subsequent batch. The final products then take alternative routes, with transfer by belt conveyors and bucket elevators, depending on the chosen packing format (with approximate masses or volumes given in parenthesis): truck (15-40 t), building-site silo (18 m^3), big bag (500 kg or 1000 kg) or small bag (5 kg or 25 kg). Product silos situated downstream of mixing and immediately upstream of packing are used for short term storage, i.e., from less than one hour up to a few days, of the final products. These silos are often filled and discharged concurrently during normal production conditions. Trucks, building-site silos and big bags are usually filled directly from product silos, whereas separate packing machines are utilized for filling of small bags. In such cases the silo contents are withdrawn via parallel outlets into separate bag fillers or via a centric outlet into a rotary packer.

Many different products are usually produced at one plant and often during the same day, and several hundred tons of final products are mixed daily. The product silo for a specific packing line, e.g., 25 kg bagging line, must nearly always be completely emptied at changes in the production sequence. This is because the vast majority of packing lines include only one product silo and all products taking this route must be temporarily stored in the silo. In special cases, a single packing line and associated product silo may be dedicated to a specific product that can then be stored for prolonged periods of time in the silo with no immediate need for complete emptying. Compared to mixing, the throughput for packing may have an even stronger effect on the production rate for the plant and, therefore, this step often comprises the bottleneck for the entire production process. Large product silos add flexibility to the production because of the alternative product routes that are possible after mixing. When the throughput rate for mixing exceeds that for packing – a relatively common situation – the product silo for this packing line becomes full at some point. Emptying of this silo continues while a product taking a different packing route can be mixed. This leads to a situation where the mixer can be operated nearly continuously. Small product silos inhibit the mixing of a different product when the mixer needs to cleaned before the product change.

Product silos usually include equipment for measuring the fill level, which can be monitored either as passing over a lower/upper level (discontinuous) or continuously. The former can be accomplished with vibrating or rotating devices and the latter with capacitive or ultrasonic instruments. Product silos are often equipped with overpressure security valves that eliminate the build-up of excessive pressures inside the silos. Pressure transducers are used in pneumatically filled silos for stopping of the filling procedure before the overpressure valves are opened, because this leads to dispersion of dust into the plant. Aside from these devices, fluidization plates are often installed in the hopper section of product silos. These reduce the friction between powder and hopper wall but do not fluidize the entire silo contents. The operation of fluidization plates is discussed more thoroughly in section 3. Further, vibrating hopper sections or outlet regions and hammers are sometimes used as discharge aids in product silos.

1.3. Segregation of construction materials

Segregation will be defined and discussed on a more general level and in more detail in section 2. In this subsection, a short introduction to the problems caused by segregation in industrial production of (dry mineral-based) construction materials will be presented.

At the start of this thesis work, several aspects of the segregation of construction materials were rather unclear to the company (maxit Group in the beginning, but today known as Saint-Gobain Weber) providing for the funding. Therefore, the scope of this thesis work was initially defined very broadly as "*Segregation of particles in the production process of powdered construction materials*". Needless to say, it is almost impossible to entirely cover such a wide topic within the scope of one single academic dissertation. However, a considerable amount of practical information was available from the production plants and, hence, the first objective of this work was to decide on a suitable starting point. On the basis of information available within the company and some initial insights into particle properties (especially particle size) affecting segregation, it was decided to focus on product silos during the early stages. Additional parts of the production process could be investigated later on. Even though some implications of segregation occurring also in other parts of the production process were obtained, segregation in product silos remained the primary interest for this dissertation.

According to the experience of on-site production personnel, by far the most common problem with and serious consequences of segregation are encountered at complete emptying of product silos (cf. Figure 2). Segregation at complete discharge of these silos manifests itself as an increase of the fines content for the output to unacceptable levels, i.e., levels exceeding the quality requirement limits. This occurs despite considerable differences in silo size, geometry, auxiliary equipment and filling procedure as well as material properties for the products. Even though segregation is qualitatively seen to increase with increasing silo volume, an explanation for this finding is not available. The effect of material properties is observed as large differences in segregation between products handled in the same silo with identical filling and emptying procedures for all products.

When the quality limit for the fines content of a product is exceeded towards the end of complete discharge from a product silo, the remainder of the silo contents must be reprocessed. Usually, segregated products are introduced as input to the production process together with other raw materials at a later stage. This has a negative impact on the maximum production rate and sustainability. Such reprocessing is also both tedious and costly with an approximate economic impact of 10 €/t for the handling of segregated material. The proportion of segregated product to total production is usually limited to a few percent or less depending on the product and production sequence, but losses up to 50 % occur in extreme cases, i.e., for short production run sizes. This means that many tons of segregated material must be taken care of on a daily basis because several hundred tons of final products are produced during one day. Overall, the total annual cost for re-processing of segregated material at Saint-Gobain Weber's production facilities is roughly estimated at €1M, because approximately 100 kt of final products must be re-processed each year. The problem is magnified at plants with wide product mixes (over one hundred different products can be produced at a single plant) as product silos must nearly always be completely emptied at changes in the production sequence for a packing line. Silos dedicated to specific products comprise the only exception and, indeed, the fill level is usually kept high in these silos in cases of strong segregation. So-called lean manufacturing principles are currently being introduced at the company's production plants. This calls for shorter production run sizes, which may lead to considerable production losses unless segregation can be minimized. Moreover, segregated products could in theory be delivered to customers by mistake, the consequences of which are, by far, the most serious outcome of segregation.

It seems fairly evident that segregation of the final products occurs in product silos because of the wide particle size distributions for these bulk solids and the conditions they are exposed to. Focusing on this part of the production process in order to suppress the detrimental effects of segregation is justified by the vicinity of end use for the products. Any measures employed for reducing segregation earlier in the process could be nullified at this stage and limited possibilities exist for correcting segregation once the products have left the plant. In summary, product silos constitute the most critical unit operation with respect to segregation in industrial production of construction materials.

2. Segregation mechanisms

Segregation can be described as the opposite of mixing. For an initially well mixed particulate solid, segregation induces partial - or sometimes nearly total - separation of the components. In principle, segregation can occur at any stage of industrial production and can be very difficult – if not impossible – to avoid. Adverse effects of segregation include reduced blend quality and flow problems in bulk solids handling equipment. According to Bates [1], segregation can occur because of differences in particle size, density, shape, surface texture, electrostatic charge, micromechanical properties, molecular surface effects, etc. Although segregation has been reported by many researchers [1,6-47], several features of this phenomenon are still not well understood.

Segregation mechanisms are often used for explaining why and how particulate solids segregate under specific circumstances, and what the outcome in terms of the spatial or temporal distribution of the constituents of a mixture will be. A total of thirteen segregation mechanisms have been identified: trajectory, rolling, displacement, percolation, sieving, air current, fluidization, agglomeration, concentration-driven displacement, push-away, impact/bouncing, embedding and angle of repose, as summarized by Tang and Puri [6]. Alternative terms are sometimes used, such as impact fluidization for fluidization of bulk solids at abrupt changes in their flow direction [1] as opposed to mixing of bulk solids with a gaseous phase during free fall or pneumatic conveying. Attempts to condense segregation mechanisms into a smaller number of primary mechanisms responsible for most particle segregation problems have also been made [6,13]. The occurrence and significance of each segregation mechanism are case-specific and depend on the properties of the bulk solid and its fractions, the handling conditions and requirements set on the homogeneity of the material composition. Therefore, it is impossible to define universal guidelines regarding the importance and magnitude of each mechanism.

The process of resolving a segregation problem in industrial settings usually starts with two tasks. Firstly, a complete picture of segregation in the entire production process should be obtained and the most critical unit operations be determined. This was elaborated at the end of the previous section for production of dry mineral-based construction materials. Secondly, the relevant segregation mechanisms for the critical unit operation(s) must be identified. In the context of the present thesis, this was performed via experiments in silos of different size

ranging from small to production scale; the results will be elucidated in forthcoming sections (section 5 and 6). Once these two steps have been completed, but rarely before that, it is possible to proceed with the implementation of countermeasures, e.g., technical solutions, against segregation. Even though several segregation mechanisms have been identified, establishing the relevant mechanisms for a specific unit operation is not a trivial task. Segregation often conflicts with intuition and many segregation mechanisms can affect a bulk solid simultaneously during a single unit operation or flow regime, i.e., segregation mechanisms rarely occur independently. This is, in particular, true for industrial handling of (dry mineral-based) construction materials in silos, where information about segregation is not available in the public domain. One truly relevant reference can be found in [38], where segregation of a multi-phase plaster (construction material) at discharge from a production scale silo is considered and different technical approaches to reduce the segregation are compared. The difficulty in applying the results of others arises from the fact that segregation depends strongly on material properties and construction materials or mixtures resembling these have rarely been investigated to date.

Segregation mechanisms relevant for the current work are sifting, rolling, embedding, fluidization and air current, and these will be briefly presented below. All of these mechanisms can occur at pouring of bulk solids onto heaps such as at filling of silos. The former two have also been reported to occur at silo discharge for free flowing materials, i.e., bulk solids characterized by a lack of significant inter-particle forces, while the latter three often require considerable free fall distances or pneumatic filling of silos. The salient feature of the aforementioned segregation mechanisms in the context of the current work is the material distribution induced at silo filling. Fine particles are accumulated at the filling point as a result of sifting and rolling whereas the opposite, i.e., concentration of fine and light particles away from the filling point, is encountered when segregation occurs because of embedding, fluidization and air current mechanisms. Different aspects of sifting and rolling have been elaborated more deeply in the open literature compared to embedding, fluidization and air current segregation. Thus, the latter three are not that well understood.

The purpose of the forthcoming description of segregation mechanisms is to familiarize the reader with the mechanisms of interest here and to provide an understanding of the overall segregation patterns or material distributions resulting from these. Furthermore, the discussion is largely restricted to circumstances commonly prevailing in silos. The reader is referred to

work cited in this section for more detailed discussions of different aspects of segregation mechanisms, such as their underlying phenomena and circumstances required for these to occur in different handling operations or flow regimes. It shall be mentioned that the references included here constitute merely a subset of information on segregation available in the public domain.

2.1. Sifting

Sifting is one of the most frequently encountered and reported segregation mechanisms. It is characterized by the entrainment and flow of small particles in the interstices of a matrix of coarse particles [1,6-19,22,23,26,27]. Sifting is often referred to as sieving and is similar to another segregation mechanism called percolation. The major difference between sifting/sieving and percolation is that the former is usually associated with dynamic conditions, such as surface flows, while the latter is related to more static conditions, i.e., to systems of particles mainly at rest. Sifting segregation can occur with bulk solids consisting of different sized particles at filling onto heaps and results in a surplus of fine particles at the filling point (horizontal or side-to-side segregation) [7,9-11,17,19], such as at the apex of a heap. Figure 3a gives a schematic illustration of this mechanism that often occurs simultaneously with rolling (see next subsection). Sifting segregation can also be active at silo discharge, especially in silos emptying in funnel flow (different discharge flow patterns in silos are elaborated below)

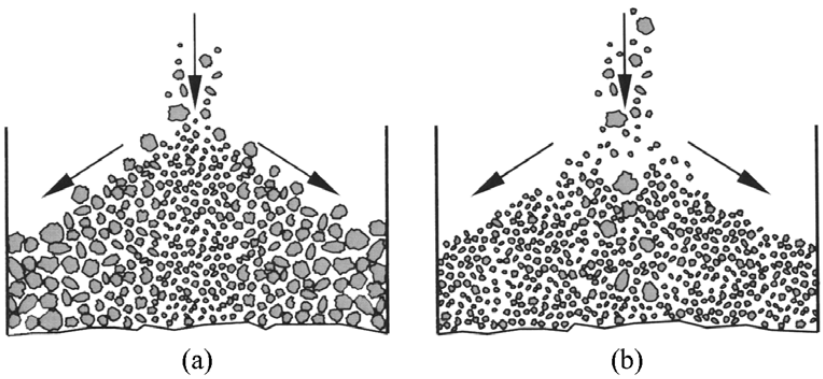

Figure 3. Schematic illustration of (a) sifting and rolling, and (b) embedding segregation (taken from [9] with permission).

but also towards the end of emptying in mass flow mode, and in other applications of particulate solid flow, e.g., in chutes, where separate regions of the solid phase move at different velocities. Carson et al. [13] defined the conditions needed for sifting segregation to occur: a difference in particle size between the individual components, sufficiently large mean particle diameter, free flowing material and inter-particle motion. Results of the current work suggest that not all components of a mixture of different bulk solids have to be free flowing for this mechanism to be active at silo filling.

2.2. Rolling

Segregation caused by rolling of large or spherical particles away from the filling point at heap formation has been well documented by other investigators [1,6-11,16,17,19,22,23,34-37]. Rolling segregation often occurs in combination with sifting. The occurrence of rolling is attributed to a higher possibility of small/non-spherical particles to be trapped in irregularities on the surface of an arrangement of particulate solids. In comparison, larger/spherical particles are not captured as easily and these are able to continue rolling for greater distances. Rolling induces a similar horizontal or side-to-side segregation pattern as sifting at filling of bulk solids onto heaps: accumulation of fine/irregularly shaped particles at the filling point and collection of large/spherical particles at the base of the heap (cf. Figure 3a). To some extent, rolling may also occur at silo discharge and in other flow regimes or processes where significant velocity gradients occur within a moving bulk solid.

2.3. Embedding

Embedding is an inertia-based segregation mechanism and refers to a process where large or dense particles penetrate the upper surface layers of a deposited particulate solid and become locked in this position. This mechanism, illustrated schematically in Figure 3b, can occur at charging of particulate solids onto heaps and causes a surplus of large/dense particles to collect at the point of impact, i.e., heap apex, with smaller or lighter particles found farther away. Hence, the (side-to-side) segregation pattern resulting from embedding is the complete opposite of the material distribution following from sifting and rolling. Even though segregation caused by the embedding mechanism has been reported earlier [1,6-11,16,17,24, 33,38,39], it

is not as well documented as some of the other mechanisms. Some authors simply refer to "density segregation" in situations where this type of segregation pattern occurs for bulk solids consisting of particles of different density [24,39].

In cases of segregation by particle size or solid density, the material distribution may also be determined by so called push-away effects. This means that large/dense particles set small/light particles in motion towards peripheral areas upon impact of additional material onto the surface of previously deposited particles. Indeed, this type of segregation (on the basis of particle size or solid density) has been defined by some investigators as a separate segregation mechanism known as push-away [7,10]. Presumably, push-away segregation is more likely to occur for particulate systems consisting of larger mean particle sizes, whereas little or no rearrangement of deposited fine/light particles occurs for bulk solids of smaller size. The present author believes that embedding of large particles (in the absence of significant push-away effects) is one of the main mechanisms, together with fluidization and air current effects, responsible for segregation of (dry mineral-based) construction materials at silo filling. Evidence of the importance of embedding segregation was, indeed, obtained in the course of this thesis work and, although not explicitly stated, this mechanism was presumably also partly responsible for the segregation reported by Kwade and Ziebell [38].

2.4. Fluidization

Fluidization refers to mixing and dispersion of a particulate solid by a gaseous phase such as air. Segregation caused by fluidization of bulk solid mixtures has been reported to induce vertical segregation with accumulation of fine or light components to the uppermost layers of a particulate bed at pneumatic or filling of silos with free fall [1,6-10,13-15]. This type of vertical segregation has also been investigated with special testers built for the purpose, where the bulk solid is filled into a vertically aligned pipe or tube and subjected to an air flow from below. A surplus of fine/light particles should be found in the upper parts of the powder column after the air flow has continued for some time when a bulk solid is susceptible to fluidization segregation [14,40]. Some researchers believe that fluidization is also induced by abrupt changes in the flow direction of a particulate solid, such as at impact of the input stream with a heap of previously deposited material at silo filling, and hence the alternative definition of impact fluidization may also be used [1]. In such situations, fluidization induces a different

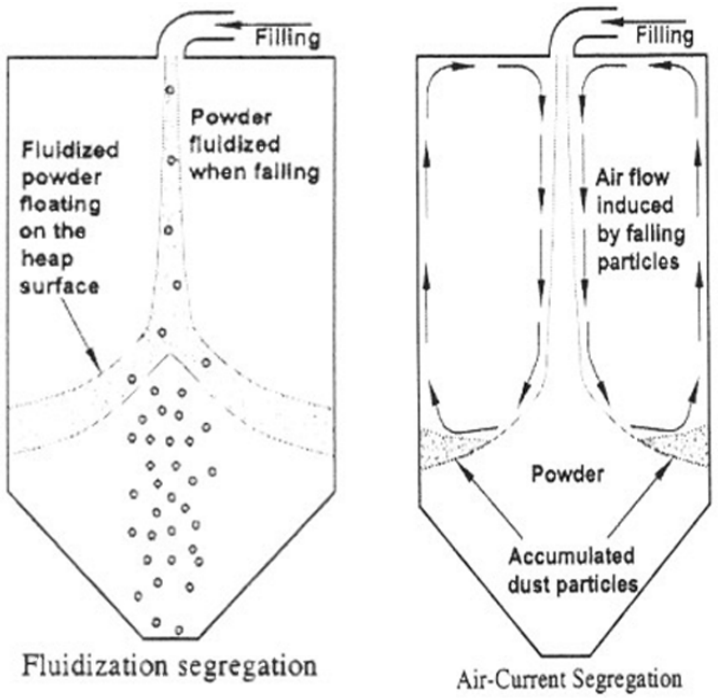

Figure 4. Schematic illustration of fluidization and air current segregation (taken from [10] with permission).

segregation pattern with accumulation of coarse/dense particles at the point of impact and small/light particles further away, as illustrated in Figure 4 (left subfigure). Clear evidence of fluidization leading to horizontal (or side-to-side) segregation with accumulation of fine/light particles away from the filling point was obtained in the context of this thesis. This phenomenon was shortly discussed by Mosby [7] and reported by Kwade and Ziebell [38], who did not explicitly state the mechanisms responsible for segregation encountered in their experiments, but the investigation was further elaborated in [9]. Segregation caused by fluidization has not been deeply investigated or reported by others, but the current work shows that it is a one of the primary segregation mechanisms (together with embedding and air current segregation) responsible for segregation of construction materials in silos.

2.5. Air current

Air-current segregation is enforced by entrainment of small, light or very non-spherical particles in gas (air) streams induced by a rapidly moving (falling) solid phase, transportation of these particles with the air flow and concentration of the entrained particles to specific positions, e.g., to silo walls, as a result of settlement caused by changes in the velocity and/or direction of the air flow [1,6-10,13,14,32,38,41-43]. Figure 4 (right subfigure) shows a schematic of the material distribution resulting from air current segregation at centric filling of silos. To the best of the present author's knowledge, previously reported work on air current segregation has been limited to free flowing materials, i.e., bulk solids characterized by the absence of significant inter-particle forces. The effect of this mechanism on segregation of cohesive bulk solids is, therefore, not entirely clear. However, evidence of the importance of air current effects was obtained in the context of this thesis and the author reckons that also this mechanism is at least partly responsible for segregation of construction materials in silos. Presumably, air currents of some magnitude are required for this mechanism to be activated and such conditions are more likely to prevail in larger silos, e.g., in the 20 m^3 and 70 m^3 silos in this work.

3. Discharge flow patterns in silos

Segregation of particulate solids in silos cannot be discussed without reference to the discharge flow pattern that designates the order of withdrawal of the contents of a silo. Segregation may be induced at silo filling, but the discharge flow pattern also affects the segregation observed at silo emptying, which is of primary interest in the majority of cases. Two main types of discharge flow patterns have been identified: mass flow and funnel flow. The latter is sometimes referred to as non-mass flow to accommodate for different forms of funnel flow discharge [1], but the terms mass flow and funnel flow will be used here. Much of the previous and current research in the field of silo flow is aimed at converting the flow pattern from funnel to mass flow, and some interesting findings in this area are discussed below. Determining the discharge flow pattern in an existing silo is not a trivial task. However, tracer or marker objects have been utilized with success. In some of the experiments in this thesis work, tracer objects were seeded into the deposited powder bed at silo filling and their order of discharge was monitored at silo emptying. Issues related to determination of discharge flow patterns with tracers are covered in the last subsection.

3.1. Mass flow

Mass flow is characterized by the movement of the entire silo contents whenever emptying occurs; Figure 5a gives a schematic illustration of this. Mass flow discharge can be achieved with steep and low friction hopper walls. Furthermore, arching, i.e., obstruction of the flow, above the silo outlet should not occur and material must be withdrawn from across the entire outlet area. The feature distinguishing mass flow from funnel flow is that no stagnant regions exist in the former whereas the presence of dead material regions is the unifying characteristic for all funnel flow silos. The discharge pattern of mass flow is sometimes referred to as “first-in-first-out”, even though this definition is not entirely correct as was pointed out by Bates [1]. The reason for Bates’ postulation lies in the velocity gradients present towards the end of complete emptying in mass flow silos. The implications of this with respect to segregation are discussed below. Mass flow is usually associated with little or no segregation because material from different radial positions is mixed at the outlet. Therefore, any horizontal or side-to-side segregation induced during filling is corrected for during emptying.

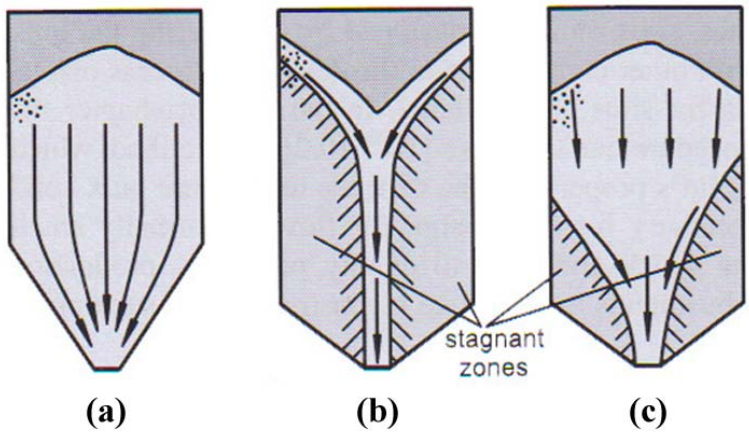

Figure 5. Illustration of different discharge flow patterns in silos: mass flow (a) and funnel flow (b and c) (taken from [9] with permission).

However, experimental results obtained in this work suggest that this is not always the case – a finding that can be attributed to the aforementioned velocity gradients. Moreover, mass flow discharge of the silo contents should be avoided when the bulk solids have been segregated in a top-to-bottom, vertical pattern (usually with accumulation of fine particles in the topmost layers) during filling. This form of segregation is not corrected for during emptying and can, in fact, remain at discharge in mass flow [9,32,47].

Criteria for the design of mass flow silos were developed by Jenike [48]. His pioneering work in the mid 1960's led to procedures that are still employed today for determining hopper angles necessary for developing slip against the container walls, and outlet sizes required for avoiding arching above the silo outlet. In the theory developed by Jenike, the critical hopper angle for mass flow is determined on the basis of measurements of the frictional properties of the bulk solids subjected to storage in a silo. In practice, this is accomplished by shear cell testers. Jenike developed a device known as the Jenike shear cell tester, which enables the characteristics of the bulk solids (internal friction and bulk density) as well as the friction between particulate solids and different wall materials to be determined. With this device it is possible to determine the instantaneous material properties as well as the effects of time consolidation, i.e., a possible increase of the bulk material strength during storage at rest. Design of silos for mass flow then proceeds with the use of design charts for different hopper geometries.

The shear cell tester developed by Jenike is not free of problems. Utilization of this device requires some experience from the operator for the results to be reliable and the analysis is also rather time consuming. Recently, automated shear cell testers have been developed to facilitate the determination of material properties and overcome the difficulties associated with shear cell testers of Jenike type [49]. A detailed elaboration of the Jenike theory is outside the scope of this dissertation and the reader is referred to Jenike's work [48] or other sources available in the open literature (for example [9]) for a more comprehensive presentation of the principles for mass flow design of silos. In this work, shear cell testing and the Jenike theory was employed for determining the critical hopper angles for mass flow and critical outlet sizes for unobstructed gravity flow from silos.

As outlined above, mass flow silos are often associated with reduced or negligible segregation. Even though this flow pattern encompasses other advantageous features, it also suffers from certain drawbacks as indicated in Table 1. One of the most significant disadvantages of mass flow is that rather steep hopper angles may be required for developing slip along the container walls. This has important (economic) consequences: a steep hopper section increases the required headroom, which can be impractical and usually increases the installation (and running) costs. The benefits of mass flow must, therefore, be weighed against the drawbacks (see Table 1) in order to reach an optimal design eventually decided on economic grounds in industrial settings. As far as segregation is concerned, it must be sufficiently reduced so that the increased installation costs for mass flow designs can be motivated.

Table 1. Benefits and drawbacks of mass flow according to Bates [1].

Benefits	Drawbacks
- Avoids indefinite storage time	- Holds less or takes more headroom
- Material flow through smaller outlets	- Higher stresses on hip and walls
- Re-mixes contents on discharge	- Wall wear with abrasive products
- Reduces prospect of 'flushing'	- Features offered may not be needed
- Predictable storage time & performance	- Outlet must not be partially restricted

One aspect of mass flow affecting segregation is the aforementioned velocity gradients that occur during the later stages of complete silo discharge. When the material level drops to below approximately 0.5-1 times the silo diameter from above the transition from hopper to vertical section, the discharging rate will be higher above the outlet compared to more peripheral regions [1,9,32]. For free flowing particulate mixtures, sifting segregation may occur as a result of these velocity gradients. For cohesive powders, side-to-side segregation induced during filling at the material levels that discharge last may not be entirely corrected for by mass flow. Thus, re-mixing from different radial sections does not necessarily occur towards the end of complete emptying. Evidence of this was obtained in the small scale experiments performed in the context of this thesis work (see section 7.3). The presence of velocity gradients towards the end of complete emptying from mass flow silos is the reason for Bates' [1] statement regarding the impreciseness of the definition "first-in-first-out" for this flow pattern.

3.2. Funnel flow

Funnel flow is characterized by the presence of stagnant regions in the silo during discharge. Different forms of this discharge flow pattern exist. The flow can, for instance, be restricted to a narrow pipe extending from the outlet upwards to the material surface and to the surface layers (Figure 5b) or the flow channel can be enlarged from the outlet and reach the silo walls at a level below the surface of the bulk solid (Figure 5c). The latter possibility makes it difficult to differentiate funnel flow from mass flow by virtue of visual inspection from the silo top. Bates [1] suggested the term non-mass flow be used whenever the discharge flow pattern is not mass flow and this definition, therefore, includes various forms of funnel flow. Nonetheless, the definition of funnel flow will be used in the current work, because it is considered more established. Funnel flow is sometimes claimed to induce "first-in-last-out" withdrawal of the silo contents in order to differentiate it from mass flow, but this is clearly an oversimplification. Compared to mass flow, funnel flow is usually associated with more severe segregation and other flow problems, such as erratic flow caused by rat-holing and subsequent flooding of fine powders when these rat-holes collapse [9]. With free flowing particulate matter, the silo contents may segregate during funnel flow discharge because of sifting segregation caused by separate regions of the bulk solid moving at different velocities [1,6,9,13,32,47]. With cohesive bulk solids, side-to-side segregation induced during filling is

not corrected for because bulk material located in different radial positions at identical vertical levels are not mixed at the outlet.

A special type of discharge flow pattern known as expanded flow (cf. Figure 6) occurs in silos where the hopper angle changes over its height. The central part of the hopper section induces mass flow while the outer (upper) hopper walls are not steep or smooth enough to develop slip of the bulk solid along the wall surface. Flow is restricted to a cross-sectional region determined by the size of the hopper at the point where the hopper angle changes and to the surface layers of the bed, or the flow channel may expand and reach the silo walls at a level below the surface of the bed. Either way, material initially deposited next to the walls of the upper hopper section and lower parts of the vertical section is discharged last at complete emptying of the silo. This has important consequences for segregation at discharge. When the material that withdraws last has been segregated in a horizontal (side-to-side) pattern during filling, considerable segregation can be expected towards the end of complete emptying simply because the silo then contains only segregated material and mixing can no longer occur. In experiments performed at a construction material producing plant, the investigated silo most likely emptied in expanded flow and significant segregation was observed at the end of the discharging process (see section 5.1).

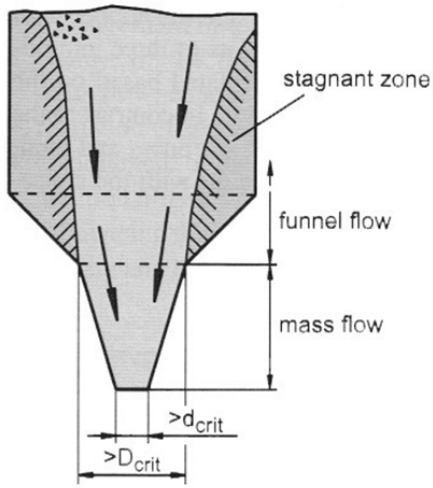

Figure 6. Illustration of silo discharging in expanded flow (taken from [9] with permission). "d_{crit}" denotes the critical outlet size for unobstructed gravity flow and "D_{crit}" expresses the minimum size of the flow channel for avoiding rat-holes.

3.3. Conversion from funnel flow to mass flow

Several solutions have been proposed for achieving mass flow in silos with shallower hopper angles than those given by the Jenike theory. In the majority of cases, this is accomplished with the installation of an insert - a kind of flow obstruction - in the lower part of the silo. Examples of such include inverted cones, double cones, cone-in-cones and the Binsert system (trademark of Jenike & Johanson, Inc.) [50-53]. These solutions reduce the requirement of headroom, but it is not a trivial task to design the inserts correctly to give mass flow.

An interesting type of flow-affecting device that should also be mentioned in this context is fluidization plates. These are normally installed in the silo's hopper section and consist of perforated plates that enable a gaseous medium (air) to pass into the silo while being impermeable to the particulate matter stored in the silo. Gas is introduced to the fluidization plates at low static pressures: 0.5-0.9 bar are typical values for the overpressure of dried air that is supplied to fluidization plates used in silos at construction material producing plants. The gas mixes with the particulate phase in the silo and exits the silo via the dust extraction device at the silo top or the silo outlet at discharge of bulk solids.

The influence of the aforementioned type of fluidization on the behavior of bulk solids in silos is not entirely clear. Some investigators have reported that introducing low pressure air slightly above the point where the area confined by the hopper walls equals the critical outlet size (as determined by shear cell testing of the powder and the Jenike theory) weakens any stable arches that may form in silos with outlets smaller than the critical value. Therefore, fluidization plates enable flow through smaller orifices [54-57]. Some practical experience supports this (for storage of dry mineral-based construction materials): reliable flow is obtained when the fluidization plates are installed slightly above the silo outlet [58]. On the other hand, fluidization plates have also been used to alter the discharge flow pattern from funnel flow to mass flow. In such cases, the best results are obtained when the fluidization plates are installed in the upper parts of the hopper section, as close as possible to the transition from hopper to vertical section [54]. One manufacturer of fluidization plates claims that, when used correctly, these should reduce friction by fluidizing a thin particulate layer adjacent to the silo walls when discharge from the silo occurs and should fluidize or aerate bulk solids in the entire hopper section when discharge does not occur [59]. Fluidization or aeration is normally associated with expansion of the particulate phase and observation of this phenomenon has been

confirmed on several occasions by visual inspection from silo roofs: The powder surface rises significantly from the level attained after periods of rest when air is supplied to the fluidization plates but no discharge of bulk material from the silo occurs [58]. Studies on the operation and process engineering of large aerated silos (with diameters between 10 m and 50 m) used for storage of fine grained bulk solids point in the same direction [60]. Apparently, a bed of bulk solids may be only partly fluidized or aerated, i.e., complete fluidization or aeration of the powder bed does not always occur and it may, therefore, not be observed on the bed surface.

Application of fluidization as a discharge aid or as a means of converting the discharge flow pattern from funnel flow to mass flow is not a trivial task. The outcome is governed by the complex behavior of multi-phase systems, which is influenced not only by features related to the gaseous phase, such as the gaseous medium and pressures used, but also by the characteristics of the particulate phase (particle size and size distribution, particle solid density, particle shape, surface properties, etc). It is clear that more work is needed in this challenging field in order to exploit fluidization plates to their fullest potential.

3.4. Determination of flow patterns

On the basis of discussions in this and the preceding sections, it is evident that knowledge of discharge flow patterns in silos is essential in the context of this thesis because of the significant effect on segregation at silo discharge. Determining the discharge flow pattern is not a trivial task; the patterns of flow in discharging silos can be very complex and, for example, visual inspection from the silo top seldom gives an accurate or useful description. This is true especially for large silos in industrial settings, where the possibilities to perform experimental investigations are normally limited. However, tracer objects have been successfully utilized for determining discharge flow patterns in silos [61-64]. Such investigations usually comprise the placement of tracer objects in specific positions of the deposited particulate bed at silo filling and determining their order of exit during discharge. Prerequisites for obtaining useful results include identification of individual tracer objects, ensuring that the tracers retain their initial positioning before discharge is commenced, and separation of the tracers from the output stream. One further aspect requiring consideration is the presentation of the results.

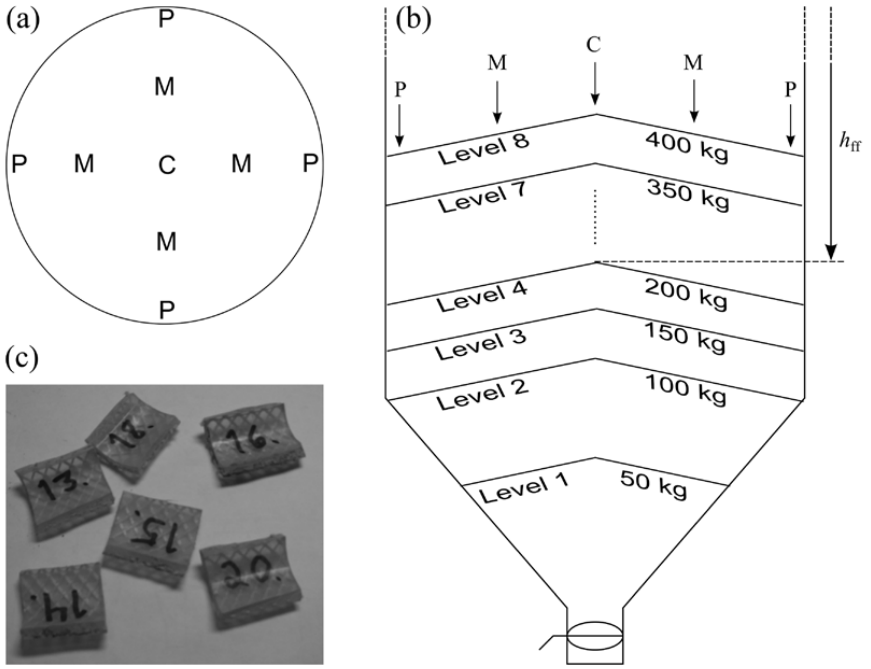

Figure 7. (a) Top view of the positions for tracer objects in small scale experiments. (b) Side view of tracer positioning together with material masses for and numbering of the fill levels used for seeding of the powder mixture with tracers. (c) Image of numbered pieces of garden hose (20 x 20 mm^2) used as tracer objects.

Tracer objects were utilized in a majority of the small scale experiments included in this thesis work for determining the flow pattern at silo discharge. The results for sampling, i.e., segregation, in these experiments are presented in forthcoming sections (chapters 5.3, 6 and 7), but an overview of the procedures used and results that can be obtained with tracers is given here. Figure 7a and b depict the vertical and horizontal positions for placement of tracer objects at silo filling. One marker was placed in each of the positions denoted by the letters C, M and P (position M was sometimes omitted). Numbered pieces of garden hose (Figure 7c) were used as tracer objects and these were later separated from the discharge stream with a wire mesh placed on top of the discharge bin situated underneath the silo outlet.

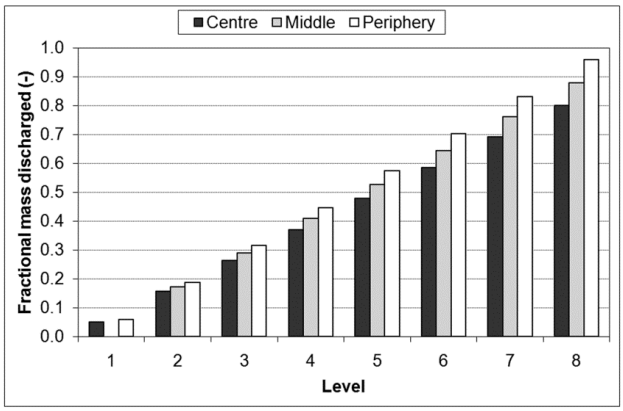

(a)

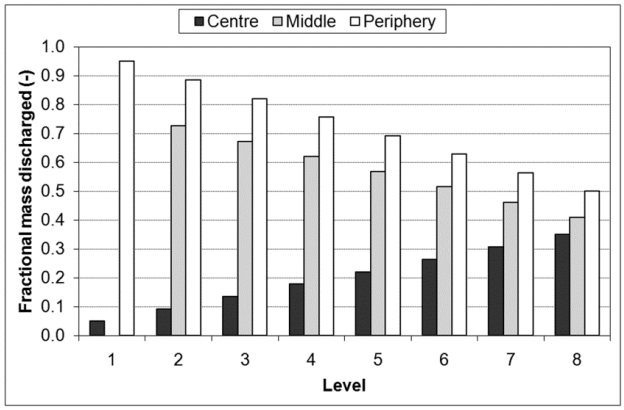

(b)

Figure 8. Illustration of the exit order for tracer objects in imaginative experiments with (a) mass flow and (b) funnel flow discharge of the silo contents. Fractional mass discharged = $m_i/m_{tot,exp}$, where m_i denotes the mass of bulk solids discharged from the silo at exit of tracer i and $m_{tot,exp}$ expresses the total mass of powder mixture used in the experiment.

Figure 8 illustrates the results for imaginative experiments with mass flow (subfigure a) and funnel flow (subfigure b) discharge of the silo contents. In this figure, the result for each tracer (m_i = mass of powder mixture discharged from silo at exit of tracer i) has been normalized against the total mass of powder ($m_{tot,exp}$) included in the experiment. Here, discharge is completely symmetric meaning that tracers seeded in identical radial positions (M or P) at the same level of fill discharge at exactly the same moment. In mass flow, the exit order for the tracers broadly follows a "first-in-first-out" pattern, i.e., tracers are withdrawn from the silo almost in the same order as they were seeded into the powder bed (starting from Level 1 and

ending with Level 8). In funnel flow, tracers associated with the same fill level exit in the order center (C), middle (M) and periphery (P). Moreover, material (tracers) from the vicinity of the silo walls (position P) at the lower levels (Levels 1-3) discharges last, which is a typical feature of funnel flow. On the basis of results presented in Figure 8b, it is clear that describing funnel flow discharge patterns as “first-in-last-out” is misleading. It should be stressed that results shown in Figure 8 represent ideal cases and deviations from these can be expected in actual experiments (see section 6). However, the difference in the overall trend for the exit order of tracer objects in silos discharging in mass flow and funnel flow, respectively, is self-evident.

4. Objectives of this work

The objectives of this thesis work were not defined in great detail at the start of the project. However, these were specified in more detail during the early stages of this study and will be briefly presented here. The remaining sections of this dissertation mainly follow the outline given below.

The first objective was to determine the critical process unit(s) with respect to segregation in the production process of dry mineral-based construction materials. Silos situated downstream of mixing and upstream of packing were identified as the most critical unit(s) for reasons elaborated in the introduction of this dissertation. Secondly, the most relevant segregation mechanisms for the handling of commercial products in silos had to be identified. This was partly discussed in the second section of this thesis and will be further elaborated in the next two sections (section 5 and 6). Thirdly, the effects of silo scale had to be determined in order to ascertain that the segregation occurring for commercial products in relatively large silos could be studied with specific mixtures in smaller silos (see section 5). Performing experiments in smaller scale is advantageous because the experimental conditions can be controlled better, it is easier to perform measurements and the work load is reduced. A fourth objective was to throw light on the effects of material properties, process conditions and silo parameters on segregation. This problem was tackled mainly through experiments in small scale with two- and three-component powder mixtures. The results of these investigations will be presented in section 7. Quantification of the effects of the aforementioned features was defined as the fifth objective of this work (see section 8). Lastly, segregation data for a longer time period were to be collected for a production plant and analyzed in order to see whether the knowledge obtained from all previous efforts could be applied in industrial practice. The results of this study are presented in section 9.

5. Investigation of the effects of silo size

Experiments were performed in silos of different size for studying the scale effects on segregation. The main objective was to clarify the possibilities of investigating the segregation of commercial construction products in large silos (with volumes of 50-100 m^3) through tests with two- or three-component mixtures in much smaller silos (< 1 m^3). Reducing the scale facilitates the performing of experiments at reduced costs, enables better control of the experimental conditions and enhances the possibilities for carrying out measurements. However, the effects of scale should be determined in order to ensure that results for small scale experiments have practical meaning, i.e., that the findings are not limited to the reduced scale but are more general and that the conclusions drawn on the basis of these apply to real industrial cases. A second objective of the work presented in this section was to identify the dominating segregation mechanisms for dry mineral-based construction materials handled in silos. This topic is partly covered here and the discussion will continue in the following section (chapter 6). Results to be presented in the forthcoming subsections were reported in Paper I and Paper II of this thesis work and the reader should turn to these articles for more details.

In all large and intermediate scale experiments, rather large samples (up to a few kilograms) were collected and these were reduced without the use of sample splitters to approximately 100 g for determining the size distribution. The size distribution for all samples was determined with a set consisting of 0.063 mm, 0.125 mm, 0.25 mm, 0.5 mm, 1.0 mm, 2.0 mm and 4.0 mm sieves, because the quality requirement limits for commercial products are defined for these size fractions. The mass fractions of small particles, i.e., the fraction less than 0.063 mm and, in particular, the cumulative undersize for 0.125 mm are used for presentation of the results. This is because segregated products are most often - if not nearly always - rejected because the quality requirement limits are exceeded for these size fractions.

5.1. Large scale

In the large scale experiments, the segregation of four commercial products (L1-L4) in a product silo at a production plant was studied. Figure 9a depicts the particle size distributions for the products that represent the arithmetic mean values for all samples collected at discharge of the silo. The exact compositions for the products cannot be given here because of

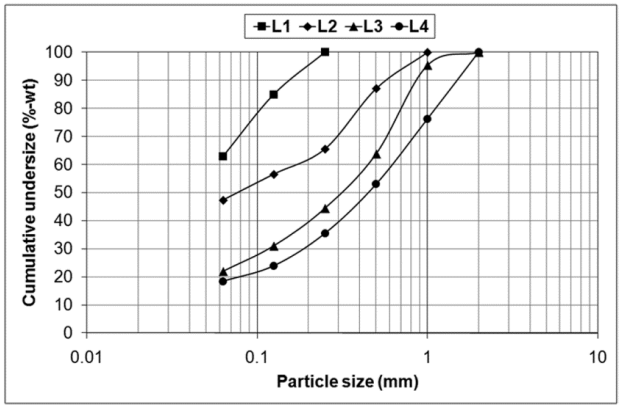

(a)

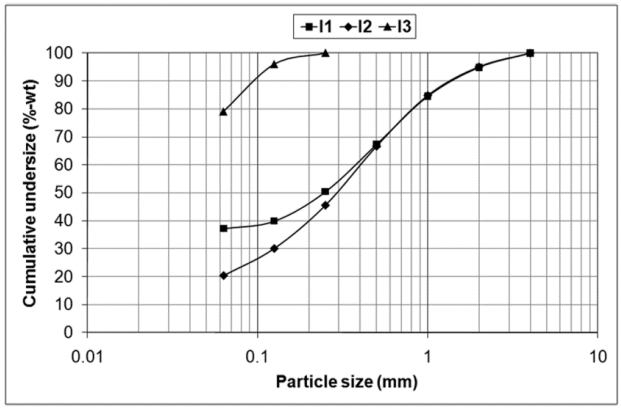

(b)

Figure 9. Particle size distributions (determined by sieving) for the commercial products included in the (a) large and (b) intermediate scale experiments.

confidentiality, but their general features were described in section 1.1. The coarse components (particle sizes > 125 μm) of all products consist mainly of different sand and limestone fractions, whereas cement comprises the greater part of the fine particles and some products also include fine limestone fractions. Moreover, product L2 includes a small amount (0.4 %-wt) of synthetic fibers. The flow properties for the products were determined with a shear cell, and silo design criteria for unobstructed mass flow were determined with the theory of Jenike [48]. Critical values for the hopper angles and outlet sizes required for mass flow in a silo made of stainless steel can be found in Paper I. The main conclusion of this analysis was that

it is unlikely that mass flow of the entire contents would occur for any of the products in the production silo under consideration here.

A schematic drawing of the 70 m^3 silo used in the large scale experiments is shown in Figure 10. The silo was built from standard steel and consists of a cylindrical vertical section with an expanded type hopper part (hopper angle varies over its height). Ideally, such silos are manufactured to give mass flow in the lower part and funnel flow in the upper part of the hopper section. The entire hopper section, i.e., upper and lower part, is almost completely covered with fluidization plates. On the basis of silo design values for stainless steel, funnel flow should occur with all products in the upper part of the hopper section whereas mass flow should be induced with the products L2-L4 and funnel flow with L1 in the lower hopper section. Even though design values for mass flow were not determined for standard steel and the influence of the fluidization plates is not entirely understood, it is reasonable to assume that the silo discharged in expanded flow (cf. Figure 6) in all experiments. Evidence of this was

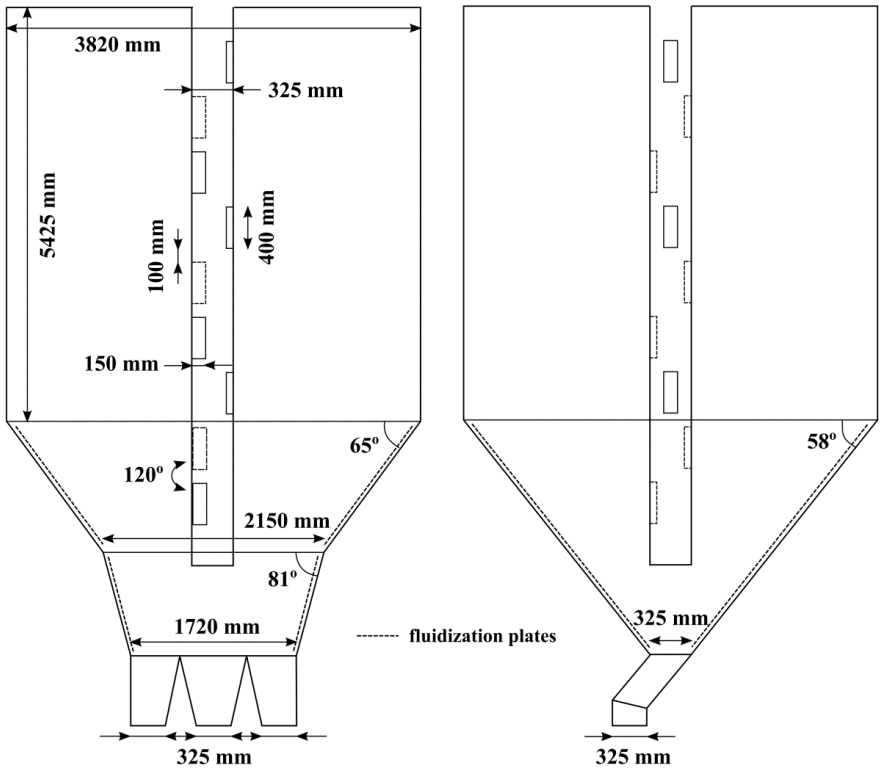

Figure 10. Large silo with view from two perpendicular planes.

obtained by visual inspection of the powder bed: material from the vicinity of the upper hopper walls discharged last. A hammer (not shown in Figure 10) is installed in the hopper section and is used during the later stages of discharge for complete emptying of the contents, which suggests that the residual material is cohesive.

During normal production conditions, raw materials are mixed in batches of three tons and are filled into the silo through the circular filling tube with an approximate rate of 27 kg/s. Filling is disrupted for a short period (10-20 s) between two subsequent batches. Material is discharge through the separate outlets into bag filling spouts at an overall rate of 7 kg/s and packed into 25 kg bags. The bag fillers operate concurrently, but each spout is closed intermittently when the bag is changed. The silo is filled and discharged concurrently. However, periods where the silo is discharged, but not filled, regularly occur because the filling rate exceeds the discharge rate. In the experiment with product L3, filling was completed before discharge started, but the other experiments were conducted during normal production conditions. In all experiments, product bags filled through the middle outlet were collected from a conveyor belt situated downstream of the bagging machine with regular intervals throughout the discharging process. A smaller sample (500-1000 g) was retrieved from each sample bag and even smaller masses (100 g) were sieved for determining the size distribution. The total masses of products discharged from the silo in the experiments varied in the range 30-108 t.

The results for the large scale experiments are shown in Figures 11 (two separate figures), where the fines content and the mass of material left in the silo are depicted versus the mass discharged from the silo. All products show a similar segregation pattern, i.e. the mass fraction of fine particles was relatively constant during most of the discharge but increased at the end of complete emptying. Segregation was clearly demonstrated by increasing amounts of the smallest particles (fraction below 0.063 mm) in all experiments. The trends for the mass fraction below 0.063 mm and the cumulative undersize of 0.125 mm were nearly identical with the exception of the experiment with L1 (subfigure 11a), where the increase at the end of emptying was somewhat steeper for the fraction below 0.063 mm. It is difficult to objectively quantify the mass of segregated material, but in practical cases this is decided by the quality requirement limits. In these experiments, roughly the last five to ten tons were segregated for L1 (subfigure 11a) whereas only the last one or two tons contained too much fines for L4 (subfigure 11d). It will be mentioned that the fines content for L2 (subfigure 11b) showed a

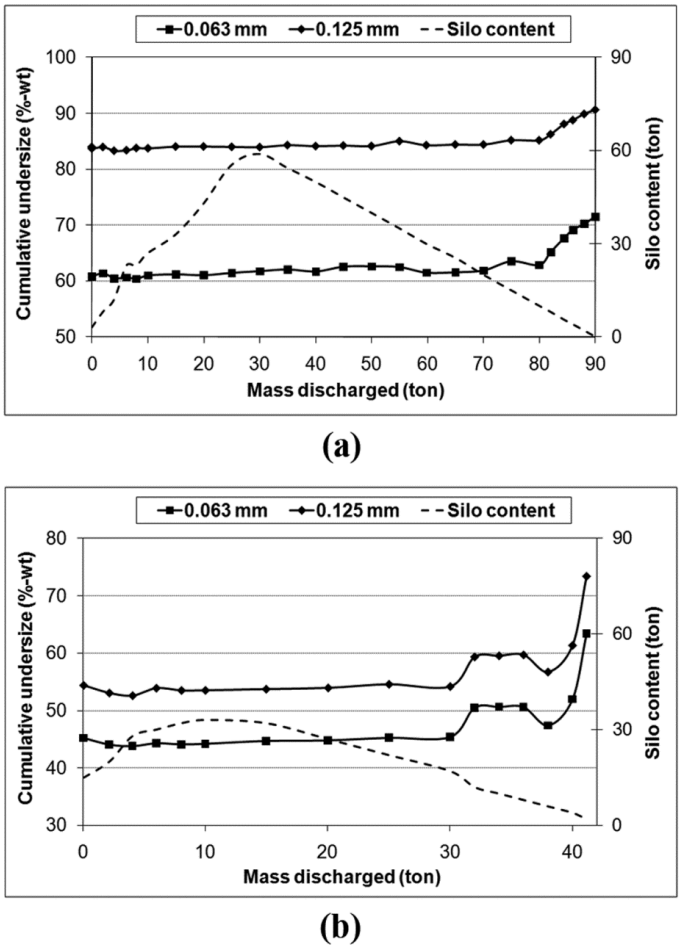

Figure 11. Results for the large scale experiments: (a) L1 and (b) L2.

peculiar evolution by increasing slightly before the end of discharge only to decrease to a more normal level before increasing once again when the silo was completely emptied. From a more academic point of view, both the amount of segregated material and the degree to which a material segregates, i.e., the actual fines content for the last samples collected at discharge, should be considered when the segregation behavior of different bulk solids is compared. However, such analysis of the results was not performed for the experiments discussed here or for other experimental results at silo discharge, but studies on the degree of segregation as a result of silo filling were performed for the majority of experiments included in this thesis work (see section 8).

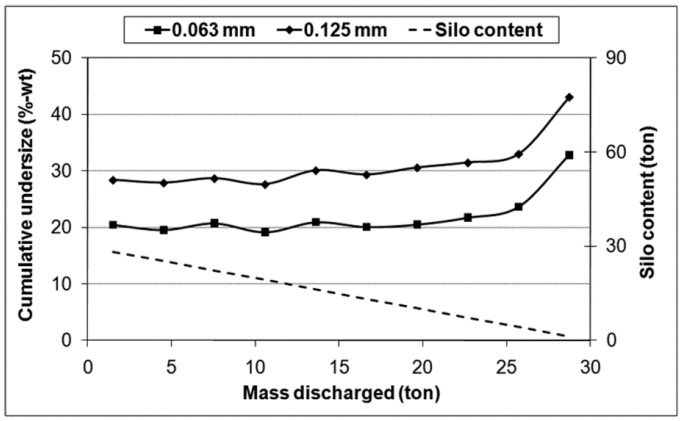

(c)

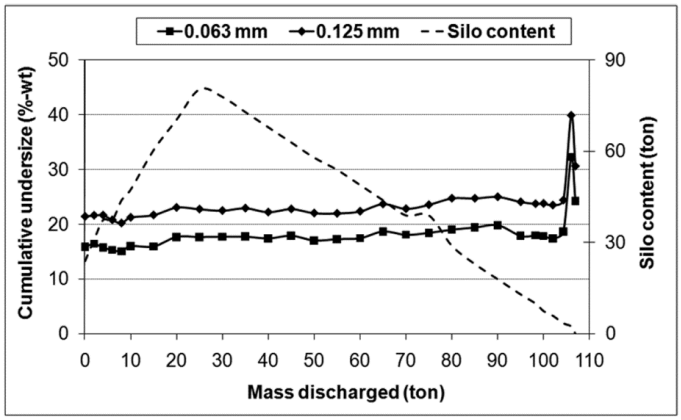

(d)

Figure 11. Results for the large scale experiments: (c) L3 and (d) L4.

It seems that the fluidization plates were not capable of reducing the friction in the upper part of the hopper section sufficiently to induce mass flow of the entire silo contents. Abrupt or steep increases of the fines content towards the end of complete emptying of the type observed in the experiments are unlikely to occur in mass flow silos, because material from different radial positions at identical levels of silo fill should be re-mixed at the outlet. This is true for cases where horizontal or side-to-side segregation is induced during filling, which could be confirmed for product L3 (see below). Visual inspection during the later stages of discharge revealed that heaps of fine particles purged to the surface of the bed together with the air flowing from fluidization plates upwards through the powder bed in very small-sized channels. However, the mass of fine particles in these heaps was negligible (measured in kilo-

grams) in comparison to the segregated material (measured in tons) withdrawn from the silo at the end of complete emptying. The effect of intermittent fill stoppages for product L1, L2 and L4 caused by the disparity between filling and discharge rate is not clear at this point. In principle, the level of fill and the surface profile of the heap could influence the material distribution at filling and impact segregation at discharge as well. This aspect was further elaborated with experiments in the small silo and will be discussed later (section 7.2). Moreover, collection of samples from the central bag filler may have influenced the monitored degree of segregation at discharge. It is possible that this outlet draws bulk solids preferentially from the silo axis and the outer bag fillers include more material from the silo walls. The material distribution in the horizontal direction should be determined at filling (see below) and samples should be collected from all bag fillers simultaneously (see section 9) to clarify the effects of the sampling procedure.

During filling in the experiment with product L3, samples were collected from the upper layers of the heap in different radial positions (silo centre, silo walls and midway) at varying levels of fill. Figure 12 depicts the distribution of fine particles after the filling of 6-24 t in intervals of six tons (corresponding to two mixing batches). The figure shows that an excess of fine particles were accumulated at the silo walls and also that the mass fractions of fines were different at opposite sides of the hopper walls for identical levels of fill. Segregation mechanisms that result in such segregation patterns at silo filling are embedding, fluidization and air current. The occurrence of these mechanisms is difficult to observe during physical experiments, but a fluidized region (approx. 20-30 cm wide) of fine particles was clearly seen next to the silo walls during sample collection. Apparently, segregation at discharge was caused by the accumulation of fine particles to the silo walls during filling in combination with the late withdrawal of material from the vicinity of the upper hopper section walls. However, the occurrence of sifting and rolling during discharge cannot be completely ruled out on the basis of the results for these experiments. The importance of these mechanisms was further investigated through small scale experiments (see section 6).

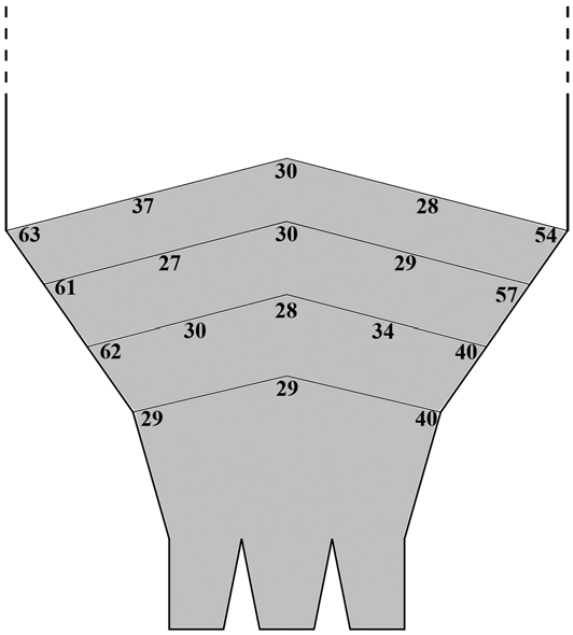

Figure 12. Distribution of fine particles (mass fraction below 0.125 mm in %-wt) for product L3 in the large silo after filling of 6 t, 12 t, 18 t and 24 t.

5.2. Intermediate scale

The experiments in intermediate scale were performed in two different silos: in a 20 m^3 product silo (silo A) at a production plant and in an 18 m^3 building-site silo (silo B). Segregation was studied for one commercial product (I1) in the former silo and for two different products (I2 and I3) in the latter. Particle size distributions for all products are given in Figure 9b. The cumulative undersize of 0.125 mm is used for presentation of the results for products I1 and I2, because results for the large silo experiments showed that this gives a good indication of segregation. However, the mass fraction below 0.063 mm is used for presenting the results for product I3 because of its small mean particle size. For this product, 96 %-wt of the particles is expected to be smaller than 0.125 mm and, therefore, this (cumulative) size fraction may conceal some of the segregation that possibly occurs. Results for the investigations in intermediate scale are presented separately starting with product I1 in silo A.

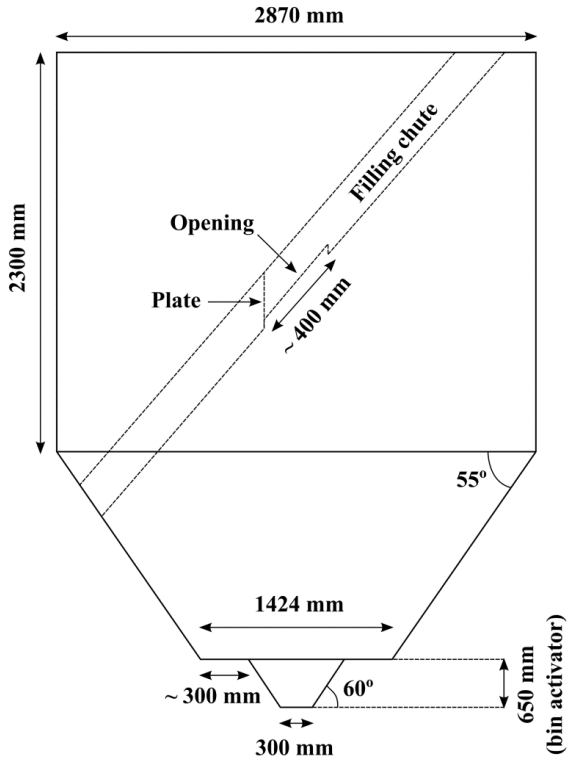

Figure 13. Intermediate silo A with vibrating bin activator at silo outlet comprising the annular horizontal surface and converging section underneath it, i.e., the lowermost 650 mm of the silo.

The commercial product (I1) used for the experiment in intermediate silo A consists mainly of cement and different sand fractions. For this product, a hopper angle of 68° from the horizontal plane is needed for mass flow in a silo constructed of standard steel on the basis of shear cell testing and the theory by Jenike [48]. Figure 13 gives a schematic drawing of silo A, which has a circular geometry and was manufactured of standard steel. The outlet region is equipped with a bin activator comprising the horizontal surface in the hopper section and small hopper beneath it. The bin activator is used only at the very end of discharge in order to empty the silo completely, which implies that the residual material contains a surplus of fine particles. During normal production conditions the raw materials are mixed in batches of two tons and transported to the silo with a conveyor belt. The filling rate is 22 kg/s and filling is stopped for short periods (10-20 s) between subsequent batches. A filling chute with an opening situated in the silo centre runs from one side of the silo roof to the opposite side down in the hopper section. The feed is directed through the opening with a plate, which causes the

silo to be filled centrally until the surface reaches the opening in the chute. However, the silo fill level is not limited to this height and filling can be continued all the way to the silo inlet (upper end of filling chute). The silo contents are discharged into bags containing one ton of product.

The experiment was performed during normal production conditions with 20 t of product I1. Filling was completed before discharge that commenced without delay. Samples were collected with a scoop from the surface layers of the heap in different radial positions (centre, walls and midway) with intervals of four ton during silo filling and also from the top of each product bag. It seems rather obvious that the silo should empty in funnel flow on the basis of mass flow design criteria and the hopper geometry. This was confirmed by visual inspection from the silo top during the experiment; a V-shaped surface clearly developed at the onset of discharge and material from the vicinity of the hopper walls discharged last.

The distribution of product I1 at filling of silo A can be studied in Figure 14, which shows that similar segregation took place as in the large scale experiment with L3: Fine particles accumulated away from the filling point when free fall occurred. The vertical distance from the opening in the filling chute to the material surface after the filling of four and eight tons was approximately 1.25 m and 0.5 m, respectively. A narrow fluidized region of material was clearly observed next to the silo walls during sampling after the filling of four tons, which implies that the segregation was caused by fluidization. Embedding of large particles into the surface layers of the heap apex most likely also occurred because of the free fall. The effects of air currents remain unclear and even though these may have contributed to the segregation, the air current mechanism was probably not as strong here as in the large silo experiments. When four tons of product I1 had been filled, the fines content next to opposite sides of the hopper walls was not the same, in similarity to the experiment with L3 in the large silo. Minor or no free fall occurred during filling from eight tons onwards, which seemed to have a strong effect on the segregation pattern. The opposite materials distribution, i.e., an excess of fine particles at the heap apex, was determined after the filling of twelve tons as a result of sifting and rolling. Here, the heap apex was situated in the silo center at the level of the opening in the filling chute. From then on, the fines content in the vicinity of the silo walls was equal to (16 t) or slightly lower than (20 t) in the centre of the silo. The central samples were no longer collected from the heap apex at the last two sampling levels because the apex moved horizontally towards the upper end of the filling chute.

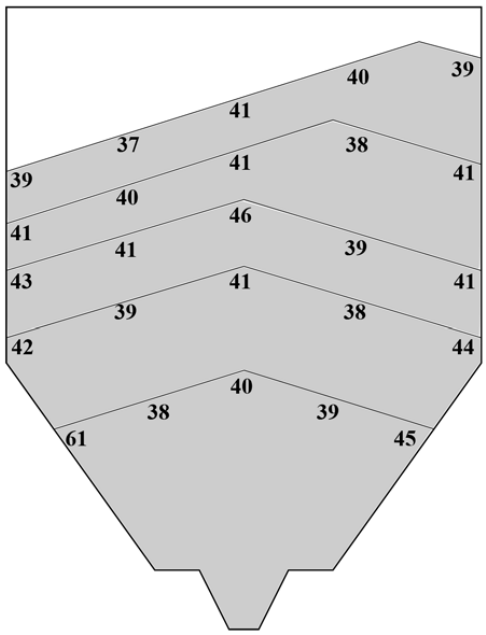

Figure 14. Distribution of fine particles (mass fraction below 0.125 mm in %-wt) for product I1 in intermediate silo A after filling of 4 t, 8 t, 12 t, 16 t and 20 t.

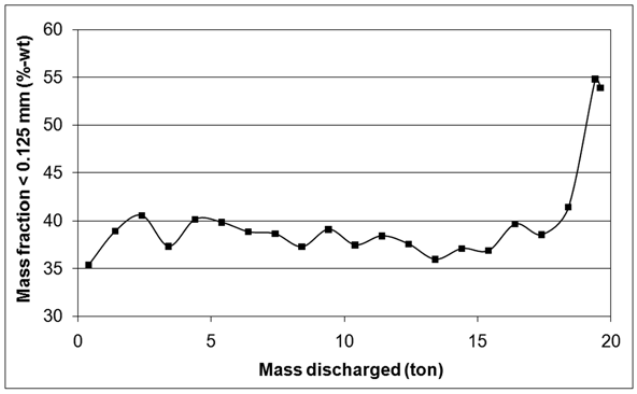

Figure 15. Results for discharge of product I1 from intermediate silo A.

The fines content was relatively constant during most of the discharge (see Figure 15), but the last one or two tons contained an excess of small particles. The fines content for the last two samples at discharge was slightly less than 55 %-wt and this practically equals the mean value (53 %-wt) for samples retrieved from the vicinity of the hopper walls after the filling of four

tons. In summary, similar segregation patterns were observed at filling and at discharge for product I1 in intermediate silo A as in the large silo experiments, despite the difference in silo size and in the auxiliary filling equipment as well as the fact that a different product was used.

Figure 16 shows a schematic drawing of intermediate silo B, which has a cylindrical geometry and was manufactured of standard steel. In the experiments, products I2 and I3 were filled from bags containing one ton of material at rates of 25-30 kg/s. The material distribution resulting from filling was determined by sampling with a scoop from the upper layers of the heap (in different horizontal positions and at varying levels of fill). Various color pigments were spread on the material surface at three or four different levels and their order of discharge was observed visually at the outlet to determine the discharge flow patterns. A total of 19 t was used in each experiment and filling was completed before discharge with a time delay of some ten hours occurring between the end of filling and beginning of discharge. The silo was emptied in batches of one ton into an open bin and sampling across the entire discharge stream was performed to determine the size distribution for the outflow.

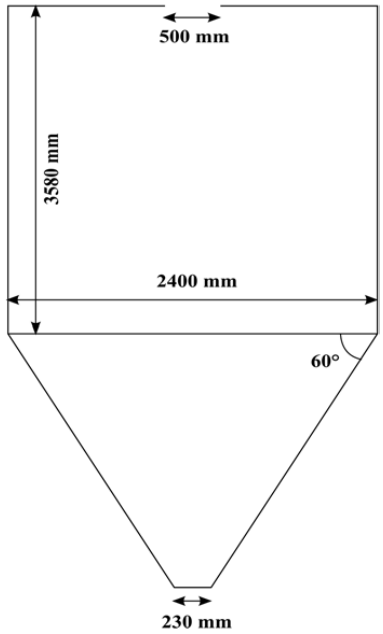

Figure 16. Intermediate silo B.

Product I2 consists mainly of cement, hydrate lime, different limestone and sand size fractions, and 0.2 %-wt of synthetic fibers. Product I3, on the other hand, is almost completely comprised of limestone. The hopper angles required for mass flow with product I2 and I3 were determined to 67° and 69° (from the horizontal plane), respectively, for axially symmetric silos made of standard steel on the basis of shear cell testing and the theory by Jenike [48]. In both experiments funnel flow discharge was confirmed by visually observing the order of discharge for the color pigments as well as by visual inspections of the powder surface during discharge. The color pigments added at the end of complete filling were the first to discharge in greater amounts. In the experiment with I2, bulk solids were withdrawn from only one half of the silo's cross section during the early stages of discharge and several rat-holes, i.e., a kind of self-supporting channel inside the powder bed, developed later. This must have influenced the determined segregation at discharge. For product I3, rat-holes were not observed and material was withdrawn quite uniformly over the cross section of the silo.

Quantitative results for sampling at filling, i.e., the distribution of fine particles in the horizontal direction at different levels of fill, for the experiments in intermediate silo B are presented in Paper II. Here, it will only be mentioned that a surplus of fines at the silo walls (up to 9 %-wt units more than in the silo centre) was determined for product I2 at all sampling levels excluding one; no clear segregation occurred at the upper end of the hopper section. This was a somewhat surprising finding with possible consequences for the determined segregation at discharge, because material from this region usually discharges last in funnel flow silos. For product I3, the material distribution was uniform or only minor segregation in either direction, i.e., accumulation of fines at silo walls or in the silo centre, was observed. This result gives an indication of the particle size distribution required for embedding, fluidization and air current segregation to occur in silos of this size that are filled with free fall.

Figure 17 depicts the fines content for the outflow with products I2 and I3. For I2 (subfigure a), some relatively large variations occurred during most of the discharge and the fines content seemed to increase towards the end. However, this trend was not as clear as for experiments in the large silo and intermediate silo A. The unexpected material distribution (no clear segregation) at the level of the upper end of the hopper section, eccentric flow during the early stages of discharge and rat-holing were the most probable reasons for these findings. For I3 (Figure 17b), the size distribution for the outflow was rather constant and no surplus of fines was withdrawn towards the end of complete emptying. It is interesting to compare the results

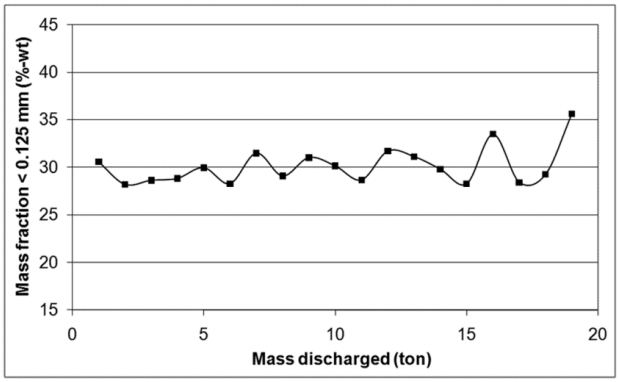

(a)

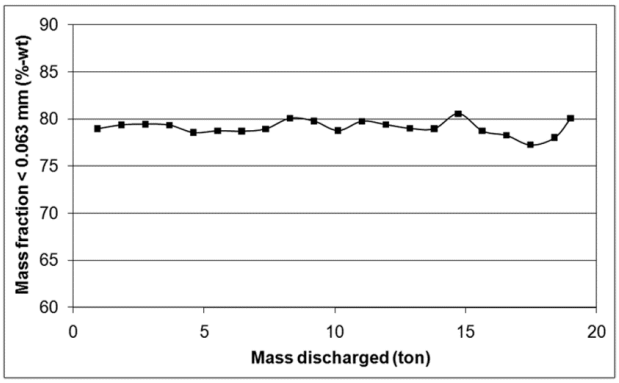

(b)

Figure 17. Results at discharge of product I2 (a) and I3 (b) from intermediate silo B.

for product I3 in intermediate silo B (18 m^3) and product L1 in the large silo (70 m^3, Figure 11a) because the size distributions for these products are similar (cf. Figure 9) at least in comparison to the other products (L2-L4, I1 and I2). Even though the material distribution as a result of filling was not determined for L1 in the large silo, it is very likely that fine particles accumulated at the silo walls at the level of the upper hopper section (cf. Figure 10) because of the determined segregation at the end of discharge. The discrepancy between the results for I3 and L1 may be partly explained by the difference in silo size. In summary, the segregation patterns observed for the experiments in the large silo and in intermediate silo A could be reproduced for product I2, but not for I3, in intermediate silo B.

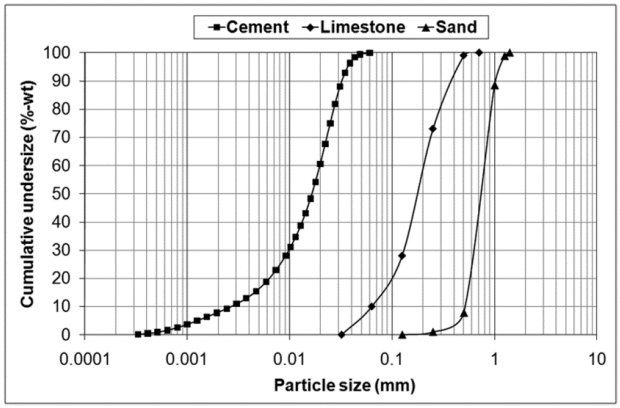

(a)

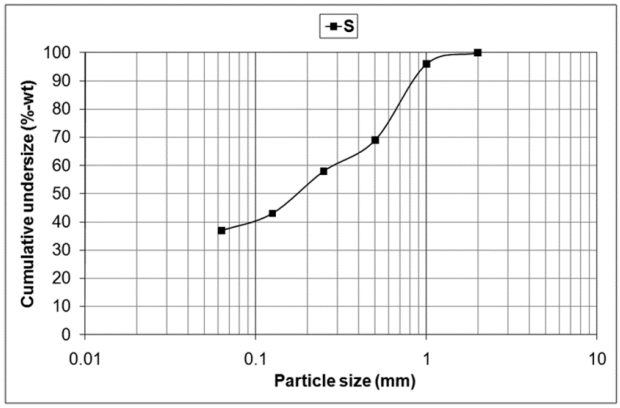

(b)

Figure 18. Particle size distributions (determined mainly by sieving) for the (a) raw materials and (b) mixture used in the small scale experiment (size distribution for cement obtained by laser diffraction and given on number basis).

5.3. Small scale

Figure 18 depicts the particle size distributions for the raw materials (subfigure a) and the mixture (subfigure b) used in the small scale experiment. The mixing of cement, limestone and sand in equal mass produces a mixture (S) with properties, i.e., fines content, mean particle size and width of size distribution, similar to the commercial products L3 and I1 included in the aforementioned experiments. These raw materials were chosen because they are commonly used in commercial construction products. Flow properties for mixture S were measured with a shear cell and the hopper angle required for mass flow in a hopper made of stain-

less steel was determined to 71° from the horizontal plane [48]. The mixture was prepared at a production plant and was packed in 25 kg bags. One experiment was performed in the small silo with a total of 400 kg of powder mixture.

A 0.5 m^3 cylindrical silo was constructed for investigating different features related to the segregation of commercial construction materials in larger silos. The essential details of the small silo are given in Figure 19 and a photograph of the silo setup is shown in Figure 20a. The silo consists of a vertical section of variable height ($H_{cylinder}$) made of standard steel and an interchangeable hopper section. Hoppers were manufactured from stainless steel with different angles (θ_{hopper}) and outlet diameters (d_{outlet}). A separate filling hopper (with outlet diameter denoted d_{inlet} in Figure 19) was aligned centrally above the silo. In this experiment d_{inlet} = 150 mm, $H_{cylinder}$ = 1500 mm, θ_{hopper} = 60° and d_{outlet} = 200 mm. The silo was filled in batches of 50 kg meaning that two bags of powder mixture were put into the filling hopper and then discharged into the silo. The filling of 400 kg was completed before discharge. The average filling rate for all batches was about 1 kg/s, but variations occurred and different mean filling rates for individual batches were observed.

During filling, samples were collected from the surface layers of the heap in the radial positions C and P at some of the levels of fill, illustrated in Figure 7a and b, for determining the initial material distribution. Sampling was also performed throughout the discharging process to determine the size distribution for the outflow. For this purpose, a sampling device was built consisting of a plywood sheet with openings large enough for the discharge stream to pass through and polycarbonate pieces for collecting the samples, see Figures 20b-d. The sampling device (subfigure b) was put on rails so that it could be slid back and forth across the silo outlet (subfigure c). This made it possible to collect samples of appropriate size despite variations in the discharge rate. Hollows were cut into the polycarbonate pieces (subfigure d) and they could be easily removed from the plywood sheet for retrieval of the powder samples. In this experiment samples of 50-150 g were collected and sieved. The silo was emptied in batches of 80 kg into bins positioned on top of a scale, which enabled sampling of the outflow at regular intervals for the withdrawn powder mass.

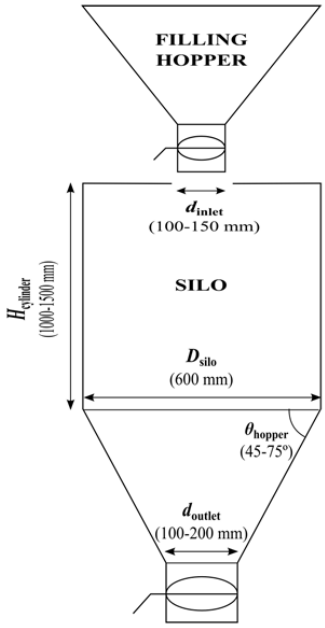

Figure 19. Small silo.

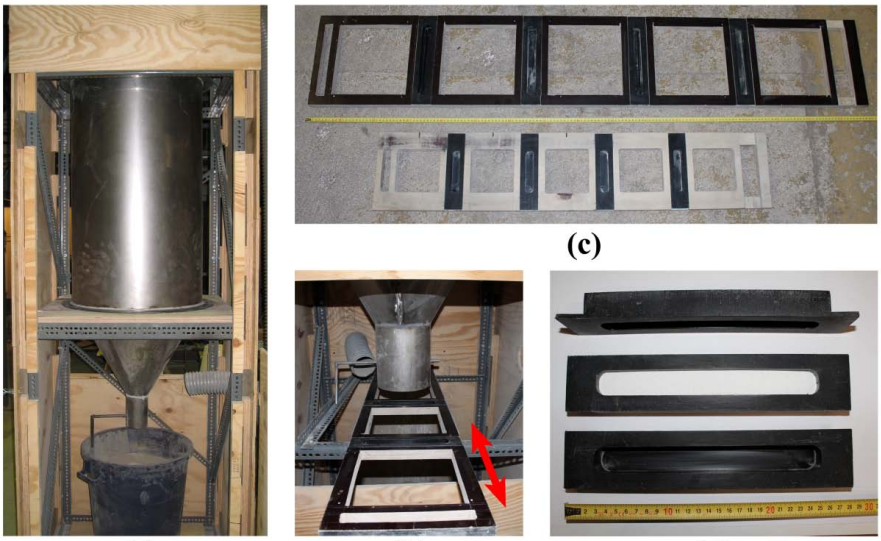

Figure 20. Images of the small silo setup. (a) Vertical section, hopper section and discharge bin (no sampling device), (b) close-up of silo outlet with sampling device, (c) two different sampling devices made of plywood sheet and polycarbonate pieces, and (d) close-up of polycarbonate sample collection pieces (middlemost filled with limestone powder).

A comparison of the hopper angle (71° from the horizontal plane) required for mass flow with mixture S and θ_{hopper} = 60° for the chosen hopper showed that funnel flow discharge should occur in the experiment. The discharge flow pattern was confirmed by visual inspection of the powder surface during discharge and also later through a similar experiment, where tracer objects were utilized for determining the emptying order for the silo contents (see next section).

Results at filling for the small silo experiment can be studied in Figure 21, which shows the distribution of fine particles (mass fraction below 0.125 m) in the silo centre and at the silo walls for levels of fill corresponding to 100-400 kg. The figure shows that a surplus of fine particles was obtained at the silo walls at all sampling levels, but less segregation, defined as the difference between the mass fraction of fines at the silo walls and in the silo centre, occurred compared to the majority of experiments in larger scale (see results for products L3, I1 and I2 above). Still, it is obvious that the segregation pattern for commercial products at filling of larger silos was reproduced in this experiment despite the smaller silo size and the considerable lower filling rates.

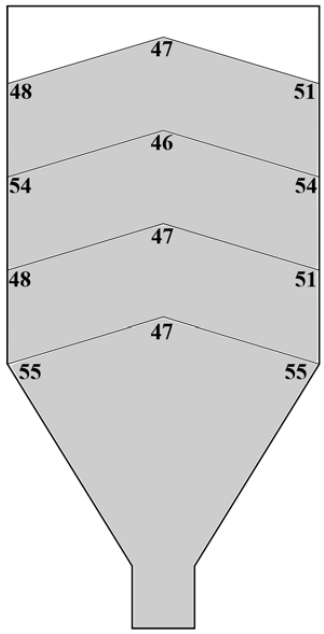

Figure 21. Distribution of fine particles (mass fraction < 0.125 mm in %-wt) for mixture S in the small silo after filling of 100 kg, 200 kg, 300 kg and 400 kg.

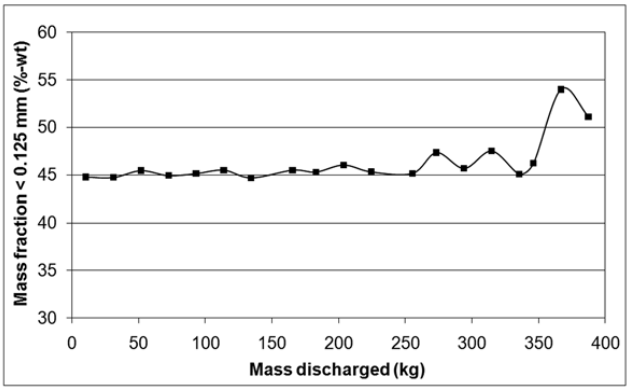

Figure 22. Results for discharge of mixture S from the small silo.

Figure 22 illustrates the results at discharge and shows that the temporal evolution for the size distribution in the outflow was similar to all large and intermediate silo experiments (excluding product I3 in intermediate silo B). More specifically, the fines content was quite constant during most of the discharge and increased at the end of complete emptying.

The experiment with mixture S confirmed that the small silo can very well be used for studying different aspects related to segregation of commercial construction products in larger silos. Even though the magnitude of segregation was different, the same segregation patterns were observed at filling and at discharge in all scales, which means that results for experiments in reduced scale are general in nature and can be applied, albeit with some caution, to practical cases. Three further experiments were performed with mixture S in the small silo in order to confirm the most significant segregation mechanisms for commercial products in larger silos (see next section) and extensive testing with different mixtures was carried out for investigating the effects of material properties, process parameters and hopper angle on segregation (see section 7). A dimensional analysis study was then performed based on all silo experiments and the results of this investigation are presented in section 8.

6. Identification of relevant segregation mechanisms

The results for experiments with commercial construction products in large and intermediate size silos were discussed in the previous section. In these experiments, accumulation of fine particles to the silo walls occurred during filling as a result of the embedding, fluidization and air current segregation mechanisms. The size distribution for the outflow was relatively constant during most of the discharge, but the fines content increased towards the point of complete emptying. It is most likely that the large silo discharged in expanded flow and the intermediate size silos emptied in funnel flow. The results presented in the previous section also showed that the segregation patterns for commercial products in large silos could be reproduced with a three-component mixture (S) in a much smaller silo. However, the extent to which sifting and rolling occurred during silo discharge was not clarified. Segregation at funnel flow discharge is affected by these mechanisms because fine particles sift through the powder matrix downwards to the hopper walls and are withdrawn during the later stages of complete emptying. Rolling of large particles on the surface of the powder bed during funnel flow discharge has the same effect, i.e., the last parts of discharge are depleted of coarse particles. In order to determine the most significant segregation mechanisms for dry mineral-based construction materials in silos, three additional experiments were performed with mixture S in the small silo. These experiments are referred as the second (S2), third (S3) and fourth (S4) experiment with mixture S while the experiment discussed in the previous section is called the first (S1). Results for all experiments with mixture S in the small silo were presented in Paper II of this thesis work.

Mixture S consists of cement, limestone and sand in equal mass. The particle size distributions for the raw materials and mixture S are given in Figure 18. Figure 19 shows a schematic drawing of the small silo and images of the experimental setup are given in Figure 20. The experimental procedures (for filling, discharge and sampling) for tests performed in the small silo were also elaborated in the previous section. Markers were utilized in the fourth experiment with mixture S (S4) to clarify whether the small silo emptied in mass flow or funnel flow. Figure 7 illustrates the initial placement for the tracer objects and illustrative results for imaginative experiments with mass flow and funnel flow discharge of the silo contents are depicted in Figure 8.

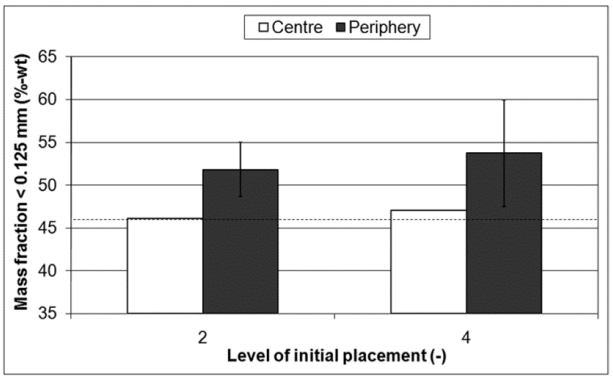

(a)

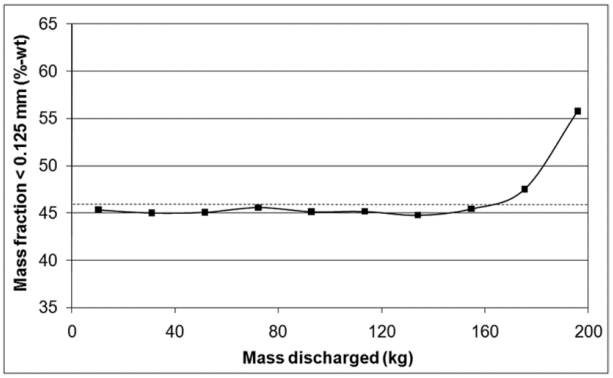

(b)

Figure 23. Results for the second experiment with mixture S (S2) at filling (a) and discharge (b) of the small silo. Mass fraction below 0.125 mm according to mixture formulation is shown by the dotted lines.

Results for the second experiment with mixture S (S2) can be seen in Figure 23. This test included a total of 200 kg of powder mixture, i.e., half of the amount used in the first experiment (S1). Subgraph (a) shows that fine particles accumulated at the silo walls at both sampling levels and subgraph (b) indicates that the size distribution for the outflow was similar to S1 (cf. Figure 22). In both experiments (S1 and S2), the fines content in the output started increasing with 40-50 kg of powder left in the silo.

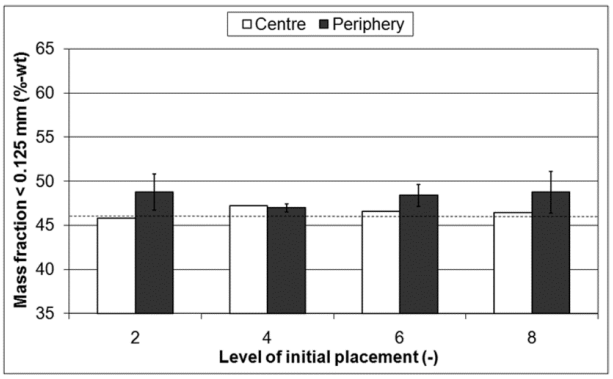

(a)

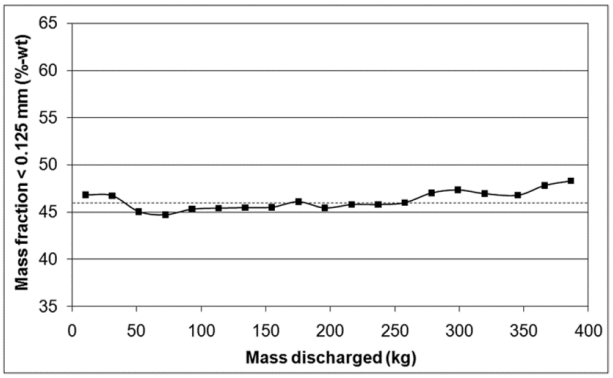

(b)

Figure 24. Results for the third experiment with mixture S (S3) at filling (a) and discharge (b) of the small silo.

Figure 24 gives the results for the third experiment with mixture S (S3). In this test, the first 200 kg (up to Level 4 in Figure 7b) were filled directly from bags containing the mixture with minimal free fall distance and the last 200 kg were filled through the filling hopper. Results for filling (Figure 24a) indicate that the average fines content in the vicinity of the silo walls at Level 2 was approximately 49 %-wt, which is a somewhat lower value compared to the results at this level of fill for S1 (55 %-wt) and S2 (52 %-wt). At Level 4, the material distribution in S3 was uniform whereas segregation clearly occurred in S1 (cf. Figure 21) and especially in S2 (cf. Figure 23). In S3, slightly higher amounts of fines were determined near the silo walls compared to the silo center at Level 6 and Level 8. The fines content for the outflow in S3 (see Figure 24b) was rather constant throughout the discharging process and no clear

increase of the fines content occurred at the end of complete emptying as in S1 and S2. This was the result of little or no segregation at the lower levels of silo fill, i.e., the material distribution over the silo's cross section was relatively uniform at Level 2 and especially at Level 4 in S3.

The fourth experiment with mixture S (S4) is identical to S1, i.e., 400 kg of powder was used and was filled through the filling hopper. The results for tracer objects in S4 are depicted in Figure 25, where the moment of exit for each tracer has been expressed as the fractional mass discharged from the silo (explained in section 3.4). The columns and error bars denote the mean and standard deviation, respectively, for all tracer objects initially placed in the M- and P-position (see Figure 7a and b) at identical levels of fill. The order of exit for tracer objects in S4 suggests that the silo discharged in funnel flow (cf. Figure 8b). Tracers seeded next to the silo walls were clearly withdrawn in a "first-in-last-out" sequence whereas markers placed halfway between the walls and the silo centre (on average) exited slightly before the peripheral ones that were originally placed at the same level. On the basis of the results for tracer objects in S4, powder mixture initially located near the silo walls at Levels 1-3 emptied last. Markers placed in the silo centre at Levels 2-7 exited later than expected, which was most likely caused by the horizontal movement of these tracers or bulk material from centre of

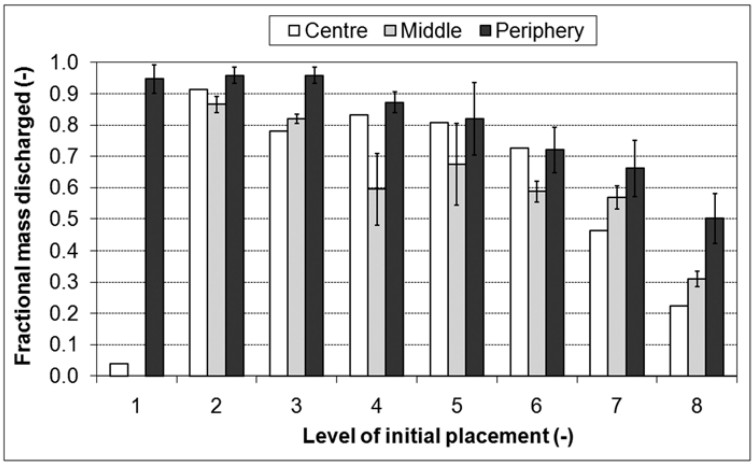

Figure 25. Results for tracer objects in the fourth experiment with mixture S (S4) in the small silo. Fractional mass discharged = $m_i/m_{tot,exp}$, where m_i expresses the mass of powder mixture discharged from the silo at withdrawal of tracer *i* and $m_{tot,exp}$ denotes the total mass of mixture used in the experiment.

the silo towards the walls before the beginning of discharge. Presumably, such reordering of the silo contents was caused by the filling of additional material.

On the basis of the results for tracer objects in S4, it can be assumed that funnel flow occurred in all small silo tests with mixture S (S1-S4) because the same hopper was used. Comparison of the results for S1-S3 shows that sifting and rolling did not occur to a significant extent during silo discharge. The main findings for the experiments S1-S3 are summarized in Figure 26, where results for filling (subfigure a) show the difference ($\Delta_{< 0.125\ \mathrm{mm}}$) for the mass fraction less than 0.125 mm between samples taken at the silo walls and in the silo centre for Level 2 and Level 4. A positive value for $\Delta_{< 0.125\ \mathrm{mm}}$ means that an excess of fines was observed next to the silo walls. Here, only the mean values for multiple samples obtained at the silo walls for a specific level are used, i.e., standard deviations are omitted. In Figure 26b, the mass fraction less than 0.125 mm for samples obtained at emptying is depicted against the mass of powder mixture left in the silo at sample collection. Segregation at the end of complete emptying was hardly affected even though the total mass of material was reduced from 400 kg in S1 to 200 kg in S2, where similar segregation occurred in the lower parts of the silo during filling. Furthermore, no significant segregation at the end of emptying was observed in S3, where the material distribution over the silo's cross section at the lower levels of fill was nearly uniform. If sifting and/or rolling would have occurred during funnel flow discharge, segregation at the end of complete discharge should have been more severe in S1 compared to S2, and some segregation at the end of emptying should have been determined in S3 as discussed in the beginning of this section. The statement that sifting does not occur is supported by the findings presented in [13,14], where the necessary conditions for the occurrence of sifting are reported. Among other features, a sufficiently large mean particle size (approx. > 100 μm) and free flowing material are required for this segregation mechanism to take place, and these requirements are not fulfilled by virtually any of the materials of interest here. Moreover, in all of the experiments discussed so far in this thesis, avalanching of small powder segments on the surface of the bed was observed during discharge. This limits the rolling of large particles because these are surrounded by and locked in a matrix of smaller particles. The large particles are mostly cubic in shape (see images of sand and limestone particles in Figure 1), which further suppresses the rolling mechanism during discharge.

The findings and conclusions presented in this section are not limited to mixture S and the small silo, because of the similarities of the results for experiments performed in varying silo

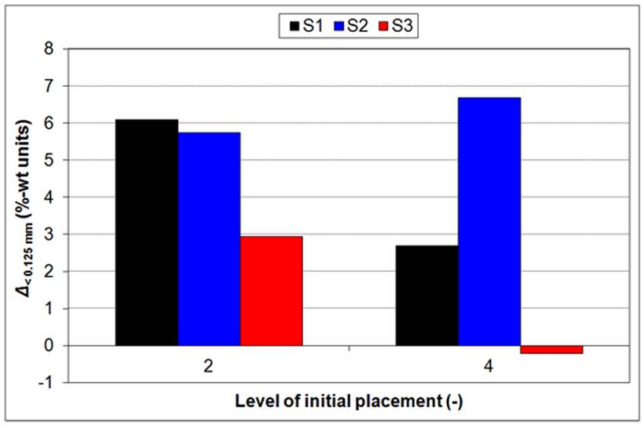

(a)

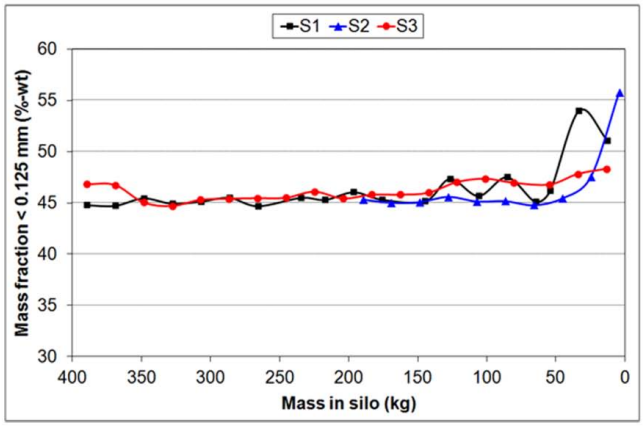

(b)

Figure 26. Results for experiments S1-S3 at filling (a) and discharge (b). $\Delta_{<0.125\ mm}$ expresses the difference for the mass fraction less than 0.125 mm between samples obtained at the silo walls and in the silo centre. Mass in silo denotes the mass of powder mixture left in the silo at sample collection.

sizes that were elaborated in the previous section. Segregation of commercial construction products at the end of complete emptying of silos is determined by the extent of horizontal segregation induced at the levels of fill that are withdrawn last. The material that discharges last is, on the other hand, determined by the discharge flow pattern. Segregation at silo filling is caused by embedding, fluidization and air current effects, and, therefore, these are the most important segregation mechanisms in the context of the systems studied in this thesis work.

7. Investigation of the effects of independent variables

In this section, a brief summary of the main findings from further experiments in the small silo are presented. These tests were performed in order to clarify the effects of material properties, process parameters and hopper angle on segregation. The results of these tests are elaborated especially in Paper III and Paper IV, and partly in Paper V of this thesis.

The raw materials utilized in these additional tests include two sand fractions, three limestone fractions, a glue, Portland cement and hydrated lime. The properties of the raw materials are summarized in Table 2, where the mean particle size (d_{50}) decreases from top to bottom, i.e., sand 1 is the coarsest raw material and hydrated lime is the finest. The particle solid density (ρ_s) is highest for cement, similar for all sand and limestone fractions, slightly lower for hydrated lime and clearly the lowest for glue. Sand 2, limestone 2 and cement obtain small negative charges, but hydrated lime becomes positively charged when electrically neutralized samples of the raw materials slide into a Faraday pail through a grounded stainless steel tube. Figure 1 gives images of the individual particles of the raw materials and shows that the shapes are mainly cubic. The flow properties for some of the raw materials were determined

Table 2. Properties for raw materials used in the small silo experiments.

Raw material	d_{10} (mm)	d_{50} (mm)	d_{90} (mm)	ρ_s (kg/m^3)	Charge [c] (nC/g)
Sand 1	1.12	1.71 [a]	2.99	2760	- [d]
Sand 2	0.51	0.76 [a]	1.04	2762	-0.38 (±0.10)
Limestone 1	0.20	0.45 [a]	0.70	2779	- [d]
Limestone 2	0.06	0.19 [a]	0.41	2600	-1.25 (±0.21)
Limestone 3	0.010	0.113 [b]	0.220	2796	- [d]
Glue	0.025	0.105 [b]	0.241	1210	- [d]
Cement	0.001	0.010 [b]	0.035	3103	-1.82 (±0.24)
Hydrated lime	0.001	0.005 [b]	0.053	2336	20.90 (±2.56)

a. Determined by sieving, distribution given on mass basis.
b. Determined with laser diffraction, distribution given on number basis.
c. Average of ten tests performed at 22 °C and 30 % relative humidity. The standard deviation of all tests is given in parenthesis.
d. Not determined.

with a shear cell and the results (not given here) showed that the degree of cohesion increases with decreasing mean particle size, e.g., sand 2 and limestone 2 are free flowing whereas cement and hydrated lime are (very) cohesive.

Experiments were performed with six binary (M1-M6) and three ternary (M7-M9) mixtures. The mixtures were prepared on mass basis with an industrial mixer at a construction material producing plant and packed in 20 kg or 25 kg bags. Table 3 gives the mixture compositions in terms of the mass fractions of raw materials. The binary mixtures M1-M3 are composed of sand 2 and cement in varying mass fractions, whereas the binary mixtures M4-M6 include sand 2 as the coarse component and either limestone 3 (M4) or glue (M5 and M6) as the fine component. Mixtures M7 (denoted mixture S in sections 5 and 6) and M8 are composed of sand, limestone and cement in equal mass, but the coarse and intermediate components are coarser for M8. In mixture M9, the fine component of M8 is substituted by hydrated lime.

Additional properties of the mixtures can be studied in Table 4. A suitable cut-off size, chosen on the basis of the raw material size distributions, was determined for each mixture in order to separate the samples collected in the experiments into fine and coarse fractions. The particle size ratio ($d_{50,c}/d_{50,f}$) expresses the ratio of the mean particle size for the coarse and fine

Table 3. Compositions, i.e., mass fractions of raw materials in %-wt, for the mixtures used in the small silo experiments. S = sand, LS = limestone and HL = hydrated lime.

Mixture	S1	S2	LS1	LS2	LS3	Glue	Cement	HL
M1		90					10	
M2		70					30	
M3		50					50	
M4		50			50			
M5		50				50		
M6		75				25		
M7 [a]		33.4		33.3			33.3	
M8	33.4		33.3				33.3	
M9	33.4		33.3					33.3

a. Denoted mixture S in sections 5 and 6.

Table 4. Additional properties for the mixtures used in the small silo experiments.

Mixture	$d_{\text{cut-off}}$ (mm)	$d_{50,c}/d_{50,f}$ (-)	$\rho_{s,c}/\rho_{s,f}$ (-)	x_{moisture} [a] (%-wt)	Flow properties [b]
M1	0.250	76	0.9	0.20	Free or easy
M2	0.250	76	0.9	0.30	Easy
M3	0.250	76	0.9	0.30	Cohesive
M4	0.300	7	1.0	0.30	- [c]
M5	0.300	7	2.3	0.50	Free
M6	0.300	7	2.3	0.40	- [c]
M7	0.125	76	0.9	- [c]	Cohesive
M8	0.125	171	0.9	0.25	Cohesive
M9	0.125	342	1.2	0.40	Cohesive

a. Determined by weight loss after drying (12 h, approx. 100°C).
b. Determined with a shear cell and with classification according to Jenike [48].
c. Not determined.

fractions. Likewise, the particle solid density ratio ($\rho_{s,c}/\rho_{s,f}$) for the coarse and fine fraction was determined for each mixture. The choice of raw materials for the mixtures was partly influenced by the desire to include a wide range of values for the particle size and solid density ratio. The moisture contents were determined by weight loss after drying, which showed that the mixtures contain very small amounts of water. Flow properties were determined for some of the mixtures with a shear cell. Classification according to Jenike [48] reveals that the mixtures range from free flowing to (very) cohesive.

A schematic drawing of the small silo is given in Figure 19. The experimental procedures, i.e., filling, discharge and sampling, for the experiments presented in this section are similar to the tests (in the small silo) discussed in sections 5.3 and 6. Samples were collected in different horizontal positions at varying vertical levels (cf. Figure 7a and b) during filling and also throughout the discharging process. In Figure 7b, the masses for the sampling levels correspond to successive fillings of two 25 kg bags and are representative of the majority of mixtures. Different values (40 kg for Level 1, 80 kg for Level 2, etc.) were obtained for M5 and M9 because they were packed in bags containing only 20 kg (compared to 25 kg for the others) as a result of the lower bulk density. In the majority of experiments, the discharge flow pattern was determined with tracer objects according to procedures explained in section 3.4.

Because some unexplainable variations are always obtained in experimental work and especially in the case of powder flow, three repeated tests were performed with mixtures M1 and M8 in order to assess the reproducibility of the experiments.

The results of sampling at filling are presented as follows: the mean mass fraction of fines for samples collected in the vicinity of the silo walls (position P in Figure 7b) was normalized against the fines content for the sample obtained in the silo centre at the same level of fill. A value exceeding unity for this "fines ratio" means that a surplus of fine particles has accumulated at the silo walls. Each sampling level was treated separately and the fines ratios are depicted against the free fall distance (denoted h_{ff} in Figure 7b), i.e., the vertical distance from the filling hopper outlet to the heap apex at the time of sampling.

The fines content for samples collected during emptying in one experiment was normalized against the mean fines content for all samples obtained at discharge in the experiment. The mass discharged from the silo at collection of sample i (m_i) was normalized against the total mass of mixture used in the test ($m_{tot,exp}$) and these normalized values are referred to as fractional mass discharged. Results for the repeated experiments with mixtures M1 and M8 (at filling and at discharge) were averaged.

7.1. Material properties

Even though segregation of powder mixtures (handled in silos) in principle could be affected by a range of material characteristics, the analysis presented in this subsection is restricted to studying the effects of the mass fraction of fines, the particle size ratio and the particle solid density ratio. Furthermore, process conditions and silo design may influence segregation, but these aspects are covered in the forthcoming subsections.

Table 5 summarizes the experimental conditions in a number tests performed for clarifying the effects of the aforementioned material parameters. The tests were done with an identical silo setup, i.e., with $H_{cylinder}$ = 1.25 m and θ_{hopper} = 60°, in order to minimize the effects of the equipment. Even though various filling hopper outlets (d_{inlet}), silo outlets (d_{outlet}), total mixtures masses ($m_{tot,exp}$) and filling batch sizes (m_{batch}) were used, the effects of these features on segregation are most likely small. Likewise, the influence of variations in the discharge rate

Table 5. Experimental conditions in the small silo tests with $H_{cylinder}$ = 1.25 m and θ_{hopper} = 60°.

Mixture	Test nr	d_{inlet} (mm)	d_{outlet} (mm)	$m_{tot,exp}$ (kg)	m_{batch} [a] (kg)	$\dot{m}_{in}$ [b] (kg/s)	$\dot{m}_{out}$ [b] (kg/s)
M1	1	100	100	500	50	6.25 ± - [c]	0.55 ± 0.03
	2	100	100	500	50	6.47 ± 0.12	0.56 ± 0.05
	3	100	100	500	50	6.52 ± 0.20	0.56 ± 0.03
M2	1	100	100	375	50	2.00 ± 0.26	0.47 ± 0.12
M3	1	100	100	500	50	Low [c]	Low [c]
M4	1	150	100	375	50	3.89 ± 2.52	0.46 ± 0.06
M5	1	150	100	320	40	3.33 ± 0.43	0.23 ± 0.04
M6	1	150	100	390	50	2.54 ± 0.15	- [d]
M7	1	150	200	400	25	0.32 ± 0.25	0.28 ± 0.06
M8	1	150	200	400	25	4.36 ± 2.33	0.20 ± 0.03
	2	150	200	400	25	4.76 ± 1.89	0.19 ± 0.04
	3	150	200	400	25	5.43 ± 2.58	0.19 ± 0.04
M9	1	150	200	380	20	6.06 ± 2.69	0.21 ± 0.01

a. Mass of material filled into the silo at a time.
b. Mean rate and standard deviation for all batches filled/discharged in the experiment.
c. Rate could not be measured accurately because flow from the filling hopper was erratic as a result of arching.
d. Not measured.

on the results can be considered negligible. The filling rate could have affected the material distribution induced during filling and, therefore, it could also have had an impact on the segregation at silo discharge (discussed in the next subsection). Results for tracer objects showed that funnel flow according to the illustration given in Figure 5b occurred in nearly all tests. In the experiments with mixture M1, where tracer objects were not used, the silo may have discharged in the (funnel flow) pattern shown in Figure 5c.

Results for the experiments with mixtures M1 and M3 are shown in Figure 27. Subgraph (a) shows that the mass fraction of fines has a significant effect on the segregation pattern at filling. At nearly all levels of fill, for M1 (low fines content) an excess of fine particles were obtained in the silo center as a result of sifting and rolling. For M3 (high fines content), the opposite material distribution was determined as a result of embedding, fluidization and air current effects. Results for M1 indicate that the unexplainable variations are rather large. For

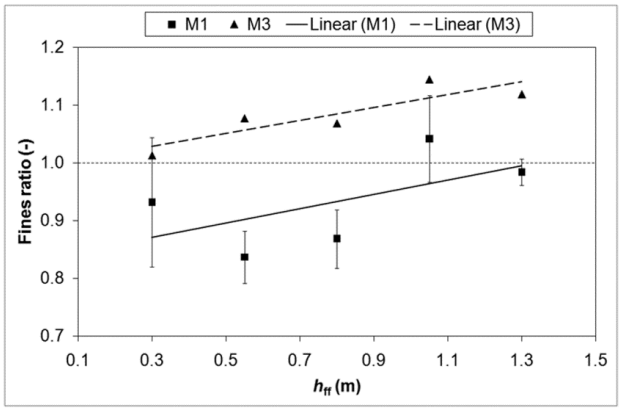

(a)

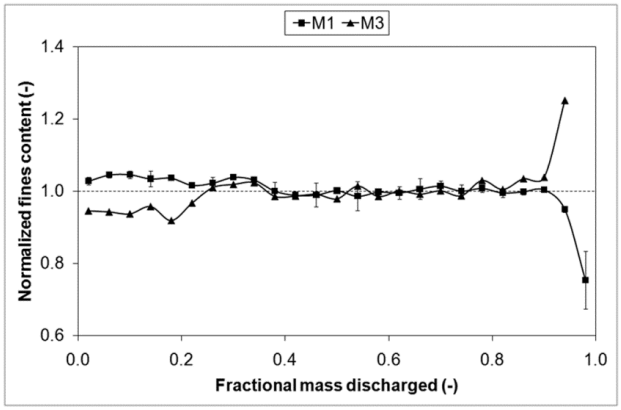

(b)

Figure 27. Results for mixtures M1 (three repeated tests) and M3 at filling (a) and at discharge (b) in the small silo experiments. Fines ratio expresses the ratio for the mean fines content of all samples collected at the silo walls and the fines content in the silo centre. The normalized fines content at discharge is obtained by normalization of the mass fraction of fines for the samples against the average fines content for all samples obtained at discharge. Fractional mass discharge = $m_i/m_{tot,exp}$, where m_i denotes the mass of powder mixture withdrawn from the silo at collection of sample i and $m_{tot,exp}$ the total mass of mixture used in the experiment.

both mixtures, the material distribution was clearly influenced by the free fall distance (h_{ff}), i.e., the mass fraction of fines at the silo walls increased with increasing h_{ff}. For M1 (giving excess fines in the silo centre) this meant reduced segregation whereas for M3 (giving a surplus of fines at the silo walls) the segregation was increased. The effect of the free fall distance will be further clarified in the next subsection. The results for mixture M2 (not given

here) were somewhere between the results for M1 and M3 meaning that the material distribution for M2 was rather uniform at nearly all sampling levels.

Figure 27b shows the results for M1 and M3 at discharge and illustrates the effect of the initial material distribution on the size distribution for the outflow. For both mixtures the fines content was quite constant for most of the discharge. However, the outflow became depleted of fines for M1 and contained a surplus of fines for M3 at the end of complete emptying. Mixing of bulk solids from various radial positions at different levels of fill presumably produced a constant size distribution for the outflow until the last stages of emptying. At some point, the silo contents became depleted of fine particles for M1 and contained a surplus of fines for M3. For M1, percolation or sifting may have occurred during discharge because the masses of fine particle for the last samples were significantly lower than the mass fraction of fines for any of the samples obtained in the vicinity of the silo walls at filling. This is true especially for those samples collected at $h_{\mathrm{ff}} \approx 1.25$ m that, presumably, correspond to the last material to discharge. The error bars for M1 in Figure 27b show that the largest variations were obtained for the last samples. However, a depletion of fines at the end of complete emptying was obtained in all three repeated tests. It will also be mentioned that rat-holing was observed during discharge of M3, which shows that the silo discharged in funnel flow, but tracer objects were not used to confirm this. Moreover, in the tests with M1 and M3 the decrease/increase of the fines content at the end of complete emptying occurred rather abruptly. For mixture M2, the size composition for the outflow was relatively constant throughout the discharging process and no clear increase or decrease of the fines content was determined.

It is interesting to compare the results obtained for mixtures M1-M3 with the findings of other investigators. For free flowing particulate solids segregation can be decreased by increasing the cohesiveness, for example, by adding small amounts of liquids [13]. However, many of the materials of interest here are not free flowing. The degree of cohesion for mixtures M1-M3 increases when the mass fraction of cement is increased (cf. Table 4). Strictly speaking, the mixture will not be the same anymore when the mass fractions of the components are changed even though the same raw materials are used. Accumulation of fine particles in the silo center was determined in the experiments with mixture M1 (free flowing) but not in the test with M2 (easy flowing), which is in accordance with the findings reported in [13]. Segregation with accumulation of fines at the silo walls was obtained for mixture M3 (cohesive), i.e., an increase of the cohesiveness induced segregation. The explanation for this discrepancy

clearly lies in the segregation mechanisms, which were different for M1 and M3. However, the results for mixtures M2 and M3 imply that segregation may increase as a result of increased cohesiveness for initially non free flowing bulk solids. The influence of fine particle concentration on segregation was also discussed in [6], where it was reported that sifting segregation in general becomes significant when the fraction of fines is 15-30 % or less and fluidization apparently leading to vertical segregation is important when the fines content exceeds 60-80 %. Results for mixture M1 are accordant with the former statement. However, the results for mixture M3 as well as the results for the majority of experiments presented in sections 5 and 6 indicate that fluidization is partly responsible for inducing horizontal segregation at values for the concentration of fine particles much lower than 60-80 %.

Figure 28a illustrates the results for mixtures M4 and M5 at filling. For all sampling levels, the material distribution for M4 (limestone as fine component) was uniform. For M5 (glue as fine component) the concentration of fine particles next to the silo walls was considerably greater than the fines content in the silo centre. This must be explained by the difference in the particle solid density for the fine components in these mixtures, because the other material properties, i.e., the mass fractions and the particle size distributions for limestone and glue, are practically identical. The solid density for glue particles is considerably lower than for limestone (cf. Table 2). This demonstrates the importance of considering the particle solid densities in studies of the segregation of particulate systems subjected to free fall, which was also stressed by Tang and Puri [6].

Comparison of the results for M3 (see Figure 27a) and M4 at silo filling, on the other hand, vividly illustrates the effect of the particle size ratio. For these two mixtures, the mass fractions of fine/coarse component (cf. Table 3) are identical. Considerable concentration of fine particles to the silo walls was obtained for the former mixture whereas no segregation was determined for the latter. This finding can only be explained by the higher particle size ratio for M3. Interestingly, the free fall distance had no effect on the outcome in light of the results for mixtures M4 and M5. For M6 (results not shown here), where the mass fraction of glue particles was reduced to half of that in M5, a surplus of fine particles at the silo walls was observed at all sampling levels. However, less segregation occurred with M6 compared to M5 and for M6 the segregation slightly decreased with decreasing free fall distance.

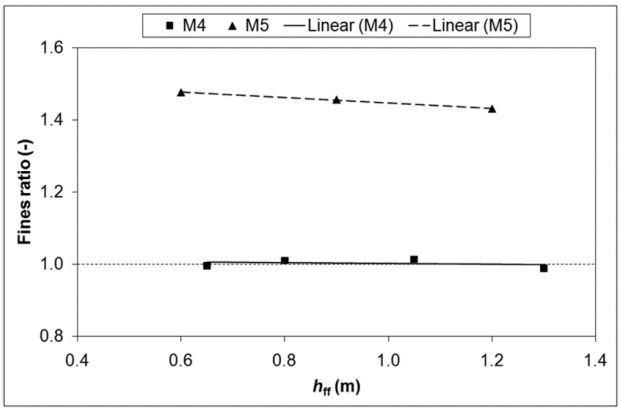

(a)

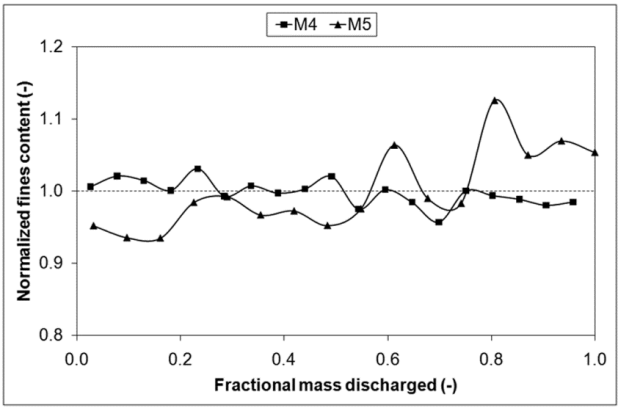

(b)

Figure 28. Results for mixtures M4 and M5 at filling (a) and at discharge (b) in the small silo experiments. Notation is clarified in the caption of Figure 27.

The size distributions for the outflows in the experiments with mixtures M4 and M5 are depicted in Figure 28b. The fines content was almost constant or slightly decreased for M4 and showed an increasing trend with rather large fluctuations for M5. Results for M4 can be explained by the initially uniform material distribution and the fact that sifting or percolation apparently did not occur during funnel flow discharge. For M5, an abrupt increase of the fines content at the end of discharge like that observed in the experiment with mixture M3 (cf. Figure 27b), was not determined. The reasons for this finding are not clear, although it may be speculated that this was caused by differences in the flow properties for the mixtures: M3 is cohesive whereas M5 is free flowing. It is possible that the discharge flow pattern was not

identical for these two mixtures even though funnel flow could be verified for both (by visual inspection for M3 and with marker objects for M5).

Figure 29a depicts results for mixtures M8 and M9 at silo filling. Fine particles were accumulated at the silo walls with both mixtures and segregation increased with increasing free fall distance. However, the segregation was much stronger for mixture M9, which was caused by the combined effect of the particle size and solid density ratio. The particle size ratio ($d_{50,c}/d_{50,f}$ in Table 4) and the particle solid density ratio ($\rho_{s,c}/\rho_{s,f}$) are higher for M9, which are the result of the slightly smaller mean particle size and the clearly lower particle solid density for hydrated lime compared to cement. Results for mixture M7 (not shown here) exhibited a similar segregation pattern, i.e., fine particles were concentrated to the silo walls at nearly all sampling levels, but the magnitude of segregation was somewhat lower than for M8. This difference must be caused by the wider particle size distribution of M8. However, the mass fraction of fines for M7 (43 %-wt) is slightly higher than for M8 (35 %-wt), which probably compensated for the effect of the particle size distribution. This is supported by the results for M2 and M3, where segregation increased (or was induced) with increasing fines content in the range 30-50 %-wt. Results for M8 show that the unexplainable variations were much smaller compared to mixture M1, especially at the higher levels of fill or with smaller free fall distances.

Results for M8 and M9 at discharge are shown in Figure 29b. Again, it can be concluded that the size distribution at the end of complete discharge was determined by the initial material distribution at the upper end of the hopper section ($h_{ff} \approx 1.25$ m). Mixing of bulk solids from different radial positions at various levels of fill led to a fairly uniform mass fraction of fine particles during most of the discharge and the fines content increased at the end of complete emptying. For M8 the temporal evolution for the fines content in the outflow was similar to the experiment with mixture M3, i.e., increased abruptly at the end. During discharge of M8, the variations of the fines content were largest for the final samples, but an increase of the mass fraction of fines occurred in all three repeated experiments. For M9, the mass fraction of fine particles started increasing earlier and this was most likely caused by the strong segregation induced during filling. Interestingly, the discharge results for M9 are rather different from the results for mixture M5 (cf. Figure 28b) that also segregated significantly during filling, but did not show an abrupt increase of the fines content at the end of complete emptying. This finding can only tentatively be explained by differences in the cohesiveness of the mixtures.

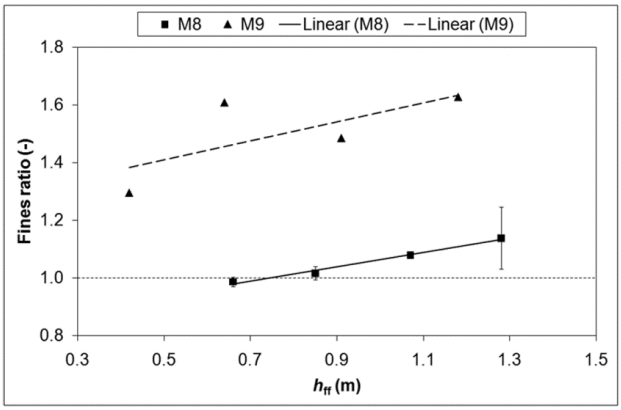

(a)

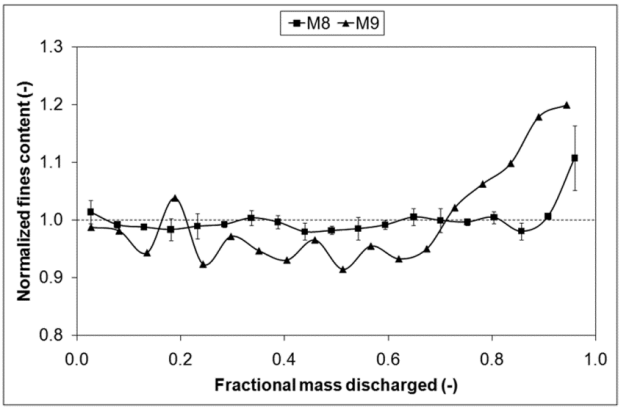

(b)

Figure 29. Results for mixtures M8 (three repeated tests) and M9 at filling (a) and at discharge (b) in the small silo experiments. Notation is clarified in the caption of Figure 27.

7.2. Process parameters

Some further experiments were performed with mixtures M7 and M8 (see Table 6) and the results from these tests were analyzed together with the results for experiments discussed in the previous subsection (cf. Table 5). The goal was to clarify the effects of certain process parameters and the hopper angle on segregation. In this subsection, the influence of the surface profile of the deposited powder bed, the free fall distance and the filling rate on segregation is elaborated. The effect of the hopper angle on segregation at silo discharge is presented in the next subsection.

Table 6. Experimental conditions for further tests in the small silo with d_{inlet} = 150 mm and d_{outlet} = 200 mm.

Mixture	Test nr	$H_{cylinder}$ (m)	θ_{hopper} (°)	$m_{tot,exp}$ (kg)	$\dot{m}_{in}$ (kg/s)	$\dot{m}_{out}$ (kg/s)	Discharge pattern
M7	2	1	75	400	0.95 ± 0.06	0.50 ± 0.11	Mass flow
M8	4	1.25	60	800	4.92 ± 2.73	0.21 ± 0.03	Funnel flow
M8	5	1.25	45	350	5.65 ± 2.92	0.23 ± 0.11	Funnel flow
M8	6	1.25	75	400	1.41 ± 1.49	- [a]	Mass flow

a. Not measured.

Figure 30 presents results for the fourth experiment with M8, where the silo was first filled with 400 kg of powder mixture, and then discharged and filled successively with 100 kg until a total of 800 kg had been filled. Accumulation of fine particles at the silo walls was determined for all sampling levels, but segregation increased during intermittent discharge and filling. During this process, the free fall distance at the time of sampling was constant, but the surface profile changed from a heap (inverted V-shape) to a V-shape as a result of material being discharged from the silo. The distribution of fine particles was clearly influenced by the shape of the powder surface and the segregation was quite strong even though the free fall distance ($h_{ff} \approx 0.66$ m) was relatively small. Again, the reason for this is not clear, but the result is important because concurrent filling and discharge of product silos regularly occurs during normal production conditions at construction material plants. Moreover, periods with discharge but no filling occur when the throughput rate for the packing machine is less than the capacity of the mixer. In such situations, the powder surface becomes V-shaped when the silo empties in funnel flow and stronger segregation may later occur at discharge, in case the level of fill is (vertically) close to the transition from hopper to vertical section. This is because of the clear relation between the material distribution at the fill levels that are discharged last and segregation at complete emptying. Results for sampling at discharge in the fourth test with M8 (not given here, but see Paper IV) showed a similar trend for the size distribution of the outflow as in the first three (repeated) experiments with this mixture: The fines content was rather constant during most of the discharging process and increased at the end. Results for tracer objects (also not shown here) indicated a reduction of the live or moving volume during intermittent discharge and filling. During this part of discharge, flow was

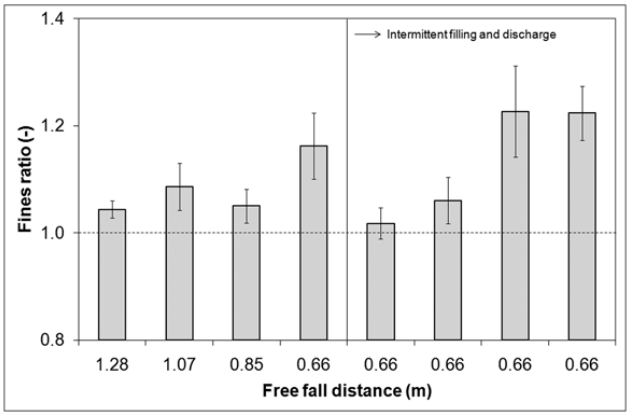

Figure 30. Effects of surface profile for powder bed on segregation at silo filling. The powder surface changes from a heap (inverted V-shape) to a V-shape as a result of material discharge, i.e., during intermittent filling and discharge.

restricted to a central channel roughly of the size of the outlet and to the surface of the powder bed, which is typical for funnel flow.

Results for many of the small silo experiments discussed so far suggest that segregation at silo filling is (strongly) affected by the free fall distance. However, definite conclusions cannot be drawn on the basis of single experiments because of the rather large variations. Therefore, the effect of the free fall distance was analyzed by use of the results for the majority of tests with mixture M8. The results of this analysis are summarized in Figure 31, which confirms that segregation does decrease with decreasing free fall distance. Similar findings were reported by Carruthers [43] for the segregation of alumina powder in large storage silos. Lower momentum for the particles suppresses the embedding mechanism and weaker air currents are induced at smaller free fall distances. Moreover, at smaller free fall distances there is less time for the powder to mix with air and this should reduce fluidization segregation. Also, fluidization caused by an abrupt change in the flow direction of the mixture at impact with the heap of previously deposited powder is decreased by the lower kinetic energy.

A similar analysis was performed for clarifying the effects of the filling rate on segregation. On the basis of the results for a majority of the experiments with mixture M8, segregation decreased with increasing filling rate at the level $h_{ff} \approx 1.25$ m, in agreement with findings reported in [41,42]. However, segregation was unaffected at smaller free fall distances

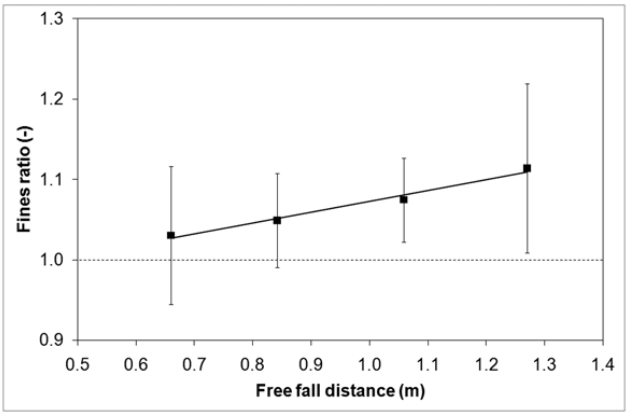

Figure 31. Effects of free fall distance on segregation at silo filling (with trend line for the mean values and error bars depicting the standard deviations). Results for the majority of experiments with mixture M8 in the small silo are included.

(h_{ff} < 0.85 m). Fluctuations in the filling rate may have affected the results of the analysis and, hence, more work is needed for elaborating the effects of this parameter on segregation at silo filling.

7.3. Hopper angle

In this subsection the effects of the hopper angle on segregation at silo emptying are discussed. Figure 32 illustrates the results for three experiments with mixtures M7 and M8, where hoppers with different angles were used. In the fifth experiment with M8 (M8/5, θ_{hopper} = 45°), where accumulation of fine particles to the silo walls occurred at all sampling levels, some rather large fluctuations (possibly partly caused by the sampling procedure) were observed during most of the discharge. An increase of the fines content similar to the first three repeated experiments (θ_{hopper} = 60°) with this mixture (cf. Figure 29b) was obtained at the end of complete emptying. This suggests that the hopper angle in a funnel flow silo does not significantly affect segregation at silo discharge and is important because the headroom required for a silo with given capacity is smaller with less steep hoppers. In existing plants, the headroom available for silos is often restricted. Moreover, it is estimated that the total investment cost for a typical construction material producing plant, where silos constitute a significant part of the processing equipment, increases by €50k when the height of the plant is

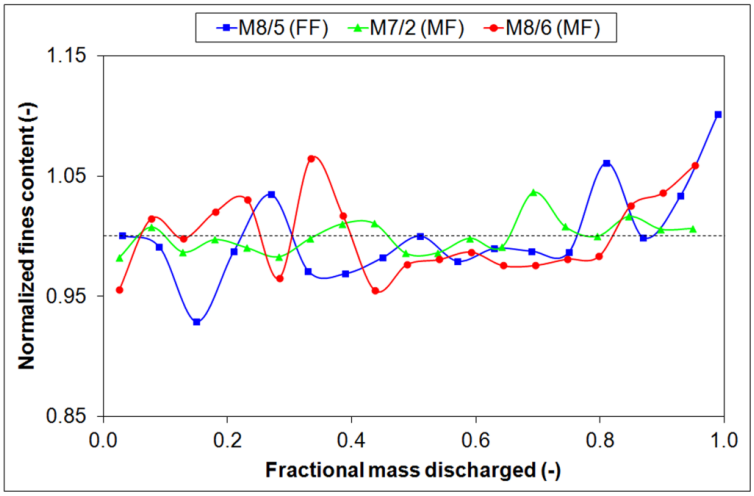

Figure 32. Effects of hopper angle on segregation at silo discharge (FF = funnel flow and MF = mass flow, see Table 6). Notation is clarified in the caption of Figure 27.

increased by one meter. The height of the plant is also usually restricted by the building permit. All of the above calls for shorter (lower) silos.

Figure 32 also depicts results for experiments with mixture M7 (M7/2) and M8 (M8/6) where a hopper (θ_{hopper} = 75°) that induces mass flow discharge of the silo contents was used. Results for filling are not elaborated here, but for M7 the material distribution was uniform at the levels that were discharged last whereas in the experiment with M8 fine particles were accumulated at the silo walls at these same levels. The difference between the results at discharge for these two experiments is fairly obvious; the fines content at the end of complete emptying was constant for M7 but increased for M8. This shows that horizontal segregation induced at the levels of fill that withdraw last is not entirely corrected for by mass flow and this is the result of the velocity gradients that always arise during the last stages of emptying in silos with this flow pattern [9,32]. The implications of this are again related to the silo height: Mass flow silos are taller than funnel flow silos of equal volume and segregation at emptying needs to be sufficiently reduced in order for the increased headroom to be justified. However, other benefits and drawbacks of mass flow (cf. Table 1) must also be kept in mind, which shows that optimal silo design is not a trivial task.

8. Regression models for segregation of powder mixtures in silos

In the experiments discussed so far, the magnitude of segregation at silo filling was qualitatively shown to depend on several factors, such as mass fraction of fines, particle size ratio or width of particle size distribution, particle solid density ratio and free fall distance. Segregation at the end of complete discharge, on the other hand, was to a large extent determined by the material distribution at filling. Little or no segregation is caused by percolation or sifting even in cases of funnel flow discharge. Moreover, mass flow silos seem incapable of completely re-mixing bulk solids at the silo outlet when considerable side-to-side segregation has occurred at filling. However, quantitative analysis is needed for this information to be disseminated and put into practical use. Based on data obtained from the experiments, this section elaborates the development of two regression models that quantitatively describe segregation at silo filling ("filling model") and at the end of complete discharge ("discharge model"). This section is essentially a summary of Paper V.

Tang and Puri [6] summarized the factors affecting the segregation of particulate solids. These include material properties, process conditions and silo parameters. Incorporating all relevant variables into models describing the related phenomena may, therefore, easily become unwieldy. The quality of fit for any model to an experimental data set may be improved by including more variables, but at some point this will result in loss of generality ("overfitting"), which should be avoided. Therefore, the aim was to find parsimonious models with reasonable descriptive capability while using a minimum number of variables. Furthermore, a goal was to use material properties, process parameters and silo characteristics that can be determined fairly easily and accurately. Procedures well-known from dimensional analysis [65] were used to derive dimensionless groups that could be combined into meaningful variables in the final models.

Results for 25 experiments in silos of different size (0.5-70 m^3) were used for parameter estimation in the filling model. This resulted in a total of 419 data points, i.e., experimental values for the mass fraction of fine particles at the silo walls. For the discharge model, the large scale (70 m^3) experiments were omitted because the hopper section, and especially its terminal construction, deviates considerably from the other silos. A total of 26 data points, or experimental values for the mass of segregated powder mixture withdrawn at the end of complete silo emptying, were available for parameter estimation in the discharge model. Schema-

tic drawings of the silos can be found in Figure 10 (large silo), Figure 13 (intermediate silo A), Figure 16 (intermediate silo B) and Figure 19 (small silo). The experimental procedures and results for the tests were elaborated in sections 5-7.

8.1. Filling

In the filling model, the quantity to be predicted is the concentration of fine particles in the vicinity of the silo walls. After extensive testing with different variables, the following initial list of variables relevant for describing the quantity of interest was arrived at

$$m_{\mathrm{f,P}} = f(m_{\mathrm{s}}, m_{\mathrm{f,tot,silo}}, m_{\mathrm{tot,silo}}, d_{50,\mathrm{c}}, d_{50,\mathrm{f}}, \rho_{\mathrm{s,c}}, \rho_{\mathrm{s,f}}, h_{\mathrm{ff}}, D_{\mathrm{silo}}, d_{\mathrm{inlet}}) \quad (1)$$

where $m_{\mathrm{f,P}}$ expresses the mass of fines in samples collected at the silo wall, m_{s} is the sample mass, $m_{\mathrm{f,tot,silo}}$ denotes the total mass of fine particles according to the formulation for the mixture in a full silo, $m_{\mathrm{tot,silo}}$ is the capacity of the silo expressed in units of mass (which for a specific silo depends on the mixture used), d_{50} and ρ_{s} are the median particle size and particle solid density, respectively, for the coarse (subscript c) and fine (subscript f) fraction. h_{ff} denotes the free fall distance at the time of sampling, D_{silo} the silo diameter and d_{inlet} the inlet diameter. Figure 33 further explains the meaning of these and other variables used in both models. The particle shape was not considered in the filling model, because mainly cubic particles (with the exception of fibers) were included in the powder mixtures.

Following the rules of dimensional analysis [65], an expression composed of only dimensionless groups was obtained from Eq. (1)

$$\frac{m_{\mathrm{f,P}}}{m_{\mathrm{tot,silo}}} = f\left(\frac{m_{\mathrm{s}}}{m_{\mathrm{tot,silo}}}, \frac{m_{\mathrm{f,tot,silo}}}{m_{\mathrm{tot,silo}}}, \frac{d_{50,\mathrm{c}}}{d_{50,\mathrm{f}}}, \frac{\rho_{\mathrm{s,c}}}{\rho_{\mathrm{s,f}}}, \frac{h_{\mathrm{ff}}}{D_{\mathrm{silo}}}, \frac{D_{\mathrm{silo}}}{d_{\mathrm{inlet}}}\right) \quad (2)$$

This can be expressed compactly as

$$Z = f(X_1, X_2, X_3, X_4, X_5, X_6) \quad (3)$$

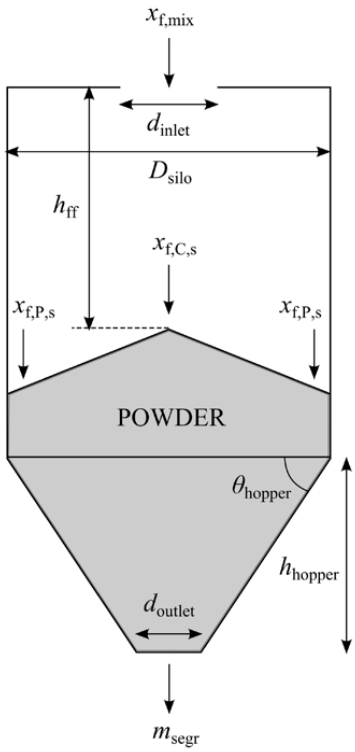

Figure 33. Schematic of silo and clarification of notation used in the regression models.

i.e., the dimensionless term Z is described by some function of the dimensionless groups X_1-X_6. Based on extensive testing with different models, the following equation was found to describe the relation

$$\frac{Z}{X_1} = \alpha_1 + \alpha_2 X_2 + \alpha_3 X_3 + \alpha_4 X_4 + \alpha_5 X_5 + \alpha_6 X_6 \qquad (4)$$

The dimensionless term on the left-hand side, Z/X_1, now expresses the mass fraction of fine particles in samples collected from the vicinity of the silo walls ($x_{f,P}$). Eq. (4) can be expressed in vector form as

$$\mathbf{Y} = \mathbf{X}\boldsymbol{\alpha} \qquad (5)$$

where $\mathbf{Y}$ and $\boldsymbol{\alpha}$ are vectors expressing the fines content at the silo wall and the parameters of the model, respectively, and $\mathbf{X}$ is the matrix that summarizes the numerical values for the selected dimensionless groups in each experiment. The model parameters $\boldsymbol{\alpha}=(\alpha_1, \alpha_2, \alpha_3, \alpha_4, \alpha_5, \alpha_6)^T$ are estimated by least sum of squares fitting to the experimental data using

$$\hat{\boldsymbol{\alpha}} = (\mathbf{X}^T\mathbf{X})^{-1}(\mathbf{X}^T\mathbf{Y}) \quad (6)$$

where $\hat{\boldsymbol{\alpha}}$ denotes the estimated parameter vector.

The numerical values for the mass fractions of fine particles at the silo walls that were used for parameter estimation (denoted by $x_{f,P,exp}$) were calculated from the fines contents of samples collected in the silo centre and at the silo walls ($x_{f,C,s}$ and $x_{f,P,s}$, respectively, in Figure 33) during the experiments by

$$x_{f,P,exp} = x_{f,mix} + (x_{f,P,s} - x_{f,C,s}) \quad (7)$$

In other words, the difference in the sampled values was added to the fines content of the mixture according to formulation ($x_{f,mix} = m_{f,tot,silo}/m_{tot,silo}$). This procedure was adopted because in some experiments both $x_{f,C,s}$ and $x_{f,P,s}$ exceeded (or fell short of) $x_{f,mix}$, but the fines content was higher (or lower) in the silo centre. In such cases, simply comparing $x_{f,P,s}$ with $x_{f,mix}$ would have suggested that fines were accumulated peripherally (centrally) when, in fact, the opposite may have occurred. In the experiments, the weight based mean fines contents at discharge were not identical to the fines contents as determined from the raw materials' size distributions and mass fractions of the mixtures; both lower and higher mean values were obtained. This indicates fluctuations in the raw material properties and/or particle attrition and breakage during mixing. Expressing the experimental values for the fines content at the silo wall ($x_{f,P,exp}$) according to Eq. (7) was therefore considered the best solution.

Results of the filling model are illustrated in Figure 34, which depicts modeled (Y_{model}) versus experimental ($Y_{experiment}$) values and shows that the overall fit for the model is quite good ($R^2 = 0.90$). As evident from the figure, there seems to be a reasonable agreement between model and experiments in the range $Y = 0.25$-0.70. The model over-predicts the fines content at the silo wall in the lower ($Y < 0.25$) and upper ($Y > 0.70$) ends of the range, as indicated by the clusters of data points in the lower left and upper right corner, respectively, in Figure 34.

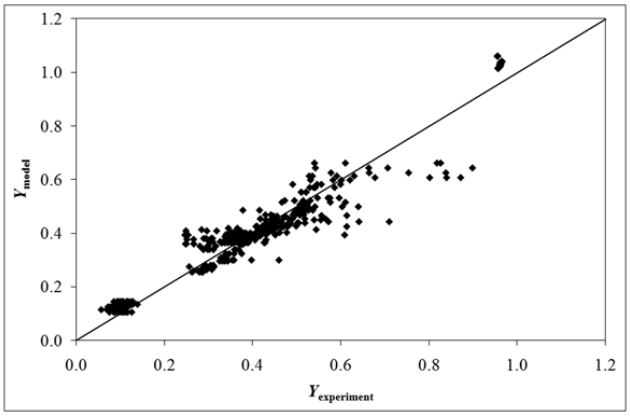

Figure 34. Results for the filling model: predicted fines content at silo walls versus experimental values (R^2 = 0.90).

These data points correspond to experiments where fine particles were accumulated at the filling point (low fines content in the mixture and low *Y*-values) or where no segregation occurred at filling (high fines content in the mixture and high *Y*-values). Sifting and rolling segregation are the main reasons for the former. For the latter, the model predicted fines contents above 100 %, which is infeasible. Some data points originating from experiments with mixtures including intermediate amounts of fines ($x_{f,mix}$ = 0.25-0.51) are under-predicted by the model (Y_{model} = 0.25-0.70, $Y_{experiment}$ = 0.25-0.90), but these are the result of very strong accumulation of fines at the silo walls. The magnitude of segregation was not always accurately captured by the model in these cases, but considerable levels of segregation were still predicted. This can be considered sufficient for practical cases, where information regarding the trend is as important as the absolute value.

Table 7 presents the numerical values for the parameters of the filling model ($\hat{\boldsymbol{\alpha}}$). With the exception of $\hat{\alpha}_1$ that acts as a bias, all parameters ($\hat{\alpha}_2$-$\hat{\alpha}_6$) obtain positive values. This was ascertained by determining 95 % confidence intervals for each parameter according to procedures given in [66]. The lower limits for the parameters $\hat{\alpha}_2$-$\hat{\alpha}_6$ were clearly positive and the upper limit for $\hat{\alpha}_1$ was negative. The signs for the parameters $\hat{\alpha}_2$-$\hat{\alpha}_6$ suggest that segregation increases with an increase in any of the dimensionless groups (X_2-X_6), which is partly consistent with the findings of other investigators.

Table 7. Parameter values and ranges for the dimensionless groups in the filling model.

Parameter	$\hat{\alpha}_1$	$\hat{\alpha}_2$	$\hat{\alpha}_3$	$\hat{\alpha}_4$	$\hat{\alpha}_5$	$\hat{\alpha}_6$
Value	-0.4018	1.1629	0.0009	0.1503	0.0361	0.0237
Dimensionless group		X_2	X_3	X_4	X_5	X_6
Range		0.11-0.96	6.7–206.6	0.9–2.3	0.0–3.7	2.6–11.8

For free flowing materials, segregation generally increases with increasing particle size ratio ($d_{50,c}/d_{50,f}$) as summarized by Tang and Puri [6]. The current experiments included both free-flowing and cohesive materials, but the same conclusion can still be drawn here. Mosby [7] performed experiments with alumina (fine component) and sand (coarse component) in heap segregation testers with minimal free fall distance. He concluded that segregation increased with increasing heap length or horizontal dimension of the tester for mixtures with low alumina content (approx. < 10 %-wt). Increasing the heap length in a segregation tester is basically equivalent to increasing the ratio between silo diameter and inlet diameter (D_{silo}/d_{inlet}). The results presented here are therefore consistent with Mosby's findings for mixtures with low fines content. Both Tang and Puri [6] and Drahun and Bridgwater [11] stressed the importance of considering the particle solid density for segregation especially in systems involving filling with free fall. Experiments included in this work show that segregation is clearly aggravated by decreasing the solid density for the fine component to well below that of the coarse component ($\rho_{s,c}/\rho_{s,f} > 2$) and this is also consistent with the model. The effect of free fall distance, in turn, seems to be more case specific [6,11]. Based on results presented in section 7, segregation defined as accumulation of fine particles to the silo walls clearly increases with increasing free fall distance or increasing h_{ff}/D_{silo} for many of the materials tested. However, at very low free fall distances (approx. < 0.5 m) in all silo scales, fine particles were quite often concentrated at the filling point because of sifting and rolling. This could also be correctly captured by the model in many cases because of the negative $\hat{\alpha}_1$.

The filling model suggests that the fines content at the silo wall ($x_{f,p}$) increases with increasing fines content ($\hat{\alpha}_2>0$). While this is true for some mixtures, the effect of this variable is more complex and cannot be examined without reference to other material properties. Consider the binary mixture M1 with low fines content ($x_{f,mix}$ = 11 %-wt), significant size ratio ($d_{50,c}/d_{50,f}$ = 76) and roughly equal solid densities ($\rho_{s,c}/\rho_{s,f}$ = 0.9) for the constituent fractions.

Segregation as a result of sifting and rolling led to accumulation of fines at the heap apex ($x_{f,P} < x_{f,mix}$) regardless of the free fall distance in the small silo. As the fines content for this binary mixture was increased to $x_{f,mix}$ = 31 %-wt (mixture M2), no significant segregation occurred and a relatively uniform material distribution ($x_{f,P} \approx x_{f,mix}$) was obtained in the small silo, again nearly regardless of the free fall distance. When the mass fraction of fine particles was increased to 51 %-wt (mixture M3), considerable accumulation of fines at the silo walls ($x_{f,P} > x_{f,mix}$) was observed at all levels of silo fill. Results for mixtures M1-M3 are therefore consistent with the statement that the fines content at the silo walls increases with increasing mass fraction of fines. Data in the interval $x_{f,mix}$ = 32-50 %-wt was not available for this type of mixture (sand/cement, $d_{50,c}/d_{50,f}$ = 76 and $\rho_{s,c}/\rho_{s,f}$ = 0.9), because of the limited number of experiments that could be performed with it. However, on the basis of the results for mixtures M1-M3 (and especially for M2 and M3), it can be assumed that segregation with accumulation of fine particles to the silo walls starts occurring and is aggravated when the fines content is increased within the aforementioned range ($x_{f,mix}$ = 32-50 %-wt). Considering the nature of segregation by the embedding, fluidization and air current mechanisms, it would not be surprising to see this type of segregation increasing even further when increasing the fines content beyond 51 %-wt for mixtures with considerable size ratios ($d_{50,c}/d_{50,f} \geq 76$) and particles with similar solid density ($\rho_{s,c}/\rho_{s,f}$ = 0.9-1.1).

However, it is not clear whether side-to-side segregation with accumulation of fines away from the filling point would occur at all if the mean particle size of a bulk solid is either decreased or increased substantially from that of the mixtures considered above. In fact, for the former case Carson [14] reported that fluidization resulted in vertical segregation with accumulation of fine particles in the topmost layers of the powder bed at pneumatic filling of silos. He concluded that top-to-bottom segregation most often occurs with mixtures of mean particle sizes less than about 100 µm, without reference to particle size distribution or particle solid densities. This vertical segregation may also be caused by a continuous filling, where some material remains fluidized throughout the filling process. On the other hand, when the mean particle size for a bulk solid clearly exceeds that of the mixtures M1-M3, the influence of embedding, fluidization and air-current effects on the material distribution may well be minor in comparison to other segregation mechanisms such as percolation, sifting, rolling and trajectory.

The mass fraction of fine particles had practically no effect on the material distribution when the particle size ratio for mixtures was significantly reduced to $d_{50,c}/d_{50,f} < 9$ from the aforementioned value of $d_{50,c}/d_{50,f} = 76$. In the experiments, a uniform material distribution was always observed regardless of the free fall distance for the binary mixture M4 with $x_{f,mix} = 50$ %-wt in the small silo and the commercial product I3 with $x_{f,mix} = 96$ %-wt in intermediate silo B. These two mixtures are also characterized by the absence of significant particle solid density differences. Interestingly, the given upper limit for the size ratio far exceeds reported values for percolation or sifting segregation for which size ratios as low as 2:1 are claimed to be sufficient [6]. This discrepancy can be explained by the fact that in the current experiments different mechanisms (embedding, fluidization and air-current effects) were mostly responsible for inducing the segregation and also by the rather wide particle size distributions for the raw materials comprising the mixtures. The wide size distributions lead to an overlapping of the particle sizes for the constituent components. Therefore, binary mixtures with small particle size ratios yield continuous particle size distributions instead of distinctly separate fractions. Moreover, the commercial product I3 has a continuous size distribution because several (> 5) raw materials of different size distribution are included.

On the other hand, experiments in the small silo with binary mixtures M5 ($x_{f,mix} = 47$ %-wt) and M6 ($x_{f,mix} = 25$ %-wt) showed that accumulation of fine particles away from the filling point increased with increasing fines content. Both mixtures are characterized by a rather small particle size ratio ($d_{50,c}/d_{50,f} = 7$), but significant particle solid density ratio ($\rho_{s,c}/\rho_{s,f} = 2.3$). In the experiments, considerably stronger accumulation of fine particles at the silo walls was determined for M5. Interestingly, an excess of fine particles was also clearly observed at the silo walls for mixture M6, which implies that the critical fines content for the occurrence of this type of segregation is also governed by the particle size and solid density ratio.

The effect of filling rate was also investigated, but including this as a variable did not improve the quality of the filling model. In some cases where the effect of the feeding rate could be isolated from the other variables, i.e., in small scale experiments with identical mixture (M8), silo parameters and free fall distance, a decreasing trend with increasing filling rate could be seen, but in other cases segregation was not significantly affected (see section 7.2). This agrees with some previously reported findings for free flowing materials [11], but disagrees with the conclusions of other investigators [33,41,42]. In industrial production of construction

materials, the feeding rate for product silos is closely associated with other factors, such as batch mixing time, plant through-put rate and constraints imposed by other equipment (belt conveyors, bucket elevators, etc.). Even in the case that segregation could be reduced by increasing or decreasing the feeding rate, it is not necessarily a straightforward task to alter this process variable in industrial settings.

8.2. Discharge

The purpose with the discharge model was to predict the mass of segregated powder (m_{segr}) withdrawn from the silos at the end of complete discharge. Therefore, a criterion had to be defined for determining the point, e.g., the mass of material left in a silo, at which the outflow becomes segregated beyond a level that can be accepted. Figure 35 exemplifies the procedure used here. The upper and lower acceptance limits for the mass fraction of fines were set at ± 2 %-wt units from the mean value at discharge ($\bar{x}_{\mathrm{f,disch}}$) in each experiment. m_{segr} takes a positive value when the fines content exceeds the upper limit and a negative value when the fines content decreases below the lower limit. Whenever the fines content stays within the limits, $m_{\mathrm{segr}} = 0$. A similar procedure is applied in practice when checking the size distribution of final products for conformity to specification at construction material producing plants. (Fines contents according to size specifications for the products are used instead of the mean mass fractions of fine particles at silo discharge.)

The initial set of relevant variables for determining the mass of segregated mixture (m_{segr}) obtained at the end of complete silo emptying was defined as

$$m_{\mathrm{segr}} = f(m_{\mathrm{f,tot,silo}}, m_{\mathrm{tot,silo}}, m_{\mathrm{f,P}}, m_{\mathrm{s}}) \tag{8}$$

where $m_{\mathrm{f,tot,silo}}$ is the total mass of fines in a full silo, $m_{\mathrm{tot,silo}}$ denotes the silo capacity in units of mass, $m_{\mathrm{f,P}}$ expresses the mass of fine particles in samples collected at the silo walls and m_{s} is the sample mass.

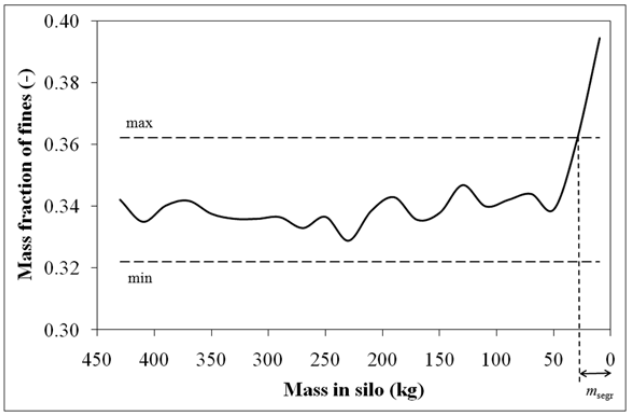

Figure 35. Procedure used for determining the mass of segregated material (m_{segr}) at the end of emptying in the discharge model. Minimum and maximum limits are given by $\bar{x}_{\mathrm{f,disch}} \pm 0.02$.

It is rather straightforward to apply dimensional analysis to the formulation in Eq. (8) as only variables expressing masses are included. Combining the dimensionless groups resulting from substitution of the unit of mass with $m_{\mathrm{tot,silo}}$ finally yields

$$\frac{m_{\mathrm{segr}}}{m_{\mathrm{tot,silo}}} = f\left(\frac{x_{\mathrm{f,P}}}{x_{\mathrm{f,mix}}}\right) \tag{9}$$

or simply

$$\tilde{Y} = f(\tilde{X}_1) \tag{10}$$

In other words, the fraction of segregated material withdrawn from the silo at the end of complete discharge is determined by some function of the ratio between the fines content at the silo wall ($x_{\mathrm{f,P}}$) and the fines content of the mixture according to the formulation ($x_{\mathrm{f,mix}}$). A simple linear model was proposed to describe this relation

$$\tilde{Y} = \beta_0 + \beta_1 \tilde{X}_1 \tag{11}$$

which is expressed more compactly as $\tilde{\mathbf{Y}} = \tilde{\mathbf{X}}\boldsymbol{\beta}$. Numerical values for the parameters $\boldsymbol{\beta}=(\beta_0,\beta_1)^{\mathrm{T}}$ were obtained with the method of least sum of squares as given in Eq. (6).

The numerical values for $x_{f,P}$ were again determined according to Eq. (7) (and are denoted by $x_{f,P,exp}$). However, only one value can be specified for this variable per experiment in the discharge model. For a given powder mixture and silo, this variable may depend on the free fall distance or level of fill in the silo according to results presented in section 7.2, which raises the question of how an appropriate value should be chosen. In experiments with funnel flow discharge, $x_{f,P,exp}$ was determined by samples collected from the transition point between hopper and vertical section, while in experiments with mass flow the results for the last material filled into the silo were used. The reason for this choice is the observation that segregation at discharge depends on the material distribution at the level of fill from which material discharges last and that no significant further segregation, such as percolation or sieving, occurs during emptying. In the small silo experiments where tracer objects were used, the last material to discharge could be determined quite accurately. In experiments without tracers, the discharge pattern was deduced in a number of different ways including visual observations, utilization of color pigments, and comparison of the hopper angle with the critical hopper angle required for mass flow with the material used in the experiment.

Figure 36 illustrates the overall results for the discharge model and indicates that it is in general but not in very good agreement with experimental data ($R^2 = 0.70$). The parameter values ($\hat{\beta}_0 = -0.275$ and $\hat{\beta}_1 = 0.282$, signs confirmed with 95 % confidence intervals [66]) suggest that only a small portion of the silo's total capacity (< 1 %-wt or $m_{segr}/m_{tot,silo} \approx 0$) will be segregated at the end of complete emptying, when the fines content next to the silo walls equals the fines content of the mixture ($x_{f,P}/x_{f,mix} = 1$) at the level of fill from which material withdraws last. Accumulation of coarse particles in this region leads to depletion of fines towards the end of discharge ($m_{segr} < 0$). A surplus of fines gives a positive value for m_{segr} and the magnitude increases (linearly) with increasing values for the ratio $x_{f,P}/x_{f,mix}$. The model is obviously affected by the procedure chosen for determining m_{segr} (cf. Figure 35).

A model including the hopper height (h_{hopper}) and the critical height required for mass flow (h_{cr}) (calculated from the theory by Jenike [48] and the geometry of the silo in question) as independent variables was also tested. Dimensional analysis put forth h_{cr}/h_{hopper} as a dimensionless group, which expresses the closeness of the hopper section to mass flow design ($h_{cr}/h_{hopper} \geq 1$ indicating mass flow). Even though this model resulted in a small increase in the explained variance ($R^2 = 0.72$) and the parameter associated with this variable obtained a positive value, the lower limit for the 95 % confidence interval for the parameter was clearly

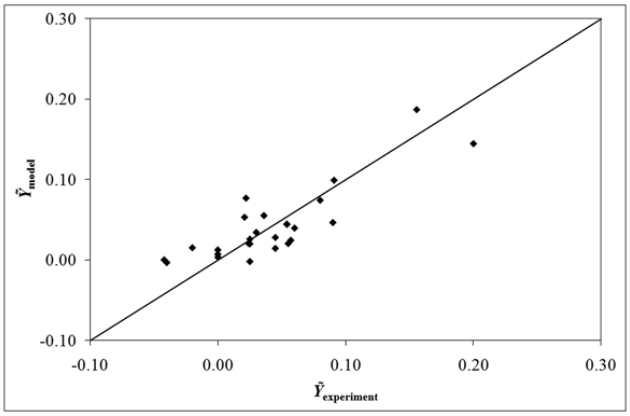

Figure 36. Results for the discharge model, i.e., normalized mass of segregated material withdrawn at the end of complete silo discharge predicted by the model versus experimental values ($R^2 = 0.70$).

negative. Therefore, it can be concluded that segregation towards the end of complete discharge is mainly determined by the material distribution at the level of fill from which material discharges last, while the discharge flow pattern (mass flow or funnel flow) has a much smaller effect. This finding is interesting since mass flow designs have been reported to correct for side-to-side segregation induced at silo filling by re-mixing the material at the outlet during discharge [6]. The explanation lies with velocity gradients that arise during the later stages of complete silo discharge, i.e., after the material surface has descended below $0.5D_{silo}$-$1.0D_{silo}$ from the transition point between hopper and cylindrical section [32]. While it was pointed out that these velocity gradients may cause sifting segregation due to inter-particle motion, the majority of particulate solids used in the present experiments do not fulfill the requirements of sufficiently large mean particle diameter and free flowing material for the occurrence of this segregation mechanism as defined in [13]. Even though the current data set contains only two experiments with mass flow discharge of the silo contents (both in the small silo), segregation at the end of complete discharge was rather well described by the proposed model including only one dimensionless group ($x_{f,P}/x_{f,mix}$ or $\tilde{X}_1$ in Eq. (11)).

One implication of the aforementioned finding is that that mass flow silos used for handling of particulate solids that are prone to segregate in a side-to-side pattern with accumulation of fine particles at the silo walls should be filled as full as possible at the end of the filling procedure. In such cases, segregation at the end of emptying should be reduced by a mass flow

discharge pattern because the material filled into and withdrawn from the silo last will be less segregated as a result of a smaller free fall distance.

Even though the discharge model yields results only in general agreement with the experimental data, the effect of the material distribution induced at silo filling on segregation at the end of complete silo discharge was demonstrated. The same conclusion was also presented qualitatively by Kwade and Ziebell [38], who investigated segregation of a multi-phase plaster (construction material) in a silo with capacity > 100 t. An estimate of segregation at the end of silo discharge can, therefore, be obtained with the filling model presented in the previous subsection together with knowledge of the overall discharge flow pattern. In principle, a regression model could have been derived to describe segregation at the end of complete discharge with the dimensionless groups of the filling model, but this appeared impossible in practice because of the limited number of experiments, i.e., data points for discharge. Such a model is presented in the next section, where segregation data for a construction material plant is analyzed.

9. Analysis of segregation data for a production plant

The work presented in this section is a summary of Paper VI, where segregation data for seven different commercial products were collected for a period exceeding one year. The goal of this investigation was to clarify the differences in the observed magnitude of segregation between the products and the reasons behind these differences. The data consist of segregated masses of products withdrawn at the end of complete discharge from a product silo situated upstream of packing (cf. Figure 2). For all products the mass fraction of fine particles increases to levels exceeding the quality requirement limits at the end of complete emptying. Preliminary tests for sifting segregation and fluidization were performed for a subset of the products with the aim of predicting the segregation pattern in the product silo a priori and differentiating between the products' segregation tendencies. These studies underlined the difficulties in translating to industrial practice the results obtained with standard lab-scale segregation testers such as those presented in [7,10,67,68]. Results for experiments with binary powder mixtures in the small silo (section 7.1) and experimental results from another construction material producing plant were utilized in the development of a regression model capable of differentiating between the products' tendency to segregate. Furthermore, the reasons for considerable variations in the magnitude of segregation for each product were elaborated and possible alternatives for retrofitting the silo for reduction of segregation are briefly discussed. It is noted that results for sampling campaigns with some of the commercial products (here denoted P1, P2, P5 and P7) were presented in section 5.1, where the products were identified differently (as L4, L3, L2 and L1, respectively).

Table 8 gives the particle size distributions for the products according to specifications and Table 9 summarizes additional material properties. Flow properties for the products were measured with a shear cell and the critical hopper angles (θ_{cr}) required for mass flow determined according to [48]. Mean particle sizes for the fractions < 0.125 mm ($d_{50,f}$) were determined with laser diffraction after representative samples of the products had passed through a 0.125 mm sieve. Average particle sizes for the coarse fractions, i.e., particle sizes > 0.125 mm, were calculated from the size specifications for the products given in Table 8. Apparent particle solid densities for the fine fractions ($\rho_{s,f}$) were determined with a helium-air pycnometer (after representative samples had passed through a 0.125 mm sieve). The term "apparent solid density" is used here as the fine fractions of the products consist of different raw materials and results obtained with the pycnometer therefore represent mean particle solid

Table 8. Mass based (%-wt) cumulative particle size distributions according to specifications for the commercial products (P1 = L4, P2 = L3, P5 = L2 and P7 = L1 in section 5).

Product	Size (mm)				
	< 0.125 [a]	< 0.25	< 0.5	< 1	< 2
P1	22	32	53	81	100
P2	30	43	62	95	100
P3	42	54	74	96	100
P4	56	69	91	100	
P5	57	73	95	100	
P6	62	86	95	100	
P7	85	97	100		

a. Mass fraction of fine particles denoted $x_{f,mix}$.

Table 9. Critical hopper angles for mass flow, mean particle sizes, solid densities and mass fractions of fibers for the commercial products.

Product	θ_{cr} [a] (°)	$d_{50,f}$ (µm)	$d_{50,c}$ (µm)	$\rho_{s,f}$ (kg/m^3)	x_{fibers} (%-wt)
P1	67	11	643	2821	0.0
P2	69	14	545	2694	0.0
P3	69	14	463	2825	0.2
P4	70	17	352	2676	0.0
P5	69	18	313	2662	0.4
P6	- [b]	16	224	2793	0.0
P7	71	20	203	2716	0.0

a. Valid for stainless steel and measured from the horizontal plane.
b. Not determined.

densities. Products P3 and P5 include small amounts of synthetic fibers (see Figure 1). The coarser components for all products consist mainly of different sand and limestone size fractions with similar particle solid density ($\rho_{s,c} \approx 2800$ kg/m^3).

A schematic drawing of the product silo is illustrated in Figure 10. On the basis of the determined values for θ_{cr}, the lower part of the hopper section enables mass flow for nearly all products, but the hopper angles for the upper hopper section (65° and 58° from the horizontal plane) are not steep enough to give mass flow for any of the products. Therefore, expanded flow most likely occurred at discharge (cf. Figure 6) meaning that material from the vicinity of the silo walls in the upper part of the hopper section and lower parts of the vertical section

(stagnant zone) were withdrawn last at complete emptying. Other features related to the operation of the product silo were elaborated in section 5.1. Moreover, it must be mentioned that, during normal production conditions, sample bags are collected at random from the different outlets for quality control of the final products.

Figure 11 illustrates results for the sampling campaigns with products P1 (L4), P2 (L3), P5 (L2) and P7 (L1) that were discussed in section 5.1. In these studies, sacks of final products were taken from the middle outlet of the product silo throughout the emptying process. The results show that the mass fraction of fine particles was rather stable during most of the discharge and increased to above the quality requirement limits for all products at the end of complete silo emptying. As the fines content for the outflow exceeds the upper quality limit for a product, the residual silo content (m_{segr}) must be rejected and is later introduced into the process as raw material. Data (m_{segr}) was obtained from daily production reports for the plant for a period exceeding one year (January 2009 - March 2010) with a minimum of five production runs for each product and a total of 110 runs for all products. The sizes of the production runs varied in the range 20-370 t. As mentioned above, during normal production conditions, sample bags of 25 kg are collected randomly from the different silo outlets for quality control of the size composition for the outflow. Samples of 1-2 kg are collected from each bag and even smaller masses (100 g) are sieved. No sample splitters are used for reducing the sample size. Preliminary analysis of the data revealed some differences in m_{segr} between the products, but these were difficult to analyze because of considerable variations in m_{segr} for each product. Possible reasons for variations in m_{segr} for each product are discussed next and differences in m_{segr} between products are elaborated later.

9.1. Reasons for variations

A possible explanation for considerable variations in m_{segr} for each product could be the size of the production run. Figure 37 depicts m_{segr} for product P2 for the runs included in the data and shows that the variations are clearly not caused by the total amount of material processed in the silo, so other explanations must be sought. Variations in the silo input for P2 are elaborated in Figure 38 showing the mass fraction of fine particles for samples collected from the belt conveyor situated downstream of the mixer during a period of six months (September

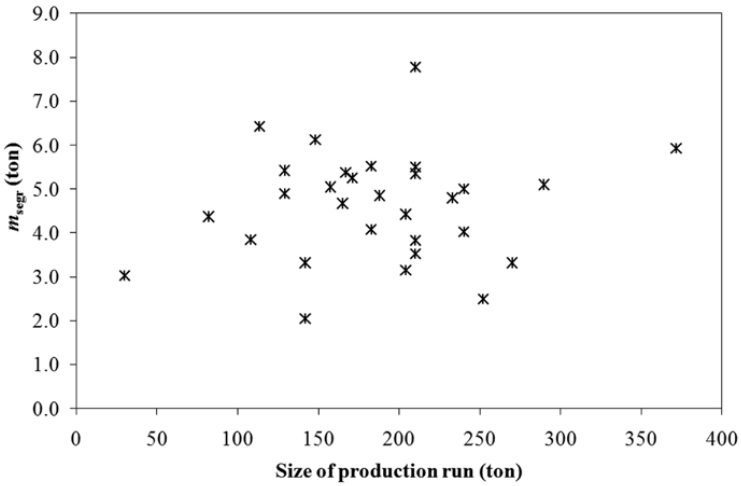

Figure 37. Rejected masses (m_{segr}) versus production run size for product P2.

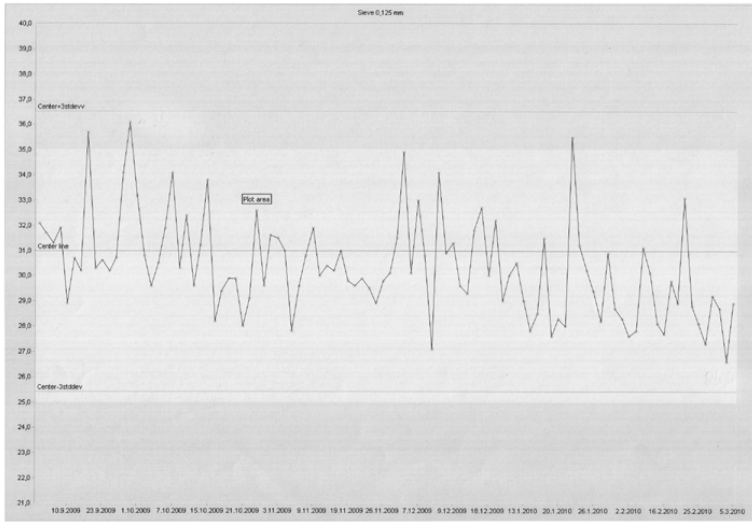

Figure 38. Variations for the fines content (mass fraction below 0.125 mm) in the silo input for product P2 during a period of six months with minimum and maximum fines content of 26.6 and 36.1 %-wt, respectively. Mass fraction of fines according to specifications for P2 is 30 %-wt, i.e., not indicated by the line marked “Center line”.

2009 - February 2010). These samples were taken at arbitrary moments and it was not possible to relate the samples to individual production runs. Nevertheless, the figure illustrates considerable variations in the size distribution for the silo input with a minimum and maximum mass fraction below 0.125 mm for the samples of 26.6 and 36.1 %-wt, respectively, during the inspected period. Such variations can be caused by varying raw material size distributions, segregation in raw material silos, and particle attrition and breakage during mixing, but apparently not by ambient air humidity (normally higher during the fall in the northern hemisphere) on the basis of the results.

Figure 12 shows the distribution of fine particles for product P2 (L3) in the product silo as a result of filling for the sampling campaign discussed in section 5.1. The material distribution was very non-uniform in the horizontal direction and the concentration of fine particles was different at opposite sides of the silo walls at the same level of fill. During discharge, the three parallel outlets presumably draw material from different regions of the silo cross section. The outer bag fillers (outlets) are most likely provided with more material from the vicinity of the silo walls whereas the middle outlet includes more material from the silo centre. The non-uniform initial material distribution and preferential draw from varying cross sectional positions to the different outlets influence the size composition of sample bags picked (randomly from different outlets) for quality control of the final products.

The combined effect of the size distribution for the silo input and sampling at random from the different silo outlets is illustrated in Figure 39, where the cumulative undersize of 0.125 mm during discharge in a separate sampling campaign for product P2 is shown. Quite large variations in the mass fraction of fine particles occurred during most of the discharge largely because of the sampling procedure and a surplus of fines was withdrawn at the end of complete emptying. However, the upper quality limit was not exceeded ($m_{segr} = 0$) as a result of the relatively low overall fines content (27 %-wt on average for all samples collected at discharge) for this production run. Comparison with the results for P2 presented in Figure 11c, with sample collection from the middle outlet only, shows the marked effect of the fines content in the input (mean value of 31 %-wt for all samples in this campaign) and the sampling strategy. The increase of the fines content towards the end of discharge and, therefore, the value obtained for m_{segr}, must be affected by the origin, i.e., center versus outer outlet, of the last samples. Because of this, it is reasonable to assume that the same value for m_{segr}

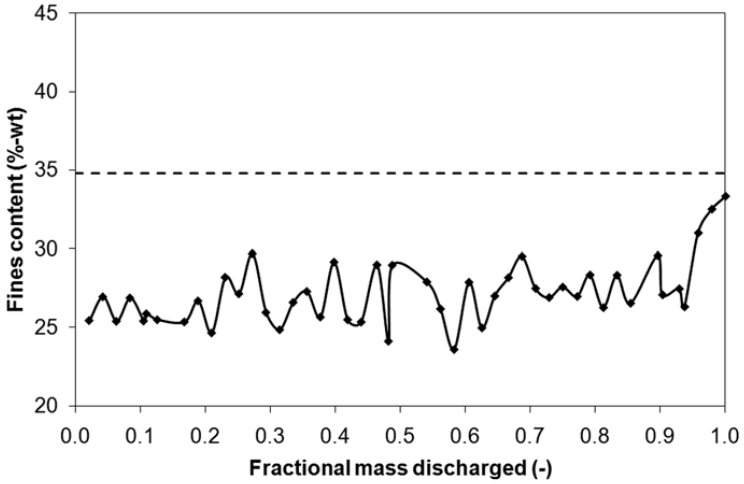

Figure 39. Result from a sampling campaign for product P2 with collection of samples at random from the different silo outlets during the discharging process. Upper quality requirement limit for the fines content (mass fraction below 0.125 mm) according to size specifications for P2 indicated by dashed line. Fractional mass discharged is elaborated in the caption of Figure 27 ($m_{tot,exp}$ = 239 t here).

would not necessarily be obtained for two different production runs of the same product even with identical fines content in the input.

Aside from the sampling strategy, the fact that no sample splitters are used for reducing the sample size for sieving analysis may also influence the determined magnitude of m_{segr}. Although this will result in some additional inaccuracy, it is believed to have a minor effect in comparison with the other sources of error discussed above. The products are also produced with different "recipes", e.g., with small amounts of rejected product used as raw material, but no correlation between the recipes used in the production runs and segregation could be seen.

9.2. Model of segregation

In section 8 of this thesis, it was shown that segregation at silo filling can be described with dimensionless groups consisting of mass fraction of fine particles ($x_{f,mix}$), particle size ratio ($d_{50,c}/d_{50,f}$), particle solid density ratio ($\rho_{s,c}/\rho_{s,f}$), ratio between free fall distance and silo diameter (h_{ff}/D_{silo}), and ratio between silo diameter and inlet diameter (D_{silo}/d_{inlet}). The concen-

tration of fine particles next to the silo walls was shown to increase with an increase in any of the dimensionless groups. Moreover, segregation at silo discharge was shown to be largely determined by the material distribution resulting from filling. The last two of the aforementioned dimensionless groups relate to silo properties and are identical for the current analysis. Therefore, a regression model is pursued that describes segregation at silo discharge on the basis of the rest of the (material dependent) dimensionless groups.

Based on results presented in section 7.1, the particle solid density ratios for the commercial products ($\rho_{s,c}/\rho_{s,f} \approx 0.99\text{-}1.05$, cf. Table 9) are rather close to unity and, therefore, the effect of this variable on segregation can be neglected here. The particle size distribution is continuous for all products and the particle size ratio ($d_{50,c}/d_{50,f}$) is thus inversely proportional (correlation coefficient = -0.94) to the mass fraction of fines ($x_{f,mix}$). Hence, it should be possible to correlate segregation with the fines content for the products. Mean segregated masses ($\bar{m}_{segr}$) versus mass fraction of fines for the products can be studied in Figure 40, where all production runs of the data have been included. Some interesting tentative conclusions can be drawn from this figure. Based on $\bar{m}_{segr}$ the products can be organized into three main groups with respect to segregation tendency: high (P2), moderate (P1, P3 and P5) and low (P4, P6 and P7). $\bar{m}_{segr}$ seems to decrease with increasing $x_{f,mix}$, or with decreasing width for particle size distribution because of the correlation, but P1 segregates less than P2 on average although the former product has a wider particle size distribution.

Segregation is also clearly aggravated by the presence of fibers (cf. Table 9, mass fraction of fibers denoted x_{fibers}), which is most vividly illustrated by comparing $\bar{m}_{segr}$ for products P4-P6 in Figure 40. The reasons for this are not entirely clear, but fibers may induce stronger segregation at filling because of their elongated shape, low solid density and tendency to form networks or large sized pseudo-particles that increases the drag force. On the basis of visual observations, for example, during sieving, the smaller particles of the powder mixtures seem to be more affected by the presence of fibers and were, in fact, often seen to "follow" the fibers during motion. The presence of fibers in a product also increases the cohesiveness (confirmed by shear cell testing) with possible consequences on the flow profile at discharge, e.g., steeper drained angles of repose may form at emptying. On the basis of all these qualitative findings a regression model for m_{segr} including linear terms for the effect of $x_{f,mix}$ and x_{fibers} was tested, but gave very poor agreement with the data ($R^2 = 0.16$).

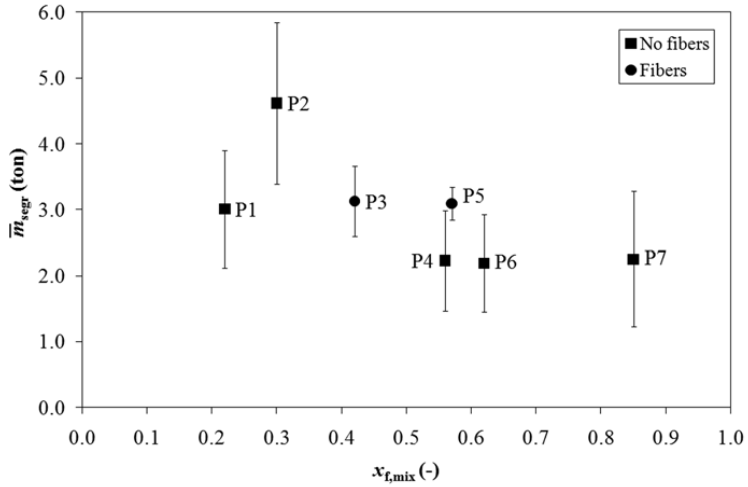

Figure 40. Average rejected product masses ($\overline{m}_{segr}$) for all production runs versus mass fraction of fines ($x_{f,mix}$) for the commercial products. Error bars depict the standard deviation for a minimum of five runs with each product.

Results presented in section 7.1 also showed that the fines content observed at the silo walls during filling increases with increasing fines content in a certain range ($x_{f,mix} \approx$ 10-50 %-wt) when other material properties, i.e., composition as well as particle size and solid density ratio, are constant. Sifting segregation (surplus of fines at the filling point) in fact occurred for the binary mixture M1 with $x_{f,mix}$ = 11 %-wt. The given limits for $x_{f,mix}$ are valid mainly for binary mixtures with considerable particle size ratios ($d_{50,c}/d_{50,f}$ = 76) and solid density ratios ($\rho_{s,c}/\rho_{s,f}$) of 0.9. It is possible that a different value for the upper limit of $x_{f,mix}$ is obtained for the powders of interest here, which exhibit continuous size distributions and more homogeneous size fractions in terms of solid density. Nevertheless, the particle size distributions and, in particular, the mass fractions of fine particles for P1 and P2 suggest that these products fall within a range where accumulation of fine particles at the silo walls during filling increases with increasing fines content. Data presented in Figure 40 support this statement.

As the fines content increases from that of product P2 ($x_{f,mix}$ = 30 %-wt), segregation (cf. Figure 40) clearly decreases with increasing fines content as a result of the decreasing particle size ratio ($d_{50,c}/d_{50,f}$). A mathematical expression capable of accounting for these effects, i.e., initial increase and subsequent decrease of segregation with increasing fines content, is therefore required for a quantitative description of the segregation. Several different functions or

frequency distributions (Gaussian, Weibull and Rayleigh) were tested, but a Gaussian distribution for quantifying the effect of fines content gave the best result. The regression model was written as

$$m_{\text{segr}} = \gamma_1 + \gamma_2 f(x_{\text{f,mix}}) + \gamma_3 x_{\text{fibers}} \quad (12)$$

where m_{segr} denotes the mass of segregated material withdrawn at the end of complete discharge from the surge silo, x_{fibers} gives the mass fraction of fibers and

$$f(x_{\text{f,mix}}) = \frac{1}{\delta_2\sqrt{2\pi}} e^{-\frac{1}{2}(\frac{x_{\text{f,mix}}-\delta_1}{\delta_2})^2} \quad (13)$$

expresses a Gaussian frequency distribution for the fines content ($x_{\text{f,mix}}$) with mean δ_1 and standard deviation δ_2. Estimates for the parameters ($\hat{\gamma}_1$-$\hat{\gamma}_3$, $\hat{\delta}_1$ and $\hat{\delta}_2$) in Eqs. (12) and (13) were obtained by minimizing the sum of square errors between model values ($\hat{m}_{\text{segr}}$) and production data (m_{segr}) with the simplex algorithm for a range of initial values (starting guesses) for δ_1 and δ_2. Identical estimated parameter values were arrived at from several different starting guesses.

Table 10 lists mean segregated masses ($\bar{m}_{\text{segr}}$) and modeled values ($\hat{m}_{\text{segr}}$) for the products together with estimated parameter values. Overall, the model is only in general agreement ($R^2 = 0.49$) with the segregation data much as a result of the large variations in m_{segr} for each product. However, as evident from Table 10, the model is capable of classifying the products according to segregation tendency. $\bar{m}_{\text{segr}}$ is accurately modeled for products belonging to groups with high (P2) and moderate (P1, P3 and P5) segregation tendency while for products with low tendency (P4, P6 and P7) only minor deviations are obtained. The same values for $\hat{m}_{\text{segr}}$ are determined for all products in the last group because a Gaussian distribution was used for describing the effect of the fines content. This gives identical values sufficiently far away, i.e., a few times the standard deviation $\hat{\delta}_2$=0.06 or 6 %-wt units, from the mean value ($\hat{\delta}_1$=0.31 or 31 %-wt).

Table 10. Production data and results for regression model ($\hat{m}_{\mathrm{segr}}$) together with classification of products according to segregation tendency.

Product	Number of production runs	Production run sizes (t)	m_{segr} [a] (t)	$\hat{m}_{\mathrm{segr}}$ [b] (t)	Segregation tendency
P1	36	63-300	3.01 ± 0.89	3.01	Moderate
P2	30	30-372	4.62 ± 1.23	4.62	High
P3	7	24-75	3.13 ± 0.53	3.13	Moderate
P4	11	51-90	2.23 ± 0.76	2.22	Low
P5	5	21-123	3.09 ± 0.25	3.09	Moderate
P6	11	45-90	2.19 ± 0.74	2.22	Low
P7	10	48-186	2.25 ± 1.03	2.22	Low

a. Mean ± standard deviation.

b. With estimated parameter values $\hat{\gamma}_1$ = 2.22 t, $\hat{\gamma}_2$ = 0.37 t, $\hat{\gamma}_3$ = 220 t, $\hat{\delta}_1$ = 0.31 and $\hat{\delta}_2$ = 0.06.

9.3. Possible remedies

Segregation in the product silo should be reduced by designing the hopper section for mass flow [38]. Even though it was stated in section 7.3 that mass flow does not entirely correct for horizontal segregation observed in the deposited powder bed at silo filling, a mass flow design would reduce the free fall distance, and therefore also the magnitude of the induced horizontal segregation in light of results presented in section 7.2, for the portions of the silo content that are discharged last. By designing the product silo to give mass flow, the free fall distance at filling for the material that discharges last from the silo will generally be smaller compared to the present situation. Material initially depositing to the silo walls in the upper part of the hopper section and lower regions of the vertical section, i.e., the portions of the silo content that currently are withdrawn last, falls for a considerable distance. A letdown chute could also be installed to reduce segregation at filling even further [47]. Mass flow could bear the additional advantage of eliminating the need for using the fluidization plates and the hammer. The presence of significant velocity gradients towards the end of complete discharge from mass flow silos was shown in section 7.3 and also by other investigators [9,32]. Because of this, segregation may not be reduced to satisfactory levels in situations with significant side-to-side segregation at the levels of fill that withdraw last. An insert that reduces these velocity gradients [9,50-53] could be installed in case a mass flow hopper and letdown chute would not suppress segregation to acceptable levels.

The sampling procedure applied during normal production conditions is not fully appropriate, but it is not a straightforward task to decide on improvements because standardized procedures do not exist. Still, it is clear that sample splitters should be used for reducing the sample sizes. Moreover, it would be advantageous to know the origin of samples, i.e., which of the three parallel silo outlets a specific sample was collected from, because the outermost outlets most likely produce material with higher amounts of fines compared to the middle outlet. This could be checked by collecting samples simultaneously from all three outlets, which resembles sampling across the entire discharge stream and is the preferred way of sampling a flowing particulate solid. However, employing such a sampling strategy for quality control purposes increases the work load considerably. Keeping in mind that the main problem caused by segregation is an increase of the fines content at the end of discharge, samples should preferably be collected from the outlet that produces the finest material. This would give an upper limit for the mass fraction of fine particles in the silo output and, therefore, more reliable information regarding correspondence with size specifications.

It is likely that size variations for the raw materials are mainly caused by two reasons: size variations in the plant input and segregation in the raw material silos. The former may be the result of natural size variations for minerals or is caused by particle attrition and breakage during transport to the plant for example by pneumatic conveying. This can be difficult to avoid even though, for example, sand and limestone are sieved to separate size fractions. The occurrence and magnitude of segregation in raw material silos should be investigated in the future. Some particle breakage and attrition presumably also occurs during mixing and the magnitude of this should also be clarified. Furthermore, timely information regarding the size distribution of the products after the mixer would be advantageous. This would give an indication of possible segregation at the end of complete emptying of product silos, because these two features are correlated, i.e., low fines content after the mixer gives less or no segregation, according to results (cf. Figure 39) presented in this section. Measurement of the size distribution after mixing need not necessarily be performed on-line, but this information should be available in time before the end of each production run.

10. Mathematical modeling of particulate systems

In the literature, different numerical methods have been used for describing the behavior of particulate systems. The advantage of mathematical modeling (compared to experimental work) is the ease of performing simulations once a working model has been established and the information that can be obtained. Experimental work is often time consuming and some features that can be studied computationally are difficult or impossible to measure experimentally. Drawbacks related to simulations of particulate systems include the definition of material properties and some numerical methods also present high computational requirements (memory and calculation time). In addition, the models are based on a number of assumptions, some of which may be crucial for the validity of the findings. The behavior of particulate systems has been modeled with the finite element method [69], the void model by Bazant [70], cellular automata [71], continuum methods [72], and the discrete element method [26-31,44-46,73-76]. In some of these investigations, segregation during silo discharge has also been studied. This section presents a short discussion on mathematical modeling of particulate systems segregation with emphasis on the discrete element method (DEM). In particular, results for preliminary DEM studies on segregation at bunker filling performed at the University of Birmingham as part of a co-operation with Åbo Akademi University are briefly presented.

DEM is a numerical method that was first reported by Cundall and Strack [73]. The advantage of DEM is that the particulate phase is not described as continuum but all particles are considered separately. Furthermore, the phase is described explicitly with parameters that at least in some cases, i.e., for larger sized particles, can be determined experimentally. Aside from silo discharge, this method also enables realistic simulations of silo filling when combined with computational fluid dynamics (CFD). This makes it possible to investigate the interdependence between particulate and fluid phase. The drawbacks of DEM are heavy computational requirements because the translational and angular motion of each particle must be calculated and the fact that it may be difficult to determine accurately material properties for very small sized particles.

Some preliminary DEM/CFD simulations of particle segregation at filling of a small sized bunker were performed during the course of this thesis work. The simulations were performed by Dr. Y. Guo under the supervision of Dr. C.-Y. Wu at the University of Birmingham in the UK [77]. In the simulations, a small bunker with dimensions width = 16 mm (x-direction),

height = 10 mm or 20 mm (y) and thickness/depth = 2 mm (z) was considered and the material distribution resulting from filling through a tube of width = 4 mm was studied. Periodic boundaries were employed in the z-direction meaning that particles passing one of the geometry boundaries in this direction were introduced at the opposite boundary with identical characteristics such as particle velocity. Spherical particles were used and calculations were performed with binary particle assemblies resembling mixtures M5 and M6 in the small silo experiments (cf. section 7.1). Coarse particles of diameter 760 μm and solid density 2762 kg/m^3 as well as fine particles of diameter 168 μm and density 1210 kg/m^3 were used giving a particle size ratio (coarse/fine) of approximately 4.5 and solid density ratio (coarse/fine) of approx. 2.3 for the mixture. Segregation was studied for mixtures with low (25 %-wt) and high (50 %-wt) mass fraction of fine particles and simulations were performed in the presence of air and in vacuum. In the presence of air, a two-way coupling between the particle and fluid phase was employed, i.e., the motion of the particle phase influences the air flow and vice versa. The bunker top was open, so air could flow freely upward. Some simulations were also performed with a closed bunker top, but this leads to air flowing upward through the particle packing in the filling tube and results in vertical segregation before all particles exit from the filling tube. The horizontal material distribution in the bunker at the end of each simulation was determined by considering the masses of fine particles in vertical segments over the width of the bunker.

The series of images in Figure 41 shows the movement of the particles at different stages of bunker filling for a simulation with low fines content in the mixture and bunker height 20 mm in the presence of air. This simulation included a total of 15816 particles with 221 coarse ones and took about two weeks to finish on a modern high speed desktop computer. In the simulation, a homogeneous particle assembly was generated in the filling tube, but an excess of fine particles can clearly be seen in peripheral areas of the filling stream soon after the particles enter into the bunker (cf. top middle and rightmost images in Figure 41). As the particles descend and reach the bunker bottom, all particles are directed peripherally and then upwards along the silo walls (cf. lower leftmost image in Figure 41). Finally, a particle bed with a V-shaped surface is obtained with the material distribution presented in Figure 42, where results for a similar simulation in vacuum are also illustrated. On the basis of results presented in this figure, it is clear that the presence of a gaseous phase has a significant influence on segregation. Fine particles are accumulated at the filling point in vacuum whereas an excess of fine particles is obtained at the bunker walls in the presence of air.

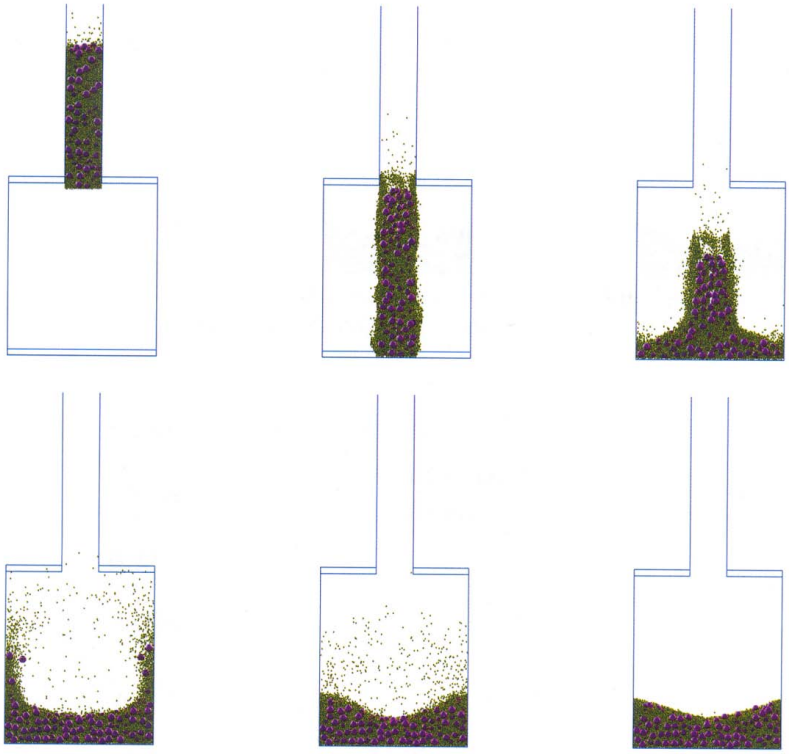

Figure 41. Illustration of particles at different stages during DEM/CFD simulation (in the presence of air) with bunker height 20 mm and mass fraction of fine particles 25 %-wt (taken from [77] with permission).

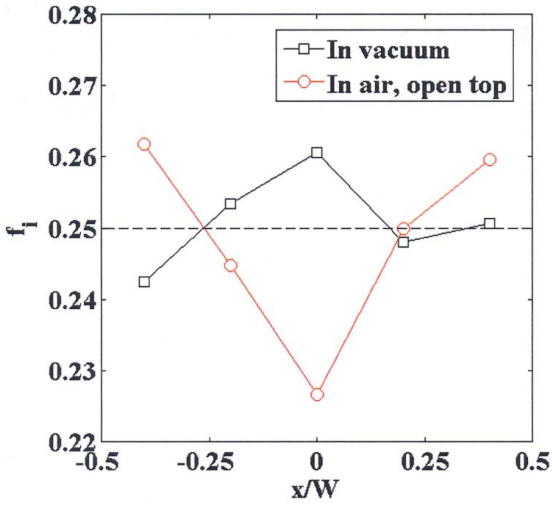

Figure 42. Distribution of fine particles at the end of the simulation illustrated in Figure 41 (in air) and a similar computation in vacuum (taken from [77] with permission).

The filling process for all simulations was somewhat different compared to the silo experiments. In the simulations, all particles enter the bunker relatively quickly without enough time for the development of a heap with the surface shaped as an inverted V. Nevertheless, the obtained distribution of fine particles (cf. Figure 42, in air) is similar to what was observed in the small silo experiment with mixture M6 despite the fact that the geometry was considerable reduced for the simulation. The finding that an excess of small particles was observed in the peripheral areas of the filling stream during particle descent in the upper and middle parts of the bunker could be explained by collisions with other (larger) particles. Compared to coarser particles, smaller particles can more easily change their flow direction upon collisions with other particles. However, it must be remembered that mixture M6 is free flowing and, therefore, it is not known to what extent the same phenomena would occur in experiments with cohesive mixtures. Results for the physical silo tests with sampling horizontally midway between the silo centre and the silo walls at filling indicated that the fine particle concentration in this point was often lower than at the heap apex (cf. Figure 12 and Figure 14). It may be speculated that if the smaller sized particles behaved similarly during free fall in the experiments as in the simulation, this could explain the observed horizontal material distribution to some extent. Small particles located in the peripheral regions of the filling stream may be thrown outwards upon impact with the deposited heap of material in the silo and reach the silo walls, where a considerable excess of fine particles was often found. Sampling positions located midway between the silo centre and the silo walls are depleted in fine particles because the small particles obtain a high horizontal velocity component upon impact with the heap. These particles are thrown upwards when reaching the silo walls and finally come to rest in this position. This was, in fact, observed for experiments in the small silo where a vertical section made of Perspex was used.

Figure 43 illustrates a simulation with low fines content in the mixture and a bunker height of 10 mm in the presence of air. In this simulation, the particles were charged in two batches with the figure showing the situation before filling of the second batch and at the end of the simulation. The horizontal distribution of fine particles included in the second batch is presented in Figure 44. The fines content next to the left bunker wall (‘x/W’ = -0.5) is approx. 30.5 %-wt, which is clearly higher than the results presented in Figure 42 (in air) despite the taller bunker used in the latter simulation. This suggests that the distribution of fine particles is influenced by the surface shape of the deposited powder bed. Similar findings were reported in section 7.2 for one experiment in the small silo where discharge and filling occurred

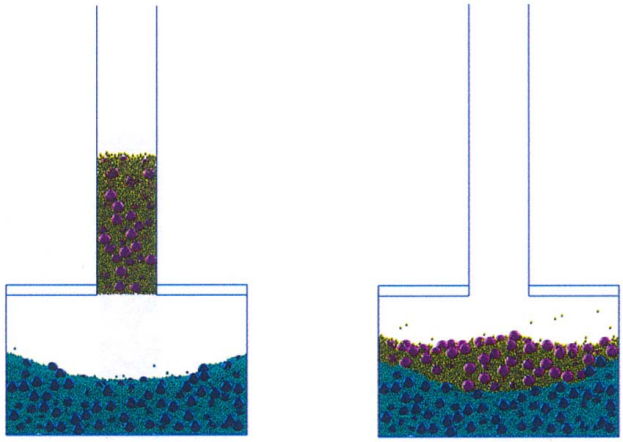

Figure 43. Illustration of simulation with bunker height 10 mm and mass fraction of fine particles 25 %-wt with filling of particles in two batches (filling of the second batch is shown) (taken from [77] with permission).

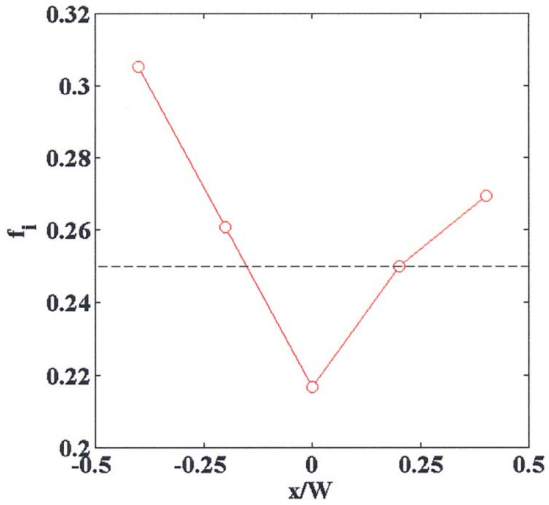

Figure 44. Distribution of fine particles for the second filling batch in the simulation shown in Figure 43 (taken from [77] with permission).

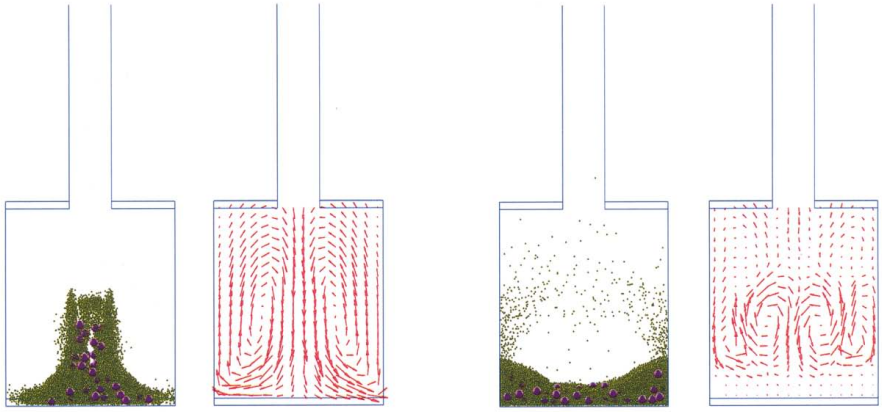

Figure 45. Illustration of particles and air velocity field at two different stages during a simulation with bunker height 20 mm and mass fraction of fine particles 50 %-wt (taken from [77] with permission).

intermittently. In this experiment, the deposited powder bed obtained a V-shaped surface after the withdrawal of a portion of the silo contents.

Figure 45 presents results for a simulation with high fines content in the mixture and bunker height 20 mm in the presence of air. In this figure, the air velocity fields corresponding to two different stages during the computation are shown. As expected, circulating air currents are generated by the falling particulate phase. The left pair of images shows that air flow is directed downwards in the central part of the bunker, towards peripheral areas along the surface of the forming heap and upwards along the bunker walls. This illustrates how air current segregation works: fine particles are carried by the air flow towards the walls of the bunker and settle in this position because of the radical change in the flow direction.

The results of the simulations presented in this section must be considered with some caution. Repeated runs should be performed in order to ascertain that the results are reproducible and not caused by stochastic processes. Nevertheless, the strength of numerical studies has been clearly shown; the generated information could not be obtained experimentally. Even though the geometry in the simulations was considerably reduced from the silo experiments, a comparison of the results (simulations versus experiments) showed some interesting similarities. Moreover, information was generated that deepens the understanding of some of the processes that potentially occur and of the results obtained in the physical silo tests.

11. Suggestions for further work

On the basis of the findings presented in this thesis, the following features deserve to be addressed in the future:

- The extent to which mass flow corrects for horizontal segregation in large sized silos with small sized outlets
- Optimal solutions for inserts placed in the lower parts of a silo for reducing velocity gradients with lower levels of silo fill in mass flow discharge and/or for converting funnel flow silos to mass flow
- Optimal designs for letdown chutes and inserts located in the top parts of the silo for reducing horizontal segregation (with accumulation of fine particles to the silo walls) induced at silo filling
- Optimal location and operation of fluidization plates (installed in the hopper section) for achieving/maintaining flow through small sized silo outlets and for converting funnel flow to mass flow
- Magnitude of segregation in raw material silos for assessing the need for mass flow designs
- Magnitude of particle breakage/attrition during mixing for determining optimal batch mixing time with respect to segregation
- More detailed studies on the effects of the free fall distance and silo diameter on segregation for clarifying optimal silo dimensions (with respect to segregation)
- Effects of pneumatic transport on segregation at silo filling
- Possibilities for reducing segregation through agglomeration of fine particles for example by the addition of small amounts of liquids (already performed for producing dust free products) or by compression/compaction

12. Conclusions

The main conclusions of this thesis work include:

- Identification of the most critical processing unit with respect to segregation for industrial production of dry mineral-based construction materials
- Clarification of the effects of silo scale on segregation of commercial construction materials
- Identification of relevant segregation mechanisms (embedding, fluidization and air current) for construction materials handled in silos
- Quantification of the effects of material properties, process parameters and silo dimensions on horizontal segregation induced at silo filling
- Segregation at silo discharge mainly determined by the material distribution obtained as a result of filling
- Horizontal segregation (induced during silo filling) not entirely corrected for at silo outlet by mass flow discharge flow pattern
- Limited possibilities of using local fluidization in the hopper section for converting funnel flow silos to mass flow
- Segregation not always reduced by increased cohesiveness for a bulk solid

Product silos located upstream of packing were identified as the most critical processing unit(s) with respect to segregation for industrial production of construction materials. Reducing the silo scale from 70 m^3 to 0.5 m^3 reduced the magnitude of segregation, but the same segregation behavior was still observed. Furthermore, segregation of commercial construction materials when handled in large sized silos can be studied with two- and three-component powder mixtures in much smaller scale. Embedding, fluidization and air current segregation were identified as the most relevant segregation mechanisms for segregation of construction materials in silos. These occur at filling of silos with free fall and result in accumulation of fine particles away from the filling point, i.e., at the silo walls when the silo is centrally filled.

The magnitude of horizontal segregation at silo filling, with accumulation of fine particles away from the filling point, was shown to increase with increasing

- mass fraction of fine particles
- particle size ratio (coarse/fine)
- particle solid density ratio (coarse/fine)
- ratio for free fall distance and silo diameter
- ratio for silo diameter and inlet diameter

On the basis of results obtained in this thesis work the feeding rate has practically no effect on segregation at silo filling, at least for the range of feeding rates tested and usually encountered in industrial operations. However, in extreme cases such as at feeding rates close to zero this may not apply anymore.

Segregation of commercial construction products at silo discharge manifests itself as an increase of the mass fraction of fine particles at the end of complete silo emptying. Segregation at the end of emptying is largely determined by the initial horizontal material distribution at the levels of fill that withdraw last. Funnel flow discharge gives severe segregation at the end of silo emptying, because fines-rich material from the vicinity of the silo walls in the upper parts of the hopper section and lower parts of the vertical section discharges last. Mass flow does not entirely correct for horizontal segregation induced at filling by re-mixing material from different radial segments at the silo outlet, because significant velocity gradients occur in the powder mixture during the last stages of emptying. The discharging velocity is greater above the silo outlet than in more peripheral regions when the silo fill level drops below 0.5-1.0 times the silo diameter from above the transition from hopper to vertical section. However, mass flow should reduce segregation at complete emptying because the free fall distance for the portions of the silo contents that discharge last is usually smaller than in funnel flow silos with identical vertical section.

This thesis work also shows that using local fluidization induced by fluidization plates in the hopper section gives limited possibilities for converting funnel flow to mass flow. However, local fluidization may be needed for achieving and maintaining flow through small sized outlets. Furthermore, even though it is often reported that segregation can be reduced by increas-

ing the cohesiveness for bulk solids, this work shows that segregation may in fact be aggravated by this. The former has been shown by other investigators for systems involving segregation of free flowing particulate solids as a result of sifting and rolling, whereas the latter seems to be true when segregation occurs partly - or mainly - because of embedding and fluidization. The cohesiveness of a particulate solid refers to the magnitude of inter-particle forces and it may be increased by adding small amounts of liquids to or increasing the concentration of fine cohesive components in the particulate solid. Air current segregation also affects the flow and the ultimate distribution of commercial construction products at silo filling by depositing fine particles away from the filling point, but it is not obvious from the work presented here whether this segregation mechanism is aggravated by increased cohesiveness for the bulk solid.

The possibilities to reduce segregation through production planning seem limited. This is because many products are nearly always produced at the same plant and a vast majority of the product silos must be completely emptied at changes in the production sequence. Segregation can be reduced or eliminated by keeping the fill level high in silos dedicated to specific products. However, this may result in degradation of product quality with time in cases of funnel flow and clear procedures must exist for controlling the level of fill.

Notation

d_{10}	10 % particle size on the cumulative distribution curve, [mm]
d_{50}	50 % particle size on the cumulative distribution curve, i.e., the mean particle size, [mm]
d_{90}	90 % particle size on the cumulative distribution curve, [mm]
$d_{\text{cut-off}}$	the cut-off size between fine and coarse fraction, [mm]
d_{inlet}	filling hopper outlet (or silo inlet) diameter, [mm or m]
d_{outlet}	silo outlet diameter, [mm or m]
D_{silo}	silo diameter, [mm or m]
H_{cylinder}	height of silo's cylindrical (vertical) section, [mm]
h_{ff}	free fall distance, [m]
h_{cr}	minimum hopper height required for mass flow, [m]
h_{hopper}	hopper height, [m]
m_i	mass of powder mixture withdrawn from silo at exit of tracer *i* or collection of sample *i*, [kg or ton]
$m_{\text{tot,exp}}$	total mass of powder mixture used in experiment or size of production run, [kg or ton]
m_{batch}	mass of filling batch, [kg]
$\dot{m}_{\text{in}}$	filling rate, [kg/s]
$\dot{m}_{\text{out}}$	discharge rate, [kg/s]
$m_{\text{f,tot,silo}}$	mass of fines (according to formulation) with full silo, [kg]
$m_{\text{f,P}}$	mass of fines in sample collected at silo wall, [kg]
m_{s}	mass of sample, [kg]
m_{segr}	mass of segregated mixture withdrawn from silo at the end of complete discharge, [kg or ton]
$m_{\text{tot,silo}}$	silo capacity (mixture dependent), [kg]
x_{moisture}	moisture content, [-]
$x_{\text{f,P,s}}$	fines content at silo wall (sampled), [-]
$x_{\text{f,C,s}}$	fines content in silo centre (sampled), [-]
$x_{\text{f,mix}}$	fines content of powder mixture according to formulation, [-]
$x_{\text{f,disch}}$	fines content at discharge, [-]
$x_{\text{f,P}}$	fines content at silo wall (model), [-]
$x_{\text{f,P,exp}}$	corrected value for fines content at silo wall in experiments, [-]

x_{fibers}	mass fraction of fibers, [-]
$Y, \tilde{Y}$	dependent variable (with tilde in discharge model), [-]
X_1-X_6	dimensionless groups in filling model, [-]
$\tilde{X}_1$	dimensionless group in discharge model, [-]

Greek letters

$\Delta_{< 0.125\ \text{mm}}$	difference in the mass fraction less than 0.125 mm between samples collected at silo walls and in silo centre, [%-wt units]
α	parameters in the filling model, [-]
β	parameters in the discharge model, [-]
γ_1-γ_3	parameters in the regression model, [ton]
δ_1, δ_2	parameters in the regression model, [-] or [%-wt] / [%-wt units]
θ_{hopper}	hopper angle from the horizontal plane, [°]
θ_{cr}	critical hopper angle (measured from the horizontal plane) for mass flow, [°]
ρ_{s}	particle solid density, [kg/m^3]

Index

f	fine fraction
c	coarse fraction

A hat above a symbol denotes a quantity estimated by linear least sum of squares. A bar above a symbol expresses the arithmetic mean value for a quantity.

References

1. L. Bates, User Guide to Segregation, Ed. G. Hayes, British Materials Handling Board, Marlow, U.K., 1997.

2. E.W. Merrow, Linking R&D to Problems Experienced in Solids Processing, Chemical Engineering Progress, 81(5), 14-22, 1985.

3. E.W. Merrow, Estimating Startup Times for Solids-Processing Plants, Chemical Engineering, 95(15), 89-92, 1988.

4. E.W. Merrow, Problems and progress in particle processing, Chemical Innovation, 30(1), 34-41, 2000.

5. T.A. Bell, Challenges in the scale-up of particulate processes - an industrial perspective, Powder Technology, 150, 60-71, 2005.

6. P. Tang and V.M. Puri, Methods for Minimizing Segregation: A Review, Particulate Science and Technology, 22, 321-337, 2004.

7. J. Mosby, Investigations of the Segregation of Particulate Solids with Emphasis on the Use of Segregation Testers, Dr. Ing. Thesis, Telemark College, Porsgrunn, Norway, 1996.

8. J.C. Williams, The Segregation of Particulate Materials. A Review, Powder Technology, 15, 245-251, 1976.

9. D. Schulze, Powders and Bulk Solids, Springer-Verlag, Berlin Heidelberg, 2008.

10. S. de Silva, A. Dyrøy and G.G. Enstad, Segregation Mechanisms and Their Quantification using Segregation Testers, in IUTAM Symposium on Segregation in Granular Flows, Eds. A.D. Rosato and D.L. Blackmore, Kluwer Academic Publishers, Dordrecht, the Netherlands, 11-29, 2000.

11. J.A. Drahun and J. Bridgwater, The Mechanisms of Free Surface Segregation, Powder Technology, 36, 39-53, 1983.

12. J.J. McCarthy, Turning the corner in segregation, Powder Technology, 192, 137-142, 2009.

13. J.W. Carson, T.A. Royal and D.J. Goodwill, Understanding and Eliminating Particle Segregation Problems, Bulk Solids Handling, 6(1), 139-144, 1986.

14. J.W. Carson, Preventing Particle Segregation, Chemical Engineering, 111(2), 29-31, 2004.

15. J.R. Johanson, Particle segregation … and what to do about it, Chemical Engineering, 85(11), 183-188, 1978.

16. R.L. Brown, The Fundamental Principles of Segregation, Glass, 422-426, November 1939.

17. G.F. Salter, Investigations into the Segregation of Heaps of Particulate Materials with Particular Reference to the Effects of Particle Size, Dr. Phil. Thesis, The University of Greenwich, London, U.K., 1999.
18. K. Shinohara, K. Shoji and T. Tanaka, Mechanisms of segregation and blending of particles flowing out of mass-flow hoppers, Industrial & Engineering Chemistry Process Design and Development, 9(2), 174-180, 1970.
19. K. Shinohara, K. Shoji and T. Tanaka, Mechanisms of Size Segregation of Particles in Filling a Hopper, Industrial & Engineering Chemistry Process Design and Development, 11(3), 369-376, 1972.
20. K. Shinohara, Mechanisms of Segregation of Differently Shaped Particles in Filling Containers, Industrial & Engineering Chemistry Process Design and Development, 18(2), 223-227, 1979.
21. K. Shinohara and S.-I. Miyata, Mechanisms of Density Segregation of Particles in Filling Vessels, Industrial & Engineering Chemistry Process Design and Development, 23(3), 423-428, 1984.
22. K. Shinohara, B. Golman and T. Nakata, Size segregation of multicomponent particles during the filling of a hopper, Advanced Powder Technology, 12(1), 33-43, 2001.
23. K. Shinohara and B. Golman, Segregation indices of multi-sized particle mixtures during the filling of a two-dimensional hopper, Advanced Powder Technology, 13(1), 93-107, 2002.
24. K. Shinohara, B. Golman and T. Mitsui, Segregation Pattern of Multi-Component Particles of Different Densities During the Filling of a Vessel, Powder Handling & Processing, 14(2), 91-95, 2002.
25. T. Tanaka, Segregation Models of Solid Mixtures Composed of Different Densities and Particle Sizes, Industrial & Engineering Chemistry Process Design and Development, 10(3), 332-340, 1971.
26. W.R. Ketterhagen, J.S. Curtis, C.R. Wassgren, A. Kong, P.J. Narayan and B.C. Hancock, Granular segregation in discharging cylindrical hoppers: A discrete element and experimental study, Chemical Engineering Science, 62, 6423-6439, 2007.
27. W.R. Ketterhagen, J.S. Curtis, C.R. Wassgren and B.C. Hancock, Modeling granular segregation in flow from quasi-three-dimensional, wedge-shaped hoppers, Powder Technology, 179, 126-143, 2008.
28. W.R. Ketterhagen, J.S. Curtis, C.R. Wassgren and B.C. Hancock, Predicting the flow mode from hoppers using the discrete element method, Powder Technology, 195, 1-10, 2009.

29. W.R. Ketterhagen and B.C. Hancock, Optimizing the design of eccentric feed hoppers for tablet presses using DEM, Computers and Chemical Engineering, 34, 1072-1081, 2010.
30. A. Anand, J.S. Curtis, C.R. Wassgren, B.C. Hancock and W.R. Ketterhagen, Segregation of cohesive granular materials during discharge from a rectangular hopper, Granular Matter, 12, 193-200, 2010.
31. Y. Yu and H. Saxén, Experimental and DEM study of segregation of ternary size particles in a blast furnace top bunker model, Chemical Engineering Science, 65, 5237-5250, 2010.
32. J.K. Prescott and R.J. Hossfeld, Maintaining Product Uniformity and Uninterrupted Flow to Direct-Compression Tableting Presses, Pharmaceutical Technology, 18(6), 99-114, 1994.
33. L.R. Lawrence and J.K. Beddow, Powder Segregation During Die Filling, Powder Technology, 2, 253-259, 1969.
34. H. Matthée, Segregation Phenomena Relating to Bunkering of Bulk Materials: Theoretical Considerations and Experimental Investigations, Powder Technology, 1(5), 265-271, 1968.
35. J.F.G. Harris and A.M. Hildon, Reducing Segregation in Binary Powder Mixtures with Particular Reference to Oxygenated Washing Powders, Industrial & Engineering Chemistry Process Design and Development, 9(3), 363-367, 1970.
36. N. Standish, Studies of Size Segregation in Filling and Emptying a Hopper, Powder Technology, 45, 43-56, 1985.
37. D. McGlinchey, Quantifying segregation in heaps: an experimental study, Powder Technology, 145, 106-112, 2004.
38. A. Kwade and O. Ziebell, Reducing the segregation of multi-phase plaster by selective alteration of the silo geometry, ZKG International, 54(12), 680-688, 2001.
39. J. Boss and M. Tukiendorf, The Influence of Filling Modes upon Mixing during Discharge from a Silo, Powder Handling & Processing, 10(4), 363-366, 1998.
40. T. Deng, K.A. Paul, M.S.A. Bradley, L. Immins, C. Preston, J.F. Scott and E.H. Welfare, Investigations on air induced segregation of pharmaceutical powders and effect of material flow functions, Powder Technology, 203, 354-358, 2010.
41. S. Zigan, R.B. Thorpe, U. Tüzün and G.G. Enstad, Air Current Segregation of Alumina Powder, Particle & Particle Systems Characterization, 24, 124-135, 2007.
42. S. Zigan, R.B. Thorpe, U. Tüzün, G.G. Enstad and F. Battistin, Theoretical and experimental testing of a scaling rule for air current segregation of alumina powder in cylindrical silos, Powder Technology, 183, 133-145, 2008.
43. A.N. Carruthers, Segregation in flat bottomed alumina silos, TMS Light Metal Committee, 116th Annual Meeting (1987), Number 492, 151-156.

44. Y. Guo, K.D. Kafui, C.-Y. Wu, C. Thornton and J.P.K. Seville, A Coupled DEM/CFD Analysis of the Effect of Air on Powder Flow During Die Filling, AIChE Journal, 55(1), 49-62, 2009.
45. Y. Guo, C.-Y. Wu, K.D. Kafui and C. Thornton, Numerical analysis of density-induced segregation during die filling, Powder Technology, 197, 111-119, 2009.
46. Y. Guo, C.-Y. Wu, K.D. Kafui and C. Thornton, 3D DEM/CFD analysis of size-induced segregation during die filling, Powder Technology, 206, 177-188, 2011.
47. J. Marinelli, Will Mass Flow Solve All Your Segregation Problems?, Chemical Engineering, 113(4), 40-42, 2006.
48. A. Jenike, Storage and Flow of Solids, Bulletin 123, Utah Engineering Experiment Station, University of Utah, Salt Lake City, 1964.
49. D. Schulze, Round robin test on ring shear testers, Advanced Powder Technology, 22, 197-202, 2011.
50. J.R. Johanson, Controlling Flow Patterns in Bins by Use of an Insert, Bulk Solids Handling, 2(3), 495-498, 1982.
51. J.W. Carson, Techniques of in-bin blending, in Bulk 2000: Bulk Materials Handling - Towards the Year 2000, IMechE conference proceedings, 247-255.
52. L. Bates, S. Dhodapkar and G. Klinzing, Using Inserts to Address Solids Flow Problems, Chemical Engineering, 117(7), 32-37, 2010.
53. A.W. Roberts, Design of bins and feeders for anti-segregation and blending, in Bulk 2000: Bulk Materials Handling - Towards the Year 2000, IMechE conference proceedings, 257-264, 1991.
54. K. Jochem and J. Schwedes, Discharging silos by aeration, ZKG International, 12, 678-686, 1997.
55. H.P. Kurz and H. Rumpf, Flow Processes in Aerated Silos, Powder Technology, 11, 147-156, 1975.
56. H.P. Kurz, The Stability of Material Bridges in Aerated Silos, Powder Technology, 13, 57-72, 1976.
57. T.A. Bell, Industrial Needs in Solids Flow for the 21st Century, Powder Handling & Processing, 11(1), 9-12, 1999.
58. M. Hjelm, Site Equipment Manager, Supply Chain Process, Saint-Gobain Weber Oy Ab, personal communication, 2010.
59. K. Saarinen, Vice President, Plaster & Mortar Technology, Lahti Precision, personal communication, 2008.

60. P. Hilgraf and A. Hilck, Functioning and process engineering design of large aerated silos, Cement International, 1, 42-60, 2009.
61. J.Y. Ooi and J.M. Rotter, Flow visualization, in Silos. Fundamentals of theory, behavior and design, Eds. C.J. Brown and J. Nielsen, Taylor & Francis, Abingdon, U.K., 745-760, 1998.
62. J.Y. Ooi, J.F. Chen and J.M. Rotter, Measurement of solids flow patterns in a gypsum silo, Powder Technology, 99, 272-284, 1998.
63. J.F. Chen, J.M. Rotter, J.Y. Ooi and Z. Zhong, Flow pattern measurements in a full scale silo containing iron ore, Chemical Engineering Science, 60, 3029-3041, 2005.
64. D.P. Graham, A.R. Tait and R.S. Wadmore, Measurement and Prediction of Flow Patterns of Granular Solids in Cylindrical Vessels, Powder Technology, 50, 65-76, 1987.
65. M. Zlokarnik, Scale-up in Chemical Engineering, Wiley-VCH, Weinheim, Germany, 2002.
66. N.R. Draper, H. Smith, Applied Regression Analysis, Wiley, New York, 1998.
67. D.L. Brone, S.A Clement, B.C. Hancock, D.B. Hedden, M.A. McCall, J.K. Prescott and T.G. Troxel, Segregation testing apparatus for powders and granular materials, US patent number 7347111 B2, 2008.
68. J.K. Prescott, S.A. Clement and J.W. Carson, Fluidization segregation tester, US patent number 6487921, 2002.
69. T. Karlsson, M. Klisinski and K. Runesson, Finite element simulation of granular material flow in plane silos with complicated geometry, Powder Technology, 99, 29-39, 1998.
70. M. Bazant, The spot model for random-packing dynamics, Mechanics of Materials, 38, 717-731, 2006.
71. J. Kozicki and J. Tejchman, Application of cellular automaton to simulations of granular flow in silos, Granular Matter, 7, 45-54, 2005.
72. N. Christakis, P. Chapelle, N. Strusevich, I. Bridle, J. Baxter, M.K. Patel, M. Cross, U. Tüzün, A.R. Reed and M.S.A. Bradley, A hybrid numerical model for predicting segregation during core flow discharge, Advanced Powder Technology, 17, 641-662, 2006.
73. P.A. Cundall and O.D.L. Strack, A discrete numerical model for granular assemblies, Geotechnique, 29, 47-65, 1979.
74. P.W. Cleary, Large scale industrial DEM modeling, Engineering Computations, 21, 169-204, 2004.

75. H.P. Zhu, Z.Y. Zhou, R.Y. Yang and A.B. Yu, Discrete particle simulations of particulate systems: A review of major applications and findings, Chemical Engineering Science, 63, 5728-5770, 2008.
76. Y. Tsuji, T. Tanaka and T. Ishida, Lagrangian numerical simulation of plug flow of cohesionless particles in a horizontal pipe, Powder Technology, 71, 239-250, 1992.
77. Y. Guo, C.-Y. Wu, DEM/CFD analysis of segregation during silo filling, internal report, School of Chemical Engineering, University of Birmingham, UK, 2011.